

INFORMATION TO USERS

This manuscript has been reproduced from the microfilm master. UMI films the text directly from the original or copy submitted. Thus, some thesis and dissertation copies are in typewriter face, while others may be from any type of computer printer.

The quality of this reproduction is dependent upon the quality of the copy submitted. Broken or indistinct print, colored or poor quality illustrations and photographs, print bleedthrough, substandard margins, and improper alignment can adversely affect reproduction.

In the unlikely event that the author did not send UMI a complete manuscript and there are missing pages, these will be noted. Also, if unauthorized copyright material had to be removed, a note will indicate the deletion.

Oversize materials (e.g., maps, drawings, charts) are reproduced by sectioning the original, beginning at the upper left-hand corner and continuing from left to right in equal sections with small overlaps. Each original is also photographed in one exposure and is included in reduced form at the back of the book.

Photographs included in the original manuscript have been reproduced xerographically in this copy. Higher quality 6" x 9" black and white photographic prints are available for any photographs or illustrations appearing in this copy for an additional charge. Contact UMI directly to order.

UMI

A Bell & Howell Information Company
300 North Zeeb Road, Ann Arbor MI 48106-1346 USA
313/761-4700 800/521-0600

NEARSHORE ICE FORMATION AND
SEDIMENT TRANSPORT IN SOUTHERN
LAKE MICHIGAN

by

Edward W. Kempema

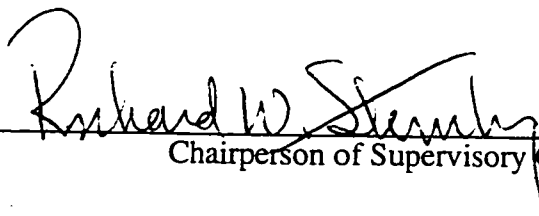
A dissertation submitted in partial fulfillment of the
requirements for the degree of

Doctor of Philosophy

University of Washington

1998

Approved by



Chairperson of Supervisory Committee

Program Authorized
to Offer Degree

Oceanography

Date

26 May 1998

UMI Number: 9836195

UMI Microform 9836195
Copyright 1998, by UMI Company. All rights reserved.

**This microform edition is protected against unauthorized
copying under Title 17, United States Code.**

UMI
300 North Zeeb Road
Ann Arbor, MI 48103

Doctoral Dissertation

In presenting this dissertation in partial fulfillment of the requirements for the Doctoral degree at the University of Washington, I agree that the Library shall make its copies freely available for inspection. I further agree that extensive copying of this dissertation is allowable only for scholarly purposes, consistent with "fair use" as prescribed in the U.S. Copyright Law. Requests for copying or reproduction of this dissertation may be referred to University Microfilms, 1490 Eisenhower Place, P.O. Box 975, Ann Arbor, MI 48106, or to the author.

Signature E. Sanfoma
Date 26 May 1998

University of Washington

Abstract

NEARSHORE ICE FORMATION AND
SEDIMENT TRANSPORT IN SOUTHERN
LAKE MICHIGAN

by Edward W. Kempema

Chairperson of the Supervisory Committee: Professor Richard W. Sternberg
School of Oceanography

The southern Lake Michigan nearshore zone is ice covered for two to four months each year. Daily observations in January 1991 document the effect of this seasonal ice on sediment transport along the Illinois shoreline of the lake. Three distinct types of ice are found in the nearshore zone. Each of these ice types has a different effect on nearshore sediment but all contribute to ice rafting sediment alongshore and cross shore.

The Nearshore Ice Complex (NIC) is a large, 'solid' mass of ice that builds lakeward from the shoreline. At Gillson Beach in southwest Lake Michigan, the NIC reached a maximum width of 180 m and formed ridges up to 4 m above lake level. The volume of this NIC was 420 m³ of ice per meter of beach width. This ice entrained 2.3 m³ of sand per meter of beach. The NIC is a dynamic feature that grows and decays in response to incident waves and the amount of slush ice in the nearshore zone. Destruction of the NIC by waves leads to ice rafting of sand.

Anchor ice is ice that is attached to the lakebed; it forms on sand, pebble and cobble bottoms in the nearshore zone. Anchor ice formation is common; it formed on 14 of 32 nights at one site. Anchor ice forms on cold, clear nights with offshore winds and is released from the bed and floats to the surface with entrained sediment when the water warms during the day. The formation and release of anchor ice transports sand in calm conditions. I estimate that anchor ice rafted 0.85 m³ of sand from each m of beach at one site during the winter of 1991. There is a continuum of anchor ice morphologies that is a function of the incident wave energy at the time of anchor ice formation.

Slush ice is mm-sized, unconsolidated, mobile ice. Slush ice consists primarily of floating accumulations of frazil ice crystals, although anchor ice and NIC ice are also incorporated into this mobile ice type. Sand is incorporated into slush ice directly from

the bed or water column and by transfer of sediment-laden anchor ice and NIC ice to the slush ice zone. Combined ice sampling, video records and drifter returns show that there is a net transport of slush ice and sand to the south and offshore along the southwestern Lake Michigan coast. This study shows that annual ice formation in southern Lake Michigan is removing sand from the sediment-starved nearshore zone.

TABLE OF CONTENTS

LIST OF FIGURES	iv
LIST OF TABLES	v
CHAPTER 1. INTRODUCTION	1
1.1 INTRODUCTION	1
1.2 BACKGROUND	2
1.2.1 Types of Lake Ice	2
1.2.2 The Study Area.....	4
1.2.2.1 Wave Climate.....	7
1.2.2.2 Gillson Beach.....	8
1.3 OBJECTIVES	13
CHAPTER 2: THE NEARSHORE ICE COMPLEX.....	14
2.1 INTRODUCTION	14
2.2 PREVIOUS STUDIES.....	14
2.2.1 Formation of the nearshore ice complex.....	14
2.2.2 Sediment in the NIC	18
2.2.3 The Effects of the NIC on Nearshore Bathymetry	20
2.2.4 Seawalls as analogs to NICs.....	22
2.3 METHODS	24
2.4 RESULTS	34
2.4.1 Bathymetry.....	34
2.4.2 NIC Growth and Destruction.....	37
2.4.3 NIC Volume and Sediment Load.....	42
2.5 DISCUSSION.....	45
2.5.1 NIC Growth and Destruction.....	45
2.5.2 The NIC as a Seawall and Winter Bathymetric Changes.....	48
2.6 CONCLUSIONS	51
CHAPTER 3. ANCHOR ICE FORMATION IN SOUTHERN LAKE MICHIGAN	53
3.1 INTRODUCTION	53
3.2 PREVIOUS STUDIES.....	54
3.2.1 Conditions for anchor ice formation	54
3.1.2 Anchor Ice in Lakes.....	57

3.3 METHODS	58
3.3.1 Wave Tank Studies.	58
3.3.2 Field Studies.....	59
3.3.2.1 Weather.....	61
3.3.2.2 Nearshore Water Conditions.....	61
3.3.2.3 Anchor Ice Observations and Analysis.	63
3.4 RESULTS	67
3.4.1 Wave Tank Results	67
3.4.2 Southern Lake Michigan Observations	70
3.4.2.1 Chicago Cribs.	71
3.4.2.2 Illinois Beach State Park.	71
3.4.3.3 Kohler-Andrae State Park.....	71
3.4.3.4 Gillson Beach.....	73
3.4.3.5 Turbulence and Anchor Ice Formation	76
3.4.3.6 Anchor Ice Morphologies	81
3.4.3.7 Sediment in Anchor Ice.....	89
3.5 DISCUSSION.....	94
3.5.1 Wave Tank Experiments and Insights into Anchor Ice Formation and Morphology	94
3.5.2 Anchor ice and sediment transport	97
3.5.3 Anchor Ice Distribution: Depths.....	100
3.5.4 Anchor Ice Distribution: Substrates.....	101
3.5.4 Anchor ice morphology and sediment concentration: a continuum.....	104
3.6 CONCLUSIONS	106
CHAPTER 4: THE SLUSH ICE ZONE	108
4.1 INTRODUCTION	108
4.2 THE VERTICAL DISTRIBUTION OF SEDIMENT IN THE SLUSH ICE ZONE.....	110
4.3 ICE RAFTING AT GILLSON BEACH, DECEMBER 1989.....	115
4.4 GILLSON BEACH OBSERVATIONS JANUARY 1991.....	117
4.5 1991 AND 1992 DRIFTERS.....	127
4.6 DISCUSSION.....	133
4.7 CONCLUSIONS	136

CHAPTER 5: AN INTEGRATED VIEW OF NEARSHORE ICE AND ITS AFFECT ON SEDIMENT TRANSPORT IN SOUTHERN LAKE MICHIGAN	137
5.1 INTRODUCTION	137
5.2 COMPARISON OF SEDIMENT FOUND IN GILLSON BEACH ICE SAMPLES	137
5.3 AN INTEGRATED VIEW OF SEDIMENT/ICE INTERACTIONS IN SOUTHERN LAKE MICHIGAN.....	139
5.4 CONCLUSIONS.....	143
BIBLIOGRAPHY.....	146

LIST OF FIGURES

<i>Number</i>	<i>Page</i>
Figure 1.1 Map of study area.	3
Figure 1.2. Cross section of the nearshore zone showing the morphologic features of the NIC and the mobile slush ice zone.	5
Figure 1.3 Map of Gillson Beach study.	11
Figure 1.4. (a) Cross section of Gillson Beach Main Line profile. (b) Mean phi grain size of sediment samples. (c) Phi standard deviation in grain size.	12
Figure 2.1. Lakeward-looking view of the NIC at Gillson Beach.....	15
Figure 2.2. Two views looking landward at the outer edge of the NIC	17
Figure 2.3a-f. Gillson Beach bathymetric profiles between 14 December 1990 and 15 March 1991.....	27
Figure 2.4. NIC profiles for lines N6 through S6 on 9, 13, 18 and 22 January 1991. ...	38
Figure 2.5. Changes in Main Line NIC width between 28 December 1990 and 2 February 1991.....	41
Figure 2.6. Topography of a small portion of the NIC.....	43
Figure 3.1. Steps in frazil and anchor ice formation in a turbulent flow and a typical cooling curve for supercooled water when frazil and anchor ice growth occurs.	56
Figure 3.2. Wave tank calibration curves.....	60
Figure 3.3. Lake Michigan map showing the four areas (dots) where anchor ice was seen during the winters of 1989, 1990 and 1991.....	62
Figure 3.4. Floating anchor ice masses released from the nearshore lakebed at Gillson Beach	64
Figure 3.5. An anchor ice sample found floating on the surface 15 m lakeward of the NIC edge on 26 January 1991.	66
Figure 3.6. Sediment concentration measured in a wave tank experiment with an OBS.	69
Figure 3.7. Weather conditions during periods of anchor ice formation.....	75

Figure 3.8. (a) Wave heights 25 m from the NIC edge on 22 January 1991. (b) Power spectra of (a).....	79
Figure 3.9. (a) Wave heights 15 m from the NIC edge at Gillson Beach on 27 January 1991. (b) The wave spectra for (a).....	80
Figure 3.10. Anchor ice sample 91-119, collected 27 January 1991. A single anchor ice crystal 7 cm x 3 cm x 2 mm thick.....	84
Figure 3.11 Bottom photograph taken at Gillson Beach on 27 January 1991 in the boulder lag at ~3.5 m water depth.	85
Figure 3.12. Bottom photograph taken at Gillson Beach on the morning of 27 January 1991 in 80 cm water depth on the crest of a nearshore bar.	86
Figure 3.13. An anchor ice sample retrieved from the bar crest 25 m from the NIC edge on 23 January 1991.	88
Figure 3.14. Massive anchor ice sample collected 28 January 1991.	90
Figure 3.15. (a) Average daily drift velocities for floating anchor ice at Gillson Beach. (b) Average wind velocities during periods when anchor ice was present.	92
Figure 4.1. Photograph from the outer edge of the NIC at Kohler Andrae State Park on 17 February 1990 showing the slush ice zone.....	112
Figure 4.2. (a) Sketch of nearshore zone at Kohler-Andre State Park on 17 February 1990. (b) Vertical sediment concentration profiles in the water column and slush ice at Kohler-Andre State Park on 17 February 1990.	113
Figure 4.3. Aerial view of Gillson Beach during ice-free conditions.	119
Figure 4.4. Vector plot of individual ice drift measurements.....	122
Figure 4.5. 1991 drifter returns.....	128
Figure 4.6. 1992 drifter returns.....	130
Figure 5.1. Sediment concentrations found in different types of ice at Gillson Beach in 1989 and 1991	138
Figure 5.2. A box plot of sample type versus mean phi size for ice and bottom samples collected at Gillson Beach in 1989 and 1991.....	140
Figure 5.3. A conceptual model of sediment entrainment pathways into Great Lakes ice (open arrows).	141

LIST OF TABLES

<i>Number.</i>	<i>Page</i>
Table 1.1. Hindcast wave statistics for the Illinois shoreline of Lake Michigan	8
Table 2.2. Dates of nearshore and NIC surveys at Gillson Beach.....	25
Table 2.3. Change in volume of Gillson Beach bathymetric profiles during the 1991 winter.....	36
Table 2.4. NIC ice volumes along survey lines at Gillson Beach during winter 1991....	40
Table 2.5. Total ice volume and sediment load in the Main Line NIC during the 1991 winter season.....	40
Table 2.6. Sediment concentration and grain size statistics for Gillson Beach NIC.....	43
Table 3.1. Anchor ice observation sites in southern Lake Michigan.	60
Table 3.2. Sediment concentration and grain size characteristics of southern Lake Michigan anchor ice samples collected from the lake bottom.....	72
Table 3.3. Sediment concentration and grain size in floating anchor ice samples and sediment concentration in lake water.	74
Table 3.4. Wave characteristics during periods of anchor ice formation	78
Table 3.5. A continuum of anchor ice types.	82
Table 4.1. Sediment concentrations in Gillson Beach slush ice samples.	116
Table 4.2. Mean video ice drift rate measurements at Gillson Beach in January 1991...	121
Table 4.3. Calculated longshore and cross shore ice rafted sediment transport.....	126
Table 4.4. February 1992 drifter release locations in southern Lake Michigan.	129
Table 4.5. 1991 drifter recoveries in southern Lake Michigan.....	131
Table 4.6. 1992 drifter recoveries in southern Lake Michigan.....	132

ACKNOWLEDGMENTS

Thanks to my committee members: Dick Sternberg, Seelye Martin, Arthur Nowell and Charlie Raymond for the guidance and encouragement they gave me during this project. Dick has been as good an advisor as anyone could ever hope to have. Thanks. Dick and Seelye deserve extra kudos for the difficult task of editing early drafts of this document. The copy here is much better because of their diligent work.

I have had three mentors through the years: Erk Reimnitz and Peter Barnes of the U.S.G.S. and, of course, Dick. All have been stimulating teachers through both thought and action, and have encouraged and supported me in my efforts to be a better scientist. Thank you.

A large crew from the U.S. Geological Survey helped collect the data for this project. My thanks to all of them for their cheerful hard work in cold, often miserable conditions. John Haines is the only person who stayed for the entire 1991 field season at Gillson Beach, and deserves acknowledgment for that alone.

Mike Chrzastowski of the Illinois State Geologic Survey has been an outstanding resource and friend throughout this entire ordeal. His encyclopedic knowledge of southern Lake Michigan and willingness to share ideas and information have been a great help. Oh, yeah, he was out in an 8' inflatable boat collecting bathymetry on many raw January days too. Rob Holman collected the video data discussed in Chapter 5. He kindly gave me the data and provided lab space and technical support so I could analyze it. Tim Kana and Nick Kraus loaned me equipment and offered advice on the best way to use it. Thanks.

There is a group of graduate students who have been good friends and colleagues through the years. I thank them for shared beers, long conversations, help with problems, insights into a larger world, and moral support. Thank you Gail Kineke, Chris Sherwood, Andrea Ogston, Craig Lee, Joanna Muench, Brian Bergamaschi, Ann Russell, Laura Landrum and Karl Newyear.

Linda Hutchison deserves the greatest thanks of all. Her support, confidence, and patience made this possible.

I gratefully acknowledge the financial support of the U.S.G.S. through cooperative agreement #14-08-001-A0600.

CHAPTER 1. INTRODUCTION

1.1 INTRODUCTION

High water levels in Lake Michigan between 1985 and 1987 resulted in extensive coastal erosion and damage to the Illinois shoreline. As a result of this damage, the United States Geological Survey and the Illinois State Geological Survey entered into a cooperative study to "... evaluate causes, effects, and the potential frequency and magnitude of future coastal erosion and lake level changes ..." (Folger *et al.* 1994b). This five year study divided into three parts: framework, lake level, and processes. The framework portion focused on the geologic structure, stratigraphy, and surficial sediment distribution in southern Lake Michigan. The lake level studies provided new information on the frequency and magnitude of prehistoric lake level fluctuations and process studies evaluated mechanisms that effect coastal erosion and nearshore change.

A special section in the *Journal of Great Lakes Research* (1994a) contains fifteen papers that report on the results of the study. The study was broad-based; a number of topics relevant to Lake Michigan coastal erosion are discussed. Topics include the large-scale geologic framework of southern Lake Michigan including littoral cells and sand deposits along the Illinois and Indiana shorelines. Three papers dealing with lake level discuss the lake level and climate history of the lake for the last 12,000 years. Processes papers deal with rates and processes of bluff erosion, wave climate and nearshore response, eolian sand transport along the southern margin of the lake, the influence of ice on coastal erosion and the development of a sediment budget for southern Lake Michigan.

This dissertation grew out of my participation in the southern Lake Michigan coastal erosion study. The dissertation focuses on the effects of ice on the nearshore zone and on how ice affects sediment transport along the southwestern shoreline of Lake Michigan. This chapter provides a general background of southern Lake Michigan, briefly describes the types of ice seen in the lake, discusses the wave climate and sediment distribution at the beach where most of the observations were made for this study, and outlines the study objectives.

1.2 BACKGROUND

1.2.1 TYPES OF LAKE ICE

Lake Michigan is a large, deep, mid-latitude lake. It is 500 km long by 190 km wide with an area of 57,000 km² and a maximum depth of 280 m. Because of its size and depth, average surface water temperatures in the middle of Lake Michigan are about 2°C throughout the winter (Figure 1.1) (Lesht and Brandner 1992; Saulesleja 1986) and the lake is rarely, if ever, completely ice covered. A partial ice cover does develop from north to south (Assel *et al.* 1983) and from the shoreline to deeper parts of the lake (Saulesleja 1986). Ice is present along the southern coastline of Lake Michigan for 2 to 4 months each year (Assel *et al.* 1983) during the period when storm-induced wave energy is high (Angel 1995; Saulesleja 1986). This coastal ice can vary in width from a few meters to 24 kilometers (Reimnitz *et al.* 1991) and changes nearshore hydrodynamics and sediment transport in ways that are poorly understood.

A number of classification schemes can be used to describe lacustrine ice types. In the broadest sense ice can be divided into two categories based on its method of formation (Foulds and Wigle 1977): (1) static ice forms on the surface of small lakes and ponds and (2) dynamic ice forms in running water or on the surface of large bodies of water agitated by wind. Static ice is relatively unimportant as a contributor to coastal erosion and sediment transport because it forms in calm conditions from the water surface downward and interacts minimally with lake sediments. Its effects on coastal erosion are not considered in this report. Because the surface of Lake Michigan does not freeze during the winter large areas of open water are agitated by winter storms resulting in predominately dynamic ice formation.

For the purposes of this study dynamic ice can be divided into three broad, interdependent sub-categories: (1) the nearshore ice complex, (2) anchor ice and (3) slush ice. These different ice types are defined briefly here; the effects of each of these ice types on nearshore dynamics and sediment transport are considered separately in Chapters 2, 3, and 4. In Chapter 5 I discuss how these different ice types interact and the net effect of nearshore ice formation on sediment transport in southern Lake Michigan.

The Nearshore Ice Complex (NIC) is the most visible component of the Great Lakes ice system. The NIC consists of a zone of relatively stable (order days to months), solidly frozen ice extending from the shoreline out into deeper water. Starting from the shoreline the NIC consists of a sediment rich icefoot and a lakeward sequence of

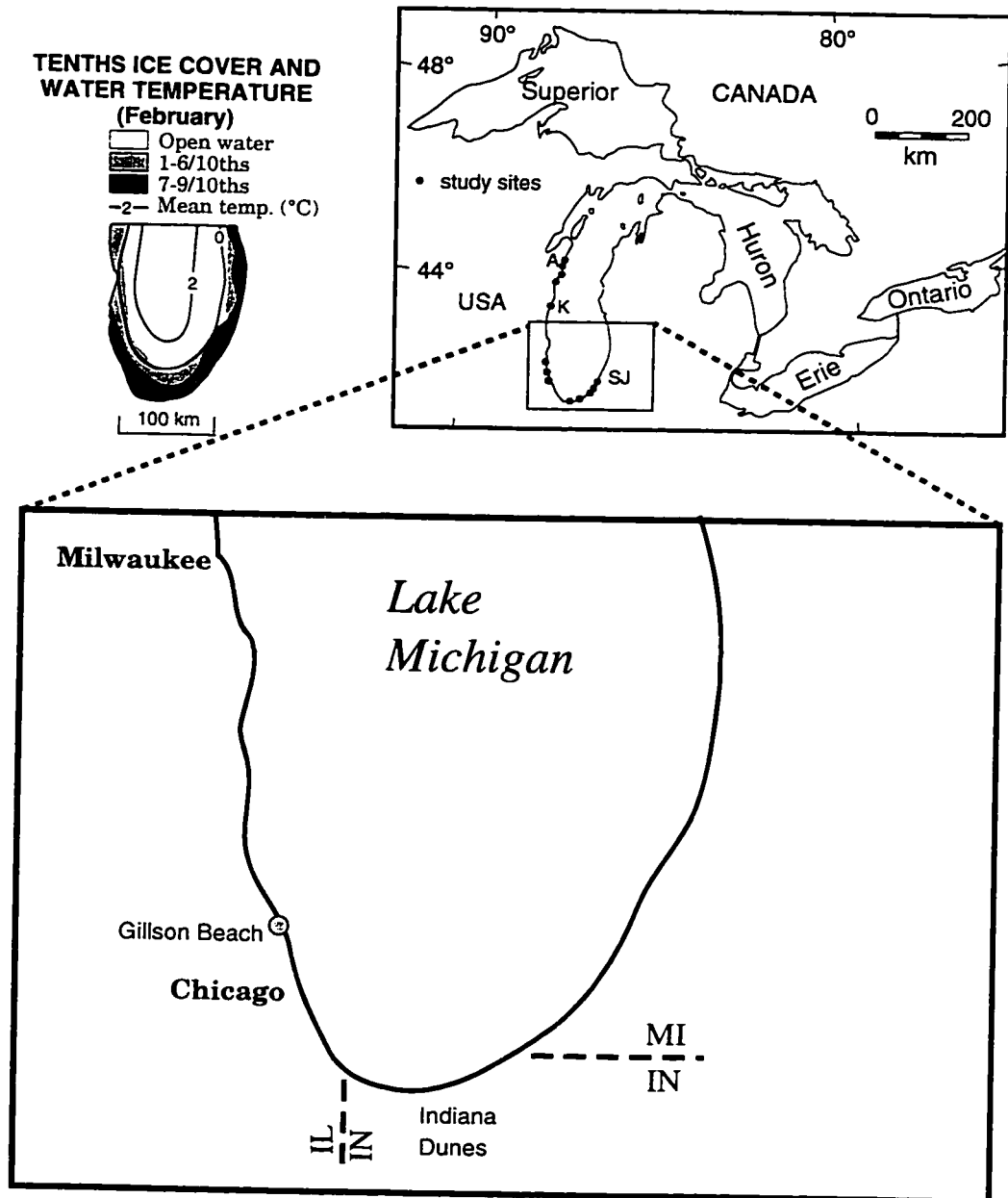


Figure 1.1. Map of study area, modified from Barnes *et al.* (1991). Upper left: typical February ice cover and water temperatures. Upper right: locations (dots) where regional nearshore ice observations were made between Algoma, Wisconsin (A) and St. Joseph, Michigan (SJ). Detailed anchor ice and slush ice observations were made at Kohler-Andrae State Park, Wisconsin during February 1990. Lower panel: location of Gillson Beach, where daily ice observations were made during January 1991.

low-relief, shore parallel ice lagoons separated by a series of ice ridges or ice volcanoes that may be up to 7 m above lake level (Figure 1.2). The ice lagoons form in low energy conditions; ice ridges and volcanoes form in high energy conditions, often on offshore bars or at the breakpoint.

Anchor ice is defined as ice attached or anchored to the bottom, regardless of the nature of its formation (Kivisild 1970). Anchor ice forms in turbulent, supercooled water. The first ice to form in turbulent conditions is frazil ice (millimeter-sized ice disks suspended in the water column) (Arden and Wigle 1972; Tsang 1982). In supercooled water frazil crystals are “active” (Carstens 1966) or sticky and readily adhere to each other or to materials on the bottom or suspended in the flow. When frazil adheres to the bottom, it becomes, by definition, anchor ice. Although the first frazil crystals that adhere to the bottom are small, the resulting anchor ice masses can grow to cover large portions of the bed (Tsang 1982).

Slush ice is a floating layer of mobile, unconsolidated or poorly consolidated ice crystals. Slush ice consists of a mixture of floating frazil ice, anchor ice, brash ice, and snow. This slush ice is often present in a zone (here called the slush ice zone) just lakeward of the NIC. Brash ice is an important component of the slush ice zone. Brash ice is solidly frozen ice fragments less than 2 m in diameter. In southern Lake Michigan most brash ice is formed by wave erosion of the NIC. The ice in the slush ice zone is mobile so the extent of the slush ice zone tends to be highly variable in time and space. The variability in the slush ice zone is driven by changes in wind direction and intensity and by changes in incident wave direction. Often, a band of slush ice will be advected onshore from over the horizon in a matter of hours after the wind changes to onshore. Conversely, the change to an offshore wind can advect coastal slush ice offshore in a short time.

Although the NIC, anchor ice and slush ice can all be considered independently, they are interdependent. For example, slush ice must be present in order for the NIC to form (Bryan and Marcus 1972). Conversely, destruction of the NIC releases brash ice to the slush ice zone and release of anchor ice from the lake bed incorporates sediment-rich ice into the slush ice zone.

1.2.2 THE STUDY AREA

Regional studies of ice effects on nearshore processes and sedimentation were made at selected sites along the Lake Michigan shoreline between Algoma, Wisconsin and

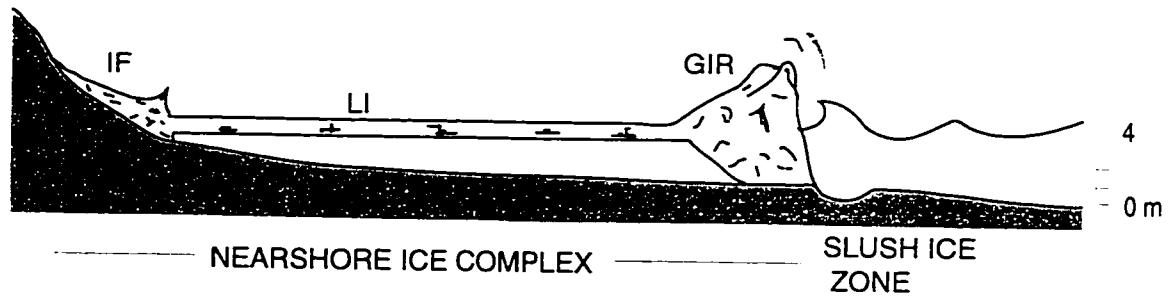


Figure 1.2. Cross section of the nearshore zone showing the morphologic features of the NIC and the mobile slush ice zone. IF: Ice foot; LI: Lagoonal Ice; GIR: Grounded Ice Ridge. Modified from Nielsen (1988), 5X vertical exaggeration.

St. Joseph, Michigan (Figure 1.1). Field work was carried out during 8-17 February 1989, 7 to 13 December 1989, February 2 to 20, 1990, 12 December 1990 to 2 February 1991, and 13 to 16 March 1991. Some results of this field work have been reported in papers by Reimnitz *et al.* (1991), Kempema and Reimnitz (1991), Barnes *et al.* (1992), Barnes *et al.* (1994) and Kempema and Holman (1994). Although some of these regional data are also used in this report, the major source of information in this report is a set of detailed observations made at Gillson Beach, Wilmette, Illinois between 1 January and 2 February 1991 (Figure 1.1).

Lake Michigan occupies an erosional trough cut into Devonian and Mississippian shale, siltstone and dolomite (Hough 1958). At depths greater than 30 m lacustrine and glacio-lacustrine silts and clays blanket the bottom (Lineback *et al.* 1972; Wickham *et al.* 1978). Shoaler depths have a veneer of sand and gravel (Chrzastowski 1992). In many places this veneer is absent and glacial till is exposed at the lakebed.

The Holocene evolution of Lake Michigan has been marked by multiple transgressions and regressions. At present, the lake level is about 177 m above mean sea level. In the past 14,500 years lake level has varied as much as 18 m above to 61 m below the present level (Hansel *et al.* 1985). For the past 4,500 years lake level has been near its present position (Chrzastowski and Thompson 1992). Along the Illinois-Indiana shoreline of Lake Michigan there is a lacustrine plain that is primarily a wave-scoured ground moraine. Prominent depositional features on this plain include relict sand spits, beaches, and beach ridge/dune complexes (Chrzastowski and Thompson 1992). Because streams contribute almost no sand to southwestern Lake Michigan wave erosion of coastal bluffs is the main source of beach sediment (Shabica and Pranschke 1994).

Since the lake has reached its present level, there has been net littoral transport to the south along both the east and west shores of Lake Michigan (Chrzastowski and Thompson 1992). Historically, these sediment transport pathways converged at a sediment sink at Indiana Dunes at the southern end of the lake (Figure 1.1). Most of the transported sediment is medium sand or finer and is susceptible to eolian transport. Loss of beach sediment to dunes at the southern end of the lake explains why there are no progradational features at the convergence zone (Chrzastowski 1990b).

In 1834 the first shore protection feature, the Chicago North Pier, was constructed along the Illinois shoreline (Chrzastowski 1990a). Based on an analysis of sediment accumulation against this and subsequent shore-protection structures, Chrzastowski

(1990b) estimates that the pre-development littoral drift along the Illinois shoreline was $78,000 \text{ m}^3 \text{ year}^{-1}$. Since the North Pier was completed, the entire Illinois shoreline has become either partially or entirely armored (Chrastowski 1990a; Chrastowski 1990b; Chrastowski *et al.* 1994; Shabica and Pranschke 1994). At present, there is “negligible” littoral transport along the Chicago shoreline (Chrastowski 1991).

Chrastowski (1990a) estimates that the southern shore of Lake Michigan (Indiana Dunes) may have been deprived of up to $12.2 \times 10^6 \text{ m}^3$ of sediment because of development along the Chicago shoreline. Not all of this sediment is trapped in the nearshore: some has never eroded from protected bluffs, some is in sand fillets associated with shore protection features, and some may have been deflected offshore. In fact, south of Waukegan Harbor the Illinois shoreline of Lake Michigan is sediment starved and in many places glacial clays are exposed in the nearshore zone. (Shabica and Pranschke 1994). Shabica and Pranschke's (1994) comparison of their 1989 to 1991 surveys with surveys done in the mid-1970's reveals that there has been a net loss of sand from beaches, nearshore bars, and nearshore sand aprons along the Illinois shoreline between the survey dates.

1.2.2.1 Wave Climate

Fox and Davis (Fox and Davis 1976) note that Lake Michigan sits across the major North Pacific storm path. Storms that make an initial landfall in the Pacific Northwest sweep across the lake as they travel across the continent. There is a predictable shift in wind direction and angle of wave approach as storms pass from west to east across the lake. The long dimension of Lake Michigan is oriented north/south so the southeastern shore of the lake has the greatest fetch to the north-northeast (Department of the Army 1971). The Great Lakes do not completely freeze during the winter and winter is the time of the strongest storms and largest wave energy in this region (Evenson and Cohn 1979; Hubertz *et al.* 1991). In an analysis of storm damage along Great Lakes shorelines Angel (1995) found that damage reports were more common during periods of high water. In addition, damage reports increase to a maximum in November, although storms are more frequent during the winter. There is a secondary peak in damage reports in April. Angel attributes the reduction of damage in the winter to formation of a nearshore ice cover.

Hubertz *et al.* (1991) have published wave hindcast data for Lake Michigan based on a 32 year history of regional winds. Their Station 4 (the station located closest to Gillson Beach) data is used to characterize the winter wave climate in the study area.

Table 1.1. Hindcast wave statistics for the Illinois shoreline of Lake Michigan

Wave Height (m)	Wave Period Range (s)	Median Wave Period (s)	Percent Occurrence
<1	0-7	3-3.9	85
1-1.5	4-9	4-4.9	10
1.5-2	4-9	6-6.9	3
2-2.5	5-9	6-6.9	1
2.5-3	6-9	7-7.9	0.5
>3	7-11	8-8.9	0.5

Table 1.1 summarizes the hindcast wave statistics. This table includes calculated significant wave height (H_s) bins, the range of wave periods and the median wave periods associated with each wave height bin, and the percentage of time that wave heights are in a given range. These data show that the majority of waves are less than 1 m high and have a median wave period in the 3 to 3.9 second range. Waves with H_s greater than 2 m are present for 2 percent of time, and the highest mean wave heights occur during the winter months (Hubertz *et al.* 1991). Booth (1994) shows that 72% of waves between 2 and 3 m and 90% of waves larger than 3 m arrive at the Illinois shore from the north to northeast, the direction of greatest fetch. The largest hindcast wave, with H_s of 6.4 m and a period of 10 s, was hindcast for a storm on 25 December 1979.

In addition to providing wave statistics, Hubertz *et al.* (1991) calculate extreme significant wave heights for recurrence intervals of 2, 5, 10, 20 and 50 years. These calculations show that the extreme wave height calculated for a 2 year return period is 5.0 m. Analysis of their data on largest hindcast H_s by month and year shows that 30 of the 32 winters had at least one event that produced waves with H_s of 3 m or more. These statistics show that the lake is a very energetic environment during winter.

1.2.2.2 Gillson Beach

The most detailed observations for this study were made at Gillson Beach (Figure 1.1), a park belonging to the city of Wilmette, so the beach is described in some detail here. Gillson Beach formed following the 1910 construction of Wilmette Harbor. The subaerial beach consists of sand trapped against the updrift (north) side of jetties that

were built to stabilize the harbor mouth (anon 1987) and 10,000 cubic yards of dredge materials from harbor construction. This subaral beach extends to near the outer edge of the jetties, a distance of 410 m lakeward from the original shoreline (Shabica and Pranschke 1994). Since 1937 Gillson Beach has existed essentially in its present form; the shoreline has only changed since then in responses to changes in water level (anon 1987).

Gillson Beach is directly updrift of a secondary littoral drift cell boundary located at Wilmette Harbor (Chrzastowski *et al.* 1994). On average, $9 \times 10^3 \text{ m}^3$ of sand is dredged from Wilmette Harbor each year (Chrzastowski and Trask 1995). This can be considered as the approximate volume of littoral drift through the study area from north to south each year. The source of the sand dredged from the harbor mouth is primarily updrift erosion of nearshore sand (Chrzastowski and Trask 1995). Shabica and Pranschke (1994) surveyed the volume of beach and nearshore sands along the Illinois coast. In 1990 at Gillson Beach they found 899 m^3 of sand per meter of beach width. The sand fillet had a maximum thickness of 3.3 m and extended out to approximately 400 m from the shoreline. A similar survey by the Illinois Geologic Survey in 1975 found 1158 m^3 sand m^{-1} of beach. The 1975 fillet had the same maximum thickness as the 1990 fillet, but extended to 600 m offshore. The reduction in sand at Gillson Beach (and the rest of the Illinois shoreline) is attributed to shore armoring which has cut off sand from coastal bluff erosion which historically nourished the beaches (Shabica and Pranschke 1994).

The littoral cell containing Gillson Beach extends 23.6 km updrift from Wilmette Harbor to Forest Park Beach (Chrzastowski *et al.* 1994). Presently, glacial till is exposed in the nearshore zone in the northern, updrift portion of the cell. As nearshore sand erosion and southerly sand transport continue, till exposures will extend southward, possibly reaching Wilmette at some future date (Chrzastowski and Trask 1995).

There is a major shoreline inflection point of 26° centered on the northern side of the entrance of Wilmette Harbor (Chrzastowski *et al.* 1994). At Gillson Beach the coastline is oriented 302° True; south of the harbor entrance the beach is oriented 328° True. Although the position of the inflection point today is controlled by the position of the harbor mouth there has always been an inflection point in this area. Before coastal development there was a natural inflection point located about 700 m south of the present harbor mouth (Chrzastowski *et al.* 1994). North of Gillson Beach the shoreline gradually shifts back to the north.

The majority of the observations for this study were made at the Gillson Beach swimming beach, located 450 m northwest of the Wilmette Harbor mouth. As part of the study, I wanted to determine if the presence of a NIC changed the beach profile, so seven survey lines were established across the swimming beach. A complete description of data collection methods and digital copies of the survey data can be found in McCormick *et al.* (1990; 1991). The seven shore normal survey lines were established between three light poles on the beach (Figure 1.3). The lines are spaced 30 m apart and are oriented at 32° True. The line that passes through the central light pole is designated the Main Line (ML), with lines North 2 to North 6 (N2-N6) increasing to the northwest and lines South 2 to South 6 (S2-S6) increasing to the southeast. A line perpendicular to the survey lines and running through the light poles marks the baseline of the beach survey area (the zero x-axis). The x values are positive offshore. The Main Line is the zero y-axis, with values increasing to the southeast. Thus the center light pole on the swimming beach has the coordinates (0,0). To establish vertical control the elevation of the base of this light pole relative to the 1955 Low Water Datum (LWD55) was established by surveying back to benchmarks on the Wilmette Harbor jetties. The zero-z value in the surveys corresponds to LWD55, which has an absolute elevation of 175.81 m.

Figure 1.4a shows 250 m of a Main Line transect along with the positions of ten bottom sediment samples. The line begins at a snow fence located 20 m lakeward of the baseline. Samples 1 and 2 are on the beach face. Sample 3 is the top of a small berm that corresponds to the upper limit of the swash zone at the time the samples were taken. Sample 5 is at the base of the swash zone (called the plunge point following local usage, see Fraser *et al.* (1991)), and samples 6-10 are in the nearshore zone.

The ten sediment samples were sieved at 0.5 ϕ intervals ($\phi = -\log_2$ (grain diameter in mm)) and analyzed by the method of moments described by Krumbein and Pettijohn (1938). The grain size distribution across Gillson Beach is similar to distributions described for other Lake Michigan beaches (Fox *et al.* 1966; Fraser *et al.* 1991). The coarsest, most poorly sorted sand along the profile is found at the plunge point (Figure 1b & 1c). Lakeward of the plunge point grain size decreases offshore except in the longshore trough. The coarse sediment size seen in the trough is unusual when compared to reports from other Lake Michigan Beaches (Fox *et al.* 1966, Fraser *et al.* 1991). To the north of the main line (Figure 1.3) the material exposed in the trough increases in size to boulders up to 25 cm in diameter. This coarse material outcropped in a zone about 10 m wide in the longshore trough. This coarse material was exposed during a period of

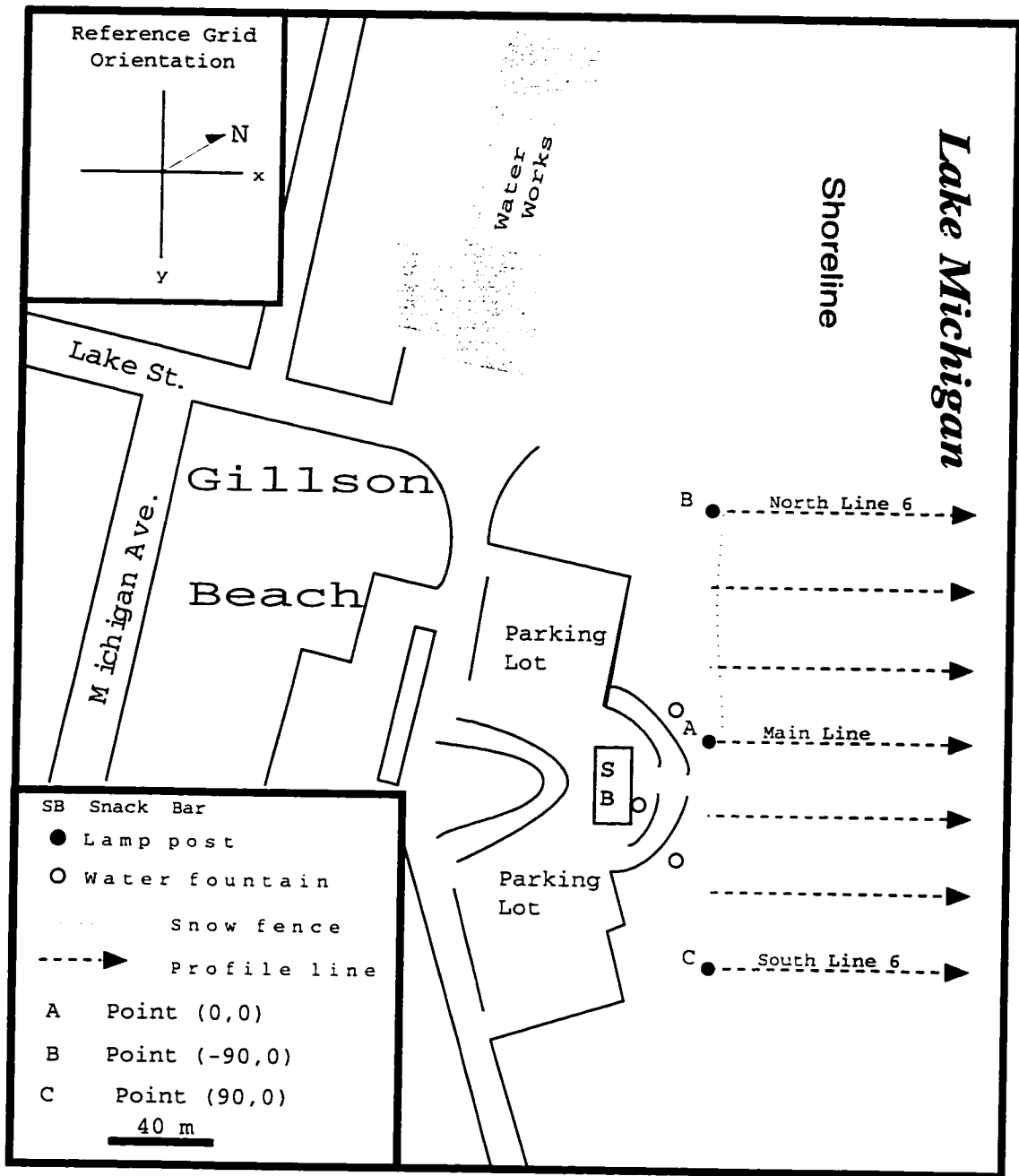


Figure 1.3. Map of Gillson Beach study area showing the location of survey lines and the reference grid orientation. From McCormick *et al.* 1991.

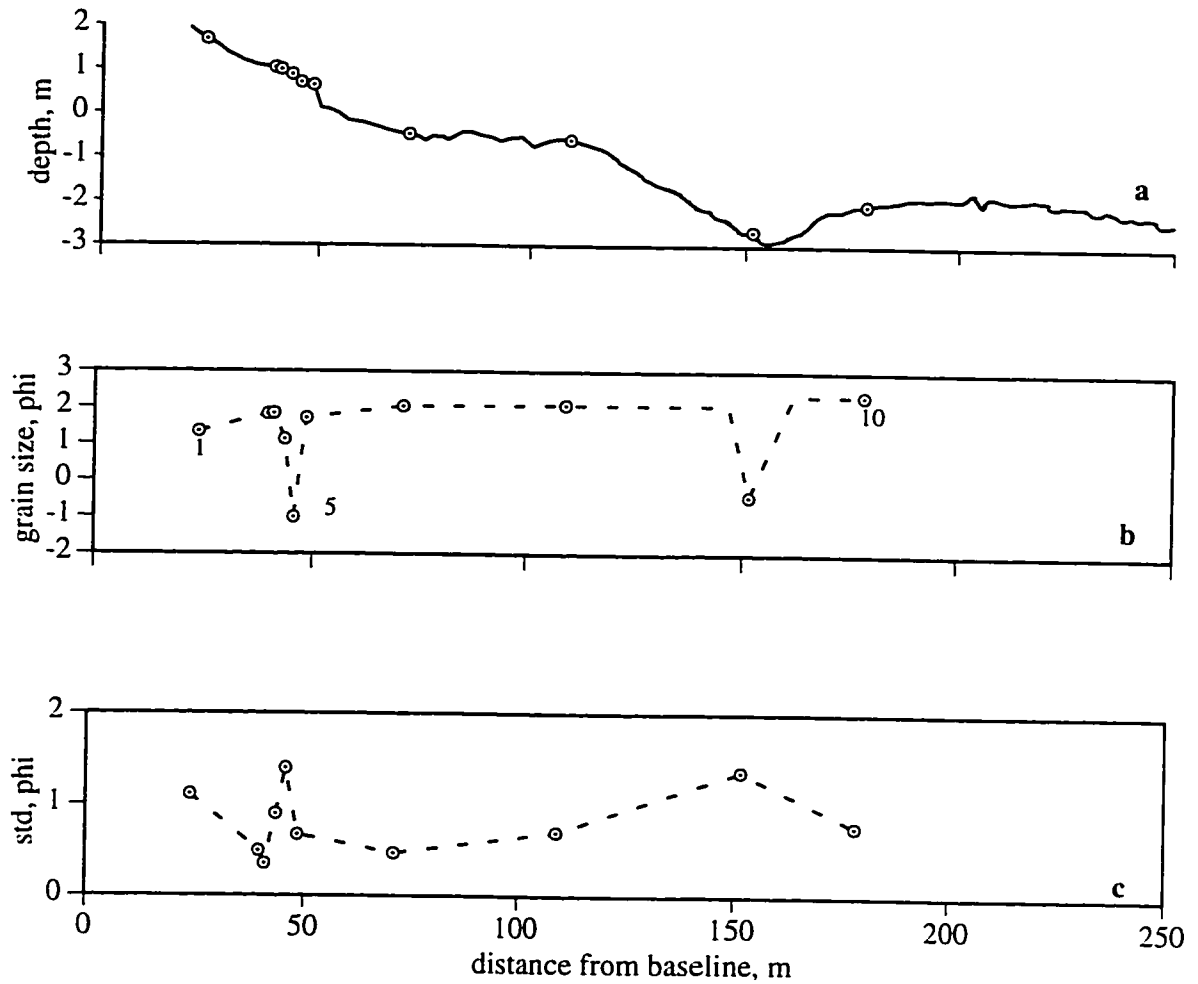


Figure 1.4. (a) Cross section of Gillson Beach Main Line profile on 14 January 1991 showing positions of sediment samples analyzed for size. Samples are numbered from 1 to 10 in a lakeward direction. (b) Mean phi grain size of sediment samples. Sample 5 is from the plunge point; sample 9 from the longshore trough is composed of a relict sand and gravel lag. (c) Phi standard deviation in grain size.

storms in December 1990. I interpret this coarse sediment to be a lag deposit eroded out of the underlying Wadsworth Till during the last Lake Michigan transgression. This lag is exposed when the thin veneer of nearshore sand shifts in response to changing wave conditions. Thus the grain size distribution at Gillson Beach is comparable with other Lake Michigan beaches with the caveat that the beach is sediment starved and the coarse material in the longshore trough is relict. During the winter, the sand most available (Samples 7, 8 and 10) for interaction with ice has a mean grain size ranging from 2.05 to 2.36 ϕ .

1.3 OBJECTIVES

The goal of this study is to determine how the presence of ice affects nearshore sedimentary processes in southern Lake Michigan. Chapter 2 describes the nearshore ice complex and its affect on nearshore bathymetry. In Chapter 3 the conditions for anchor ice formation are presented, and an estimate of the importance of anchor ice for sand transport is discussed. Chapter 4 discusses sediment content and textures in slush ice and sediment transport by slush ice. Finally, in Chapter 5, the interdependent nature of the NIC, anchor ice and slush ice is discussed, and the major findings of this study are summarized.

CHAPTER 2: THE NEARSHORE ICE COMPLEX

2.1 INTRODUCTION

The Nearshore Ice Complex (NIC) is the most visible, distinctive form of coastal ice in southern Lake Michigan. It is a zone of relatively stable, solidly frozen ice attached to the coast. Because of its prominence, the NIC is the most studied type of coastal ice in the Great Lakes. Barnes *et al.* (1992) describe the distinctive NIC morphology and present the terminology used in this dissertation. From the shoreline the NIC consists of an icefoot and a lakeward sequence of ice ridges separated by intervening, shore parallel, low relief ice lagoons (Figures 1.2 and 2.1).

Marsh *et al.* (1976) note that “[The NIC]. . . is an important component of the sediment mass balance of the shore and backshore. It forms a natural seawall along low relief sandy shorelines and is itself a reservoir of sediment.” The concept of the NIC as a seawall and the observation that sediment is incorporated into the NIC are found in most of the literature on Great Lakes NICs. Unfortunately, very few studies document sediment concentrations and grain size distributions found in NIC ice or document bathymetric changes associated with NIC development.

In this chapter, I describe the growth and decay of the NIC at Gillson Beach in southern Lake Michigan (Figure 1.1) through the 1991 winter. The littoral zone was repeatedly surveyed to determine the effect of the NIC on nearshore bathymetry. Sediment samples were collected to determine the amount and type of sediment that is incorporated into the NIC during winter.

2.2 PREVIOUS STUDIES

2.2.1 FORMATION OF THE NEARSHORE ICE COMPLEX

Bryan and Marcus (1972) list four critical criteria for formation of the NIC: (1) freezing air and water temperatures, (2) large bodies of water, (3) onshore wind and storm waves, and (4) a supply of brash and slush ice. These conditions are met repeatedly during the winter months in the Great Lakes, where NICs are common.

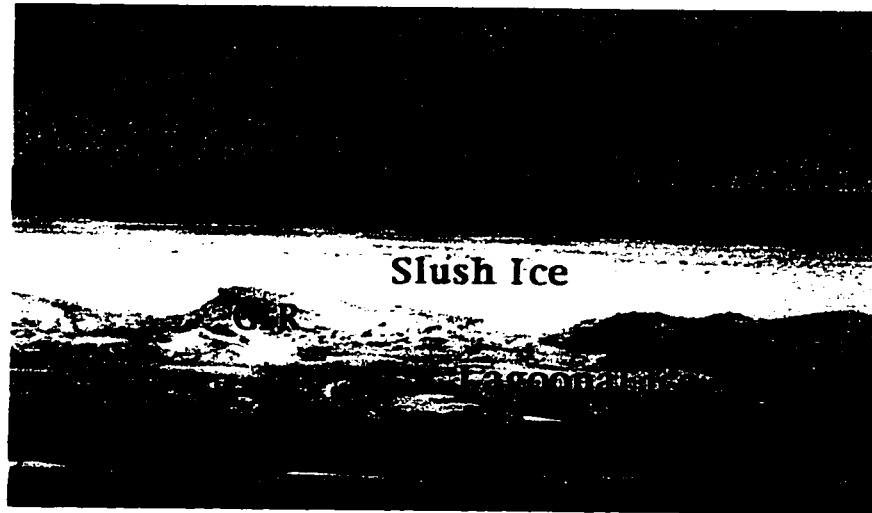


Figure 2.1. Lakeward-looking view of the NIC at Gillson Beach on 29 January 1991. This view shows the subaerial beach, the rough, sediment-laden ice foot, a zone of low-relief lagoonal ice and the grounded ice ridge (GIR) which marks the outer edge of the NIC. Lakeward of the NIC there are discontinuous bands of ice extending to the horizon. View is to the northeast.

NIC formation begins at the shoreline and the NIC grows lakeward with time and favorable conditions (O'Hara and Ayers 1972). A frozen beach face is the first coastal ice feature to form. This ice-bonded beach face may be undercut by waves, resulting in an erosional scarp. Thin slabs of ice-cemented sandstone are dislodged by undercutting, then are distributed along the beach at the shoreline (O'Hara and Ayers 1972, Davis 1973, Nielsen 1988, Dillon and Conover 1965). When lake water reaches the freezing point, slush and brash ice form in the nearshore zone. This uncongealed material is readily driven against the coast by onshore winds and waves. Slush and brash are worked by waves into a stratified icefoot at the shoreline (Figures 1.4 and 2.1). The icefoot usually is several meters wide, and is marked at its outer edge by a vertical scarp a meter or more high (Davis 1973; Evenson and Cohn 1979; Miner 1990; Miner and Powell 1991). Once established, the icefoot locks beach face sediment in place while focusing wave energy at its outer edge. As conditions change, the icefoot can be destroyed and rebuilt several times through a single winter season (Miner 1990, Miner and Powell 1991, Davis 1973).

With freezing conditions and the presence of onshore wind and waves, a thick, wide mass of mobile brash and slush ice will accumulate against the outer edge of the icefoot. As the brash and slush ice band thickens, it effectively dampens incident wave energy (Dozier *et al.* 1976). For a given set of wave conditions, there is a slush ice thickness and width that will absorb all incident wave energy. Once this threshold is passed, the landward portion of the mobile ice band no longer moves. When air temperatures are below freezing, the surface of this stationary ice freezes into a solid mass of repeated, irregularly spaced, low relief undulations that are roughly parallel to the beach. This feature is called an ice lagoon (Figures 1.4 and 2.1) (Barnes *et al.* 1994; Seibel 1986).

Normally, a grounded ice ridge forms at the outer edge of the ice lagoon. Ice ridges form when wave energy is large (Miner and Powell 1991). Wave energy is large at the breakpoint, which is often located near an offshore bar so ice ridges are often grounded on bars (Bajorunas and Duane 1967; Barnes *et al.* 1992; Davis *et al.* 1976; Seibel 1986). However, not all ridges are associated with bars, and ridges do not form on all bars (Marsh *et al.* 1973). Ridges form when waves pile slush ice onto the outer edge of an ice lagoon (Evenson and Cohn 1979; Fahnestock *et al.* 1973; Miner and Powell 1991; O'Hara and Ayers 1972). Ice ridges are grounded, shore-parallel features (Figures 2.1 and 2.2) with near-vertical to overhanging lakeward faces and gentle landward slopes.



Figure 2.2. Two views looking onshore towards the lakeward edge of the NIC at Gillson Beach in January 1991. The vertical scarps of the NIC grounded ice ridge are 3 to 4 m high and ridge is firmly grounded in 1 m of water.

Ridges tend to have a porous, open structure, with porosity ranging from 22 to 57 percent (Miner and Powell 1991). Their submerged parts are less indurated than subaerial portions, except for random blocks of brash (O'Hara and Ayers 1972). Ice ridges commonly rise one to two meters above water level, but ridges with heights to seven meters above water level have been reported (Marsh *et al.* 1973). Several episodes of ridge building may occur throughout the winter, resulting in NICs that consist of several shore-parallel bands of lagoonal ice and ice ridges. These NICs may be up to 300 m wide and terminate in water 4 m deep (Davis *et al.* 1976; Evenson and Cohn 1979; Miner and Powell 1991; Seibel 1986; Seibel *et al.* 1976).

Barnes *et al.* (1994) report that the NIC is ubiquitous in the southern portion of Lake Michigan, although the degree of development varies with location. The most extensive NICs form off exposed sand beaches. Where the shoreline is protected by engineered structures (revetments, seawalls, and timber or sheet pile bulkheads), the NIC is poorly developed or absent.

Although it is relatively stable compared to other types of lake ice, the NIC is still a dynamic feature which changes continuously with changing weather conditions and sea states. The NIC is destroyed by wave action or by *in situ* melting, depending on temperature and wave conditions. Some researchers report that NIC decay occurs in the same order as growth, i.e. outward from the shoreline (Davis 1973; Evenson and Cohn 1979; Marsh *et al.* 1973; O'Hara and Ayers 1972). Other researchers disagree, stating that NIC decay most often occurs by wave-induced erosion at the outer edge (Miner and Powell 1991, Seibel 1986, Dozier *et al.* 1976). Miner (1989) and Miner and Powell (1991) estimate that over 90% of the NIC formed during the 1989 winter at Gillson Beach was destroyed by wave action rather than by melting. All of this eroded NIC ice is introduced into the mobile slush ice zone for transport.

2.2.2 SEDIMENT IN THE NIC

Most papers dealing with Great Lakes NICs note the presence of sediment in the ice. Sediment in the NIC is important for two reasons: (1) The presence of sediment in NIC ice indicates that some scour of the lakebed is occurring just lakeward of the NIC. This topic will be discussed in the next section. (2) Sediment in ice can potentially be ice rafted. If the NIC is destroyed by wave action rather than by melting in place, sediment-laden ice is released into the nearshore zone. With ice supplying the buoyancy to hold the

entrained sediment near the top of the water column, this sediment can be transported alongshore or offshore by prevailing winds and currents, affecting the sediment balance of the beach (Barnes *et al.* 1992; Evenson and Cohn 1979; Marshall 1966; Miner and Powell 1991). This section reviews the published observations of sediment in the NIC.

Many papers note the presence of sediment in the NIC and suggest mechanisms for incorporating sediment into the nearshore ice complex. These papers are important because they document the wide-spread distribution of sediment in NIC ice, but they contain little information about sediment concentrations found in the ice.. Papers that fall into this category include Davis *et al.* (1976) who report that sand is incorporated into NIC ridges along the eastern shore of Lake Michigan. Marshall (1977) looked at the regional distributions of ice in the Great Lakes, and mentions that sand is found in the NIC, but attaches no significance to this observation. Seibel (1986) also reports sand incorporated into NICs in southeastern Lake Michigan. Bajorunas and Duane (1967) and Zumberge and Wilson (1953) also observed sand in Great Lakes' NICs.

A number of papers give more detailed information about sediment in the NIC. O'Hara and Ayers (1972) studied NIC development along both shores of Lake Michigan and along the southeast shore of Lake Ontario. They collected two samples of 'clean' ice that had a sediment concentration of about $3 \text{ cm}^3 \text{ l}^{-1}$ ($\sim 5 \text{ g l}^{-1}$). In their study of NICs in the Grand Marais region of Lake Superior, Marsh *et al.* (1973) report that sediment concentrations are so large in some NIC ice that the ice sinks when it is eroded from the NIC. This indicates a sediment concentration of $>127 \text{ g l}^{-1}$ (section 3.4.2 of this dissertation). In another report on Lake Superior NICs Marsh *et al.* (1976) present a graph of sediment concentration in NIC ice versus distance from the shoreline. This graph has 32 samples plotted, and shows decreasing sediment concentrations with increasing distance from shore. Sediment concentrations range from 3.6% by weight for samples collected near the shoreline to 0-0.6% for samples collected up to 150 m from the shoreline. Fahnestock *et al.* (1973) report that sand, silt, clay, wood fragments and boulders weighing up to 20 kg were incorporated into a Lake Erie NIC near Dunkirk, New York. Bryan and Marcus (1972) studied NIC development at Grand Marais in southeastern Lake Superior. They present sediment grain size distributions for six NIC samples. All six samples were sand with a mode of 2ϕ . Although they do not give any information on sediment concentrations in these ice samples, they state the sediment content was low compared to other Great Lake sites based on visual observations. They

also report that other sites along Lake Superior contain high percentages of pebbles and gravel in the NIC.

The two published reports that contain the most information on NIC sediment are by Barnes *et al.* (1992) and Miner and Powell (1991). Barnes *et al.* studied nearshore ice around southern Lake Michigan. They collected a total of 24 NIC samples during February 1989 and February 1990. These samples had sediment concentrations ranging from 1 to 59 g l⁻¹. The mean sediment concentration for eleven 1989 samples was 21.3 g l⁻¹. The thirteen samples collected in 1990 had a mean sediment concentration of 19.5 g l⁻¹. The sediment in all the samples was predominately sand, although a few samples contained small amounts of silt or gravel. Comparison of sediment in ice with sediment from the adjacent lake shore showed similar grain size distributions, indicating that the sand in the ice was locally derived.

Miner and Powell (1991) report on the results of a long term study of NIC formation at Gillson Beach during the winters of 1987/88 and 1988/89. Through a series of daily to weekly observations, they found that the NIC is a dynamic feature that changes on almost a daily basis. At Gillson Beach they found that reduction in NIC volume results mostly from destruction by large waves as opposed to melting. In 1988/89, the NIC had a total ice volume of 548 m³ m⁻¹ of beach width, with a sediment load of 5.1 x 10³ kg m⁻¹ of beach width (3.8 m³ of sand m⁻¹ of beach). The largest NIC volume observed was 279 m³ of ice per m of beach. Although Miner and Powell document the dynamic nature of the NIC and the amount of sediment incorporated into the NIC, they do not give any information about the type of sediment found in NIC ice. They note that destruction of the NIC releases this sediment into the water column for ice-enhanced transport.

2.2.3 THE EFFECTS OF THE NIC ON NEARSHORE BATHYMETRY

Many NIC studies conclude that grounded ice ridges act as natural seawalls (Bajorunas and Duane 1967; Davis 1973; Davis *et al.* 1976; Evenson and Cohn 1979; Marsh *et al.* 1976; Marsh *et al.* 1973; Sadler and Serson 1981; Seibel 1986; Seibel *et al.* 1976; Zumberge and Wilson 1953). Although this comparison is commonly made, no one has taken the results of seawall research and applied them to grounded ice ridges. In this section I review some aspects of NICs in the Great Lakes and some results of seawall research that might apply to grounded ice ridges.

As NICs grow, the surf zone is displaced progressively lakeward and the beach is protected from erosion. In a study on Lake Ontario, Evanson and Cohn (1973) calculated that more than 60% of all incoming wave energy occurs during the winter months when the beach is protected by grounded ice ridges. They concluded that beach retreat rates are significantly reduced because of the ice. Angel (1995) analyzed storm damage reports for the Great Lakes between 1959 and 1990. He found that damage reports increase to a maximum in November. The number of damage reports decreases in winter and increases to a second maximum in April even though the greatest number of storms occur during the winter. Angel concludes that the nearshore ice cover is important for lessening midwinter storm damage to Great Lakes shorelines. Marsh *et al.* (1973) compared longshore sediment transport rates at Point Barrow Alaska, Lake Superior and typical ice-free mid-latitude coasts. They found that the estimated $1.3 \times 10^5 \text{ m}^3 \text{ year}^{-1}$ littoral transport rate in southern Lake Superior is midway between arctic beaches ($\sim 10^4 \text{ m}^3 \text{ year}^{-1}$) and ice-free beaches ($2\text{-}3 \times 10^5 \text{ m}^3 \text{ year}^{-1}$). Marsh *et al.* conclude that this intermediate transport rate results from an intermediate-length ice season relative to arctic and temperate coasts, because a nearshore ice complex protects the beach from wave-induced erosion. This conclusion must be viewed skeptically because Marsh *et al.* failed to consider differences in factors such as fetch, storm severity, and wave climate when comparing the different coastal regions.

While it is generally acknowledged that NICs protect the beach from erosion, questions remain about the effects of ice ridge/wave interactions in the nearshore zone. As the nearshore ice complex grows lakeward during the winter, the surf zone is progressively shortened, so wave energy is dissipated across a shorter section of lake bottom (Marsh *et al.* 1973). Bajorunas and Duane (1967) state that nearshore ice ridges direct some of the force of impinging waves downward, resulting in lake bottom scour and suspension of bed sediment. Once suspended, sediment can be advected along shore or can be thrown onto the growing NIC by successive waves. Bajorunas and Duane state that scouring at the base of grounded ice ridges results in over-steepening of the bottom. When the ice ridges melt, the bottom is unstable and subject to wave modification. O'Hara and Ayers (1972) report that waves scour sand from beneath ice ridges, leading to the collapse of ridge sections. Seibel *et al.* (1976) state that scouring at the base of ice ridges may destroy offshore bars. This destruction may lead to increased shoreline and bluff erosion in the spring because the bars are no longer there to dissipate wave energy.

Although all of these authors conclude that interactions between ice ridges and waves lead to scour, none of them have conclusively shown that scour depressions form lakeward of ice ridges. Marsh *et al.* (1973) surveyed a beach in Lake Superior and concluded: "Although it is evident that part of the wave energy is concentrated downward at the ice front, profiles reveal negligible net erosion of the bottom in this zone."

Two studies do document scour depressions associated with the NIC. Nielsen (1988) reports on a study conducted in Denmark where a section of beach was surveyed regularly over a two year period. Nielsen found that during the winter when an ice ridge was present there was a net loss of sediment between the 60 and 100 cm contours. Nielsen concluded that this loss resulted from a reflective wave environment caused by grounded ice ridge build up in the nearshore zone. Nielsen surveyed to 1 m depth, so the final disposition of the lost sediment is not known; it could have been deposited offshore. Barnes *et al.* (1992) measured bathymetric profiles lakeward of grounded ice ridges at a number of locations around southern Lake Michigan. They report that a small erosional trough is a persistent feature along the outer edge of ground ice ridges. These troughs were commonly 10 to 15 cm deep, but reached maximum depths of 50 cm and widths of 2-3 m. These troughs were apparently ephemeral features, filling in and reforming as the NIC eroded or expanded.

2.2.4 SEAWALLS AS ANALOGS TO NICs

Seawall research is concerned with both longshore and cross shore changes associated with seawall construction. NICs commonly extend for many kilometers in the longshore direction, so the present discussion deals only with onshore/offshore effects of seawalls. Dean (1986) proposed an approximate principle that for a two-dimensional situation the scour immediately fronting a seawall will be less than or equal to the volume that would have been eroded from the whole nearshore zone if the seawall was not present. This principle has been verified with physical model tests. The net result of a seawall is a flattening of the profile in front of the seawall as sand moves offshore.

In tank studies, Chestnutt and Schiller (1971) found that maximum local scour occurred when a seawall was placed in a "critical region" located between 1/2 and 2/3 of the way across the surf zone from the shoreline. This is a region where grounded ice ridges commonly form; this observation suggests that grounded ice ridges located in the mid-surf zone should result in maximum scour. However, when Chestnutt and Schiller

moved the seawall to a position landward of the "critical region", the scour depression began to fill immediately with wave-transported sediment, suggesting scour depressions associated with NICs should fill once the NIC is gone.

Weggel (1988) states that seawalls located on an active shoreface will modify the nearshore beach profile and the cross-shore distribution of longshore currents and longshore sediment transport. He notes that a reflecting seawall will cause standing waves. Standing waves presumably cause more scour, but the relationship between scour depth and wave conditions is not well understood. Weggel states that the rule of thumb that local scour depth is equal to the height of the highest breaking waves over predicts scour depth at a seawall.

Kraus (1988) published a comprehensive review of seawall literature, and drew a number of conclusions about the effects of seawalls on the nearshore zone. Kraus and McDougal (1996) updated this review with over forty new articles; many of the conclusions from the 1988 review have changed in light of these new studies. For this reason, I will mainly focus on the new findings reviewed by Kraus and McDougal (1996). The most surprising result of the last ten years of seawall study is that scour does not necessarily occur at the foot of seawalls. Also, reflected waves are not a significant contributor to beach profile change or scour in front of seawalls. The final result relevant to grounded ice ridges is that during storms, the beach profile in front of a wall retains the same amount of sand as a beach without a wall. The main difference is that the profile lakeward of the wall is flatter than the adjacent non-walled profile.

McDougal *et al.* (1996) is a companion paper to Kraus and McDougal (1996) that reports on the results of the large-scale SUPERTANK wave tank experiments. In three experiments with seawalls in the surf zone, McDougal *et al.* found that scour depressions did form, but the depressions were much smaller than anticipated. Sand from the scour depressions went into forming a longshore bar at the breakpoint. They determined a relationship between scour depth and breaking wave height:

$$\frac{S_w}{H_b} = 0.51m^{3/4} \left(\frac{h_w}{D_{50}} \right)^{1/3} \quad (2.1)$$

where S_w is the scour depth, H_b is the breaker height, h_w is the still water depth at the seawall, m is beach slope, and D_{50} is the mean grain diameter of local bottom sediment.

McDougal *et al.* point out that scour depth relationships are specific to initial profile conditions so care is needed to apply this relationship to other sites. Numerical modeling shows that larger waves produce deeper scour depressions and displace the bar seaward. The tank and numerical studies show that waves reflected from seawalls do not influence profile change, but more studies are needed to verify this. One effect that reflected waves do have is to cause incident waves to break farther offshore and to be smaller across the surf zone. The SUPERTANK study also showed that scour depth increases rapidly in the first few hours of a storm. Fifty percent of the scour associated with storm waves occurs within the first 2200 waves. For waves with a 10 s period, this corresponds to 6 hours. This short response time implies that scour could readily occur lakeward of grounded ice ridges.

In summary, review of the seawall literature indicates that grounded ice ridges form in the region of the surf zone where they would contribute to the greatest amount of scour but this scour may be rapidly infilled following destruction of the NIC. Seawall research shows that scour depressions can form in short time periods, so scour could readily occur lakeward of ephemeral grounded ice ridges. However, the amount of scour may not be very great (McDougal *et al.* 1996).

2.3 METHODS

Several methods were used to study the winter beach and NIC at Gillson Beach. Nearshore bathymetric profiles and profiles of the upper surface of the NIC at Gillson Beach were made on six different occasions between 14 December 1991 and 16 March 1991 (Table 2.1). The even-numbered lines established by McCormick *et al.* (1990; 1991) are used in this study. These lines are labeled North 6 (N6) to the Main Line (ML, the zero y axis of the survey grid) to South 6 (S6). The spacing between adjacent shore normal survey lines is 30 m, so the seven survey lines span 180 m of beach front (Figure 1.3). Although some survey sets took more than one day to complete (Table 2.1), I use just the first day of the survey to identify the set (e.g. 14 December 1990 refers to bathymetric profiles made between 14 and 18 December 1990). The surveys were made using a leveled, acclimatized electronic distance meter. Vertical errors in the surveys are estimated to be less than ± 5 cm. The complete survey technique, a description of the initial data reduction and digital copies of the survey data can be found in McCormick *et al.* (1991). It was assumed there were no changes to the NIC surface shoreward of the

Table 2.1. Dates of nearshore and NIC surveys at Gillson Beach

Date of Survey	Lake Level (m)	Date and Time of lake level reading
14-18 December 1990	0.36	14 January @ 1608
9-10 January 1991	—	—
13-14 January 1991	0.33 0.39	13 January @ 1300 14 January @ 1310
18 January 1991	-0.05	18 January @ 1130
22 January 1991	0.09	22 January @ 1650
15-16 March 1991	—	—

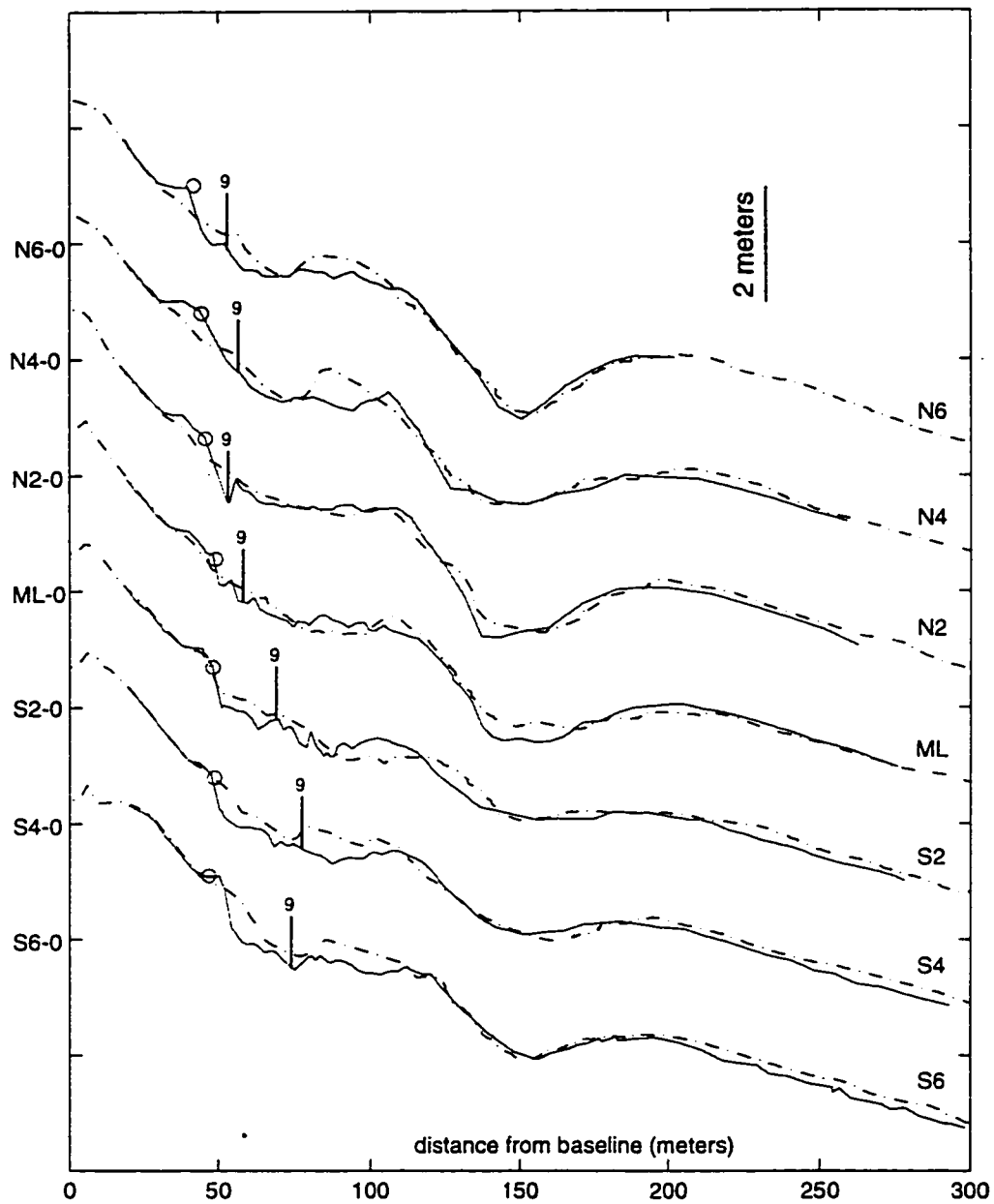
outermost, active grounded ice ridge between surveys or to the bottom below the initial NIC, so surveys after 9 January 1991 were only carried to the point where they intersected the unchanged surface of the NIC.

Changes in sand volume along the seven survey lines between 40 and 300 m from the baseline (Figure 1.3) for the 14 December and 13 January surveys, the 13 January and 15 March surveys, and the 14 December and 15 March surveys were determined using the trapezoid rule assuming a one-meter-wide strip perpendicular to the survey line. The 13 January date was chosen for the comparison because it is the only January data set that extends to 300 m offshore. The 13 January surveys do not extend to the shoreline (Figure 2.3b), so the 9 January inshore survey data were merged with the 13 January data to make complete profiles.

To document changes in shore-normal NIC width between survey dates, the distance from a known point to the outer edge of the Main Line (ML, Figure 1.3) was measured every one to three days during January 1991. Gillson Beach was visited daily during this period, and the NIC width was measured whenever a noticeable change occurred. The beach was not visited between 2 and 7 February 1991. The final winter visit to Gillson Beach occurred on 7 February. At that time, the NIC consisted of a 5-m-wide icefoot. This was the last ice formation of the 1991 winter (Michael Chrzastowski, Illinois State Geological Survey, personal communication).

The total NIC ice volume of an assumed 1-m-wide strip along the ML for the 1991 winter was found by using the trapezoid rule to determine the change in ice volume for each period of NIC erosion and then summing the eroded ice volumes. To find the change in NIC volume, I assume that NIC ice extended to the lake bed, and found the volume between the upper surface of the NIC and the lake bed. Changes in grounded ice ridge, lagoonal ice and icefoot volumes are calculated separately. For periods when there was NIC growth and then erosion between surveying dates (Table 2.1), I assume grounded ice ridges had an elevation of 2 m and lagoonal ice had an elevation of 0.5 m above the survey datum. The lake level was typically around 0.3 m during January 1991 (Table 2.1), so this results in an assumed ridge elevation of ~1.7 m above lake level, and an assumed lagoonal ice freeboard of ~20 cm. To determine variability in the alongshore NIC volume, ice volumes were calculated for all seven survey lines for the days 10, 13, 18 and 22 January by integration of the entire NIC width. The mean, standard deviation and fractional uncertainty (σ/mean) (Taylor 1982) for each day was calculated. The mean

Figure 2.3a-f. Gillson Beach bathymetric profiles between 14 December 1990 and 15 March 1991. The "o's" mark the position of the inner edge of the icefoot (the shoreline) on 9 January 1991. The numbered vertical lines mark the lakeward edge of the NIC for the day in January represented by the number. The values on the vertical axis are the zero points for each survey line (LWD55). For example, N4-0 is the zero datum for Line N4. Survey lines are separated by 30 m horizontally (Figure 1.3); adjacent profile zeros are offset by 2 m in this figure.



a. 14 December 1990: dotted; 9 January 1991: solid

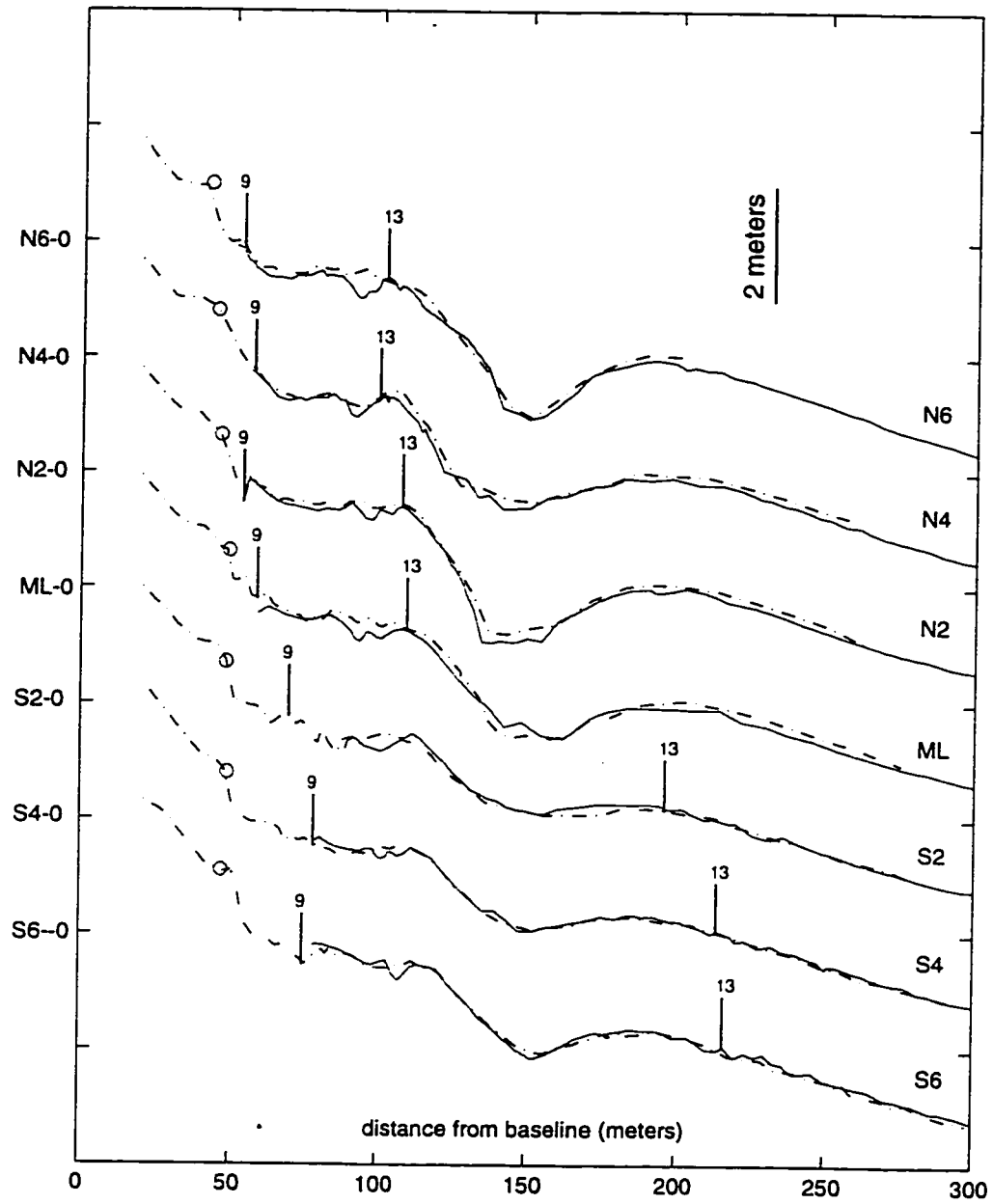


Figure 2.3 (continued) b. 9 January 1991: dotted; 13 January 1991: solid

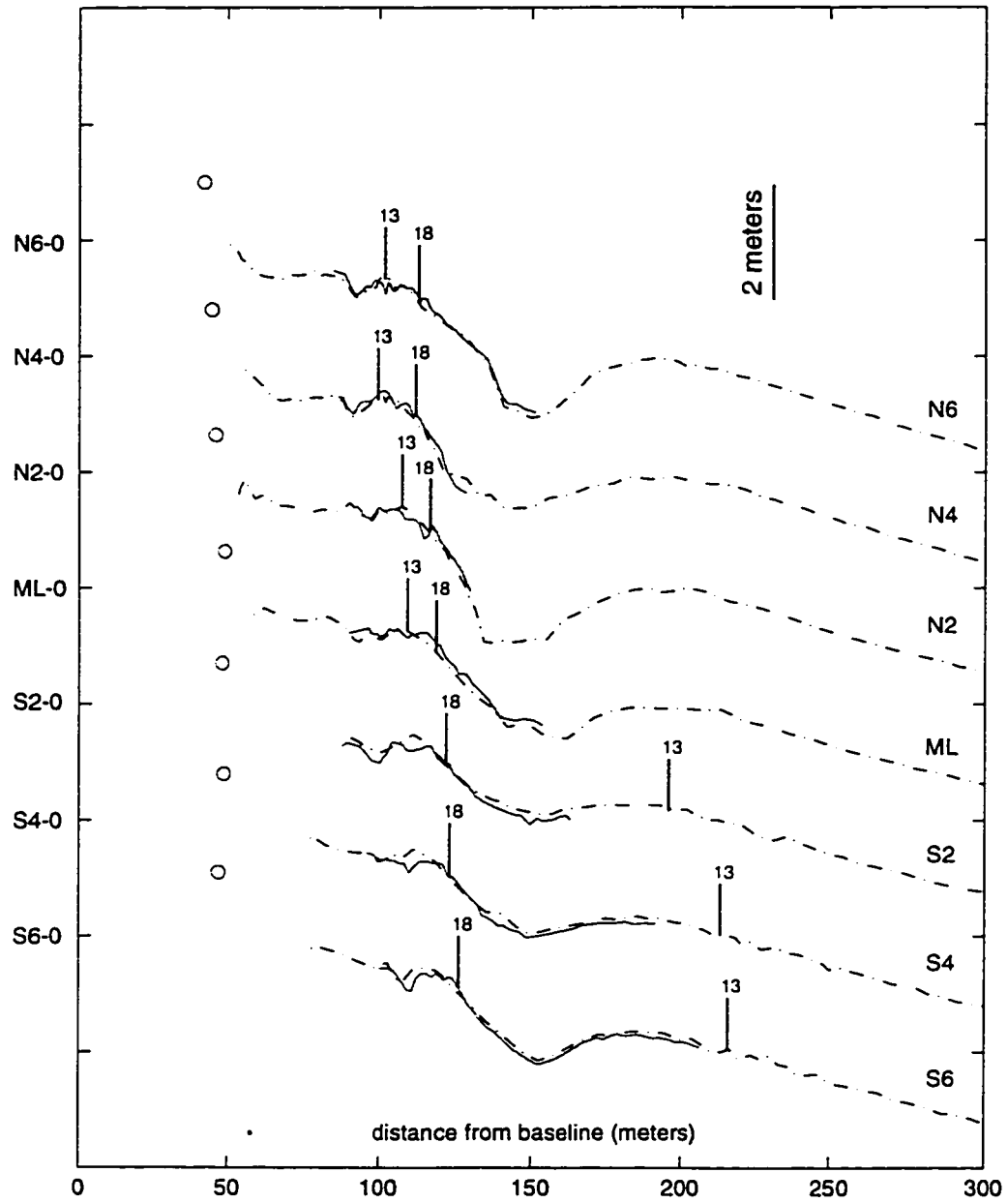


Figure 2.3 (continued) c. 13 January 1991: dotted; 18 January 1991: solid

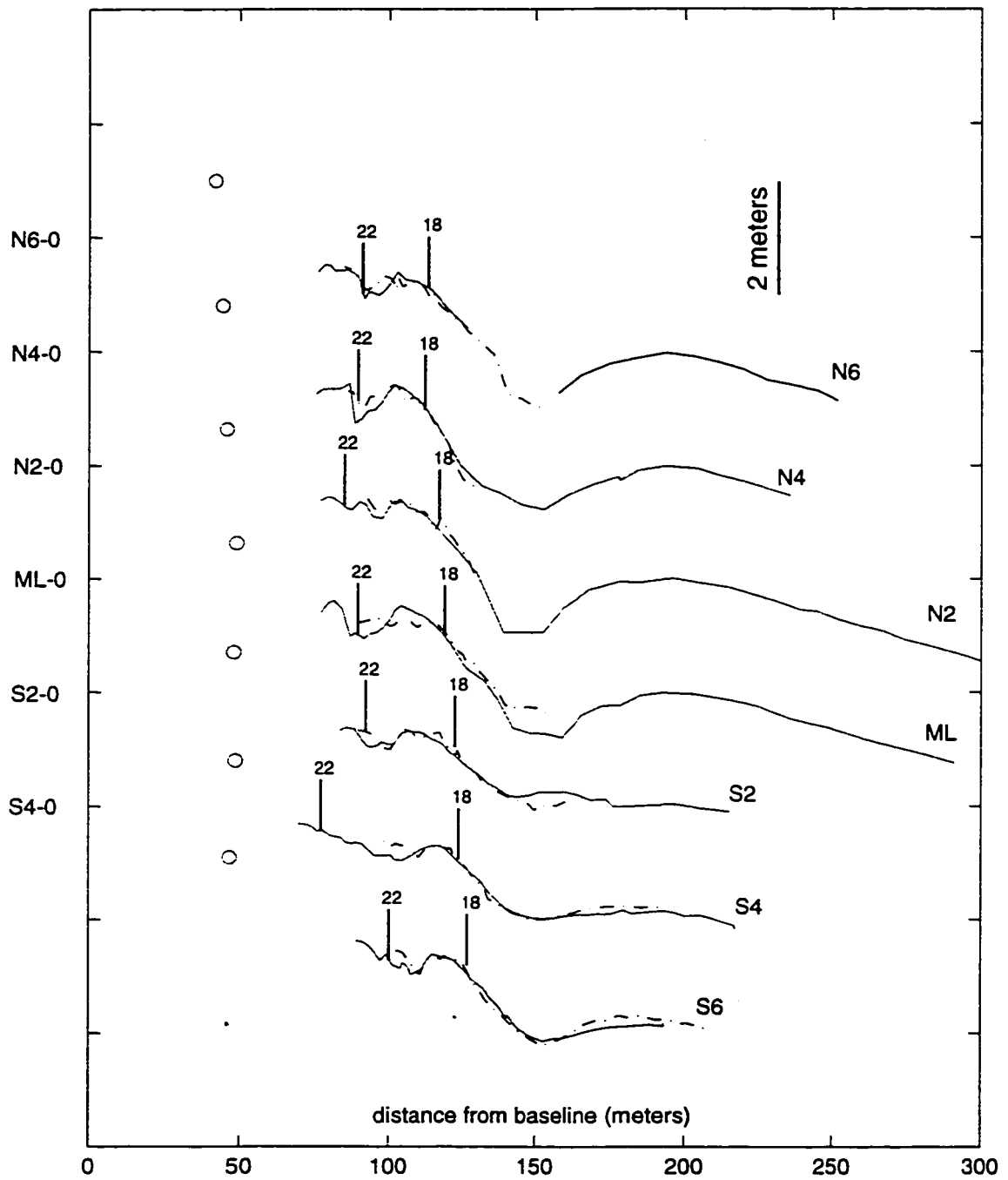


Figure 2.3 (continued) d. 18 January 1991: dotted; 22 January 1991: solid

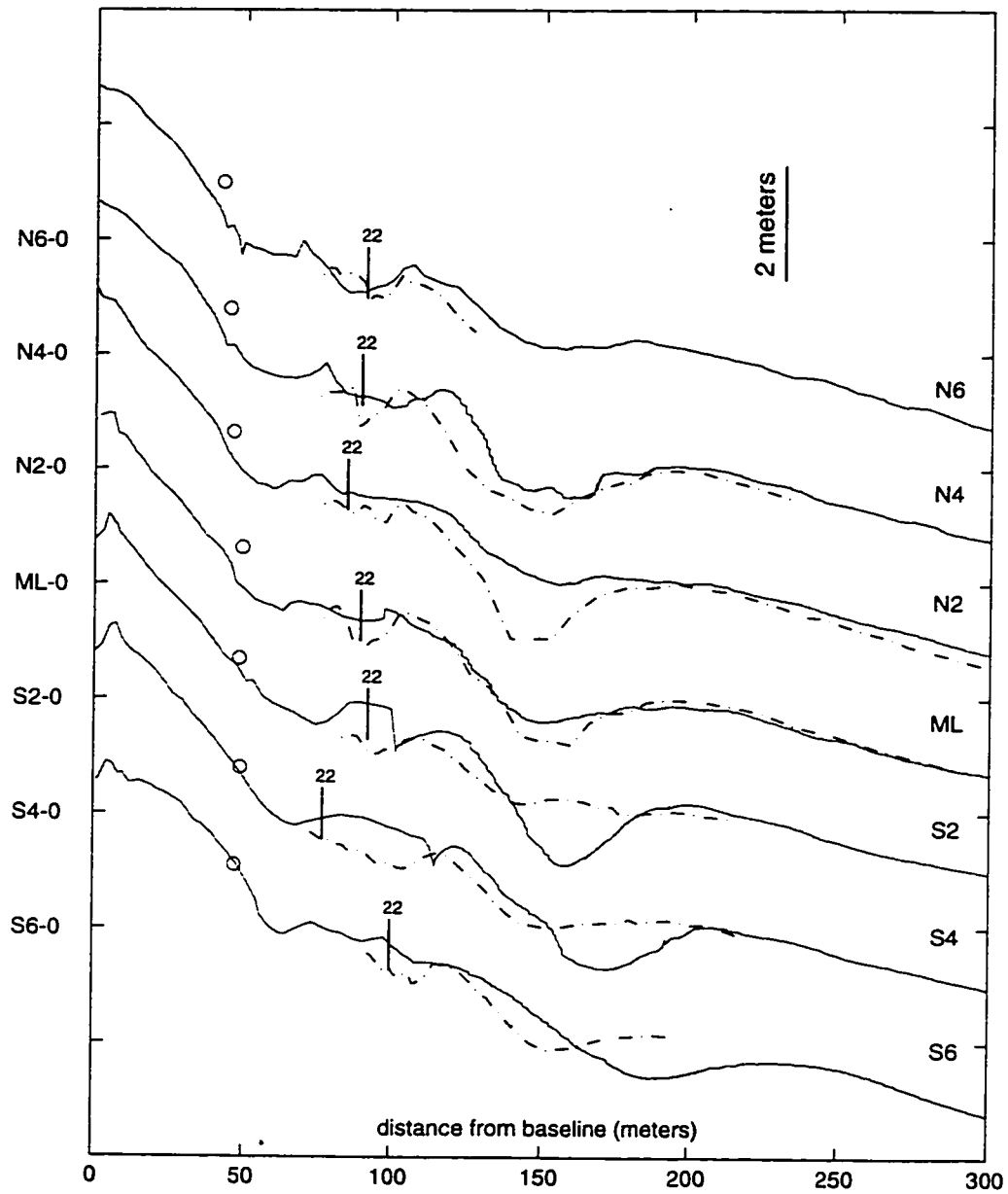


Figure 2.3 (continued) e. 22 January 1991: dotted; 15 March 1991: solid

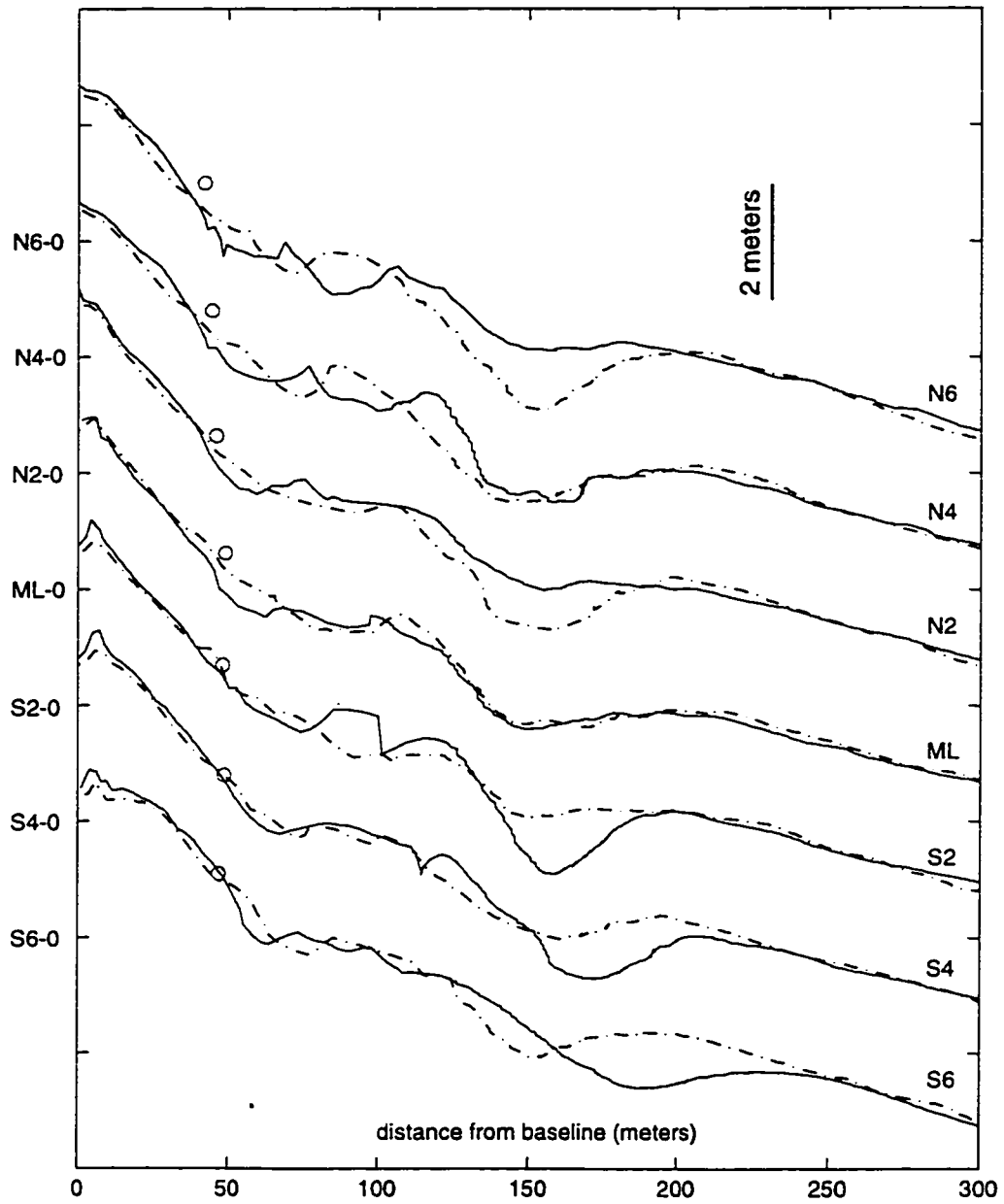


Figure 2.3 (continued) f. 14 December 1990: dotted; 15 March 1991: solid

of the fractional uncertainties for the four days is taken as a measure of the alongshore variation in NIC volume.

In addition to cross-shore surveys, a 25 m by 25 m area of the outer edge of the NIC was surveyed on 27 January 1991 to document the variability typically seen along a small portion of a the grounded ice ridge. Ten ice cores were collected from known locations in this small survey area to document the inhomogenous sediment distribution in the NIC.

A total of 56 NIC ice cores were collected in the survey area. These cores were collected with a motor-driven ice corer that could collect cores up to 1 m long and 8 cm in diameter. Extensions could be added to the core barrel to collect longer core lengths, when this was done, the two lengths of core collected in the same hole were counted as individual samples. NIC ice is very porous; the amount of ice in a core was determined by melting the core and measuring the melt water. The melt water volume was converted into an ice volume assuming an ice density of 0.917 g cm^{-3} and ice concentration was determined by dividing the ice volume by the core volume. This ice concentration is expressed as a decimal value between zero and one. Sediment concentrations in NIC samples were determined by decanting the melt water from the sediment, and drying and weighing the sediment. NIC sediment concentrations are expressed in two ways: (1) The sediment concentration for a given NIC volume, expressed as g dm^{-3} , was determined by dividing the sediment mass by the core volume. I use the units g dm^{-3} ($= \text{g l}^{-1}$ of bulk volume) as a reminder that the concentration is for a volume of ice, pore space and sediment. (2) The sediment concentration in ice was determined by dividing the sediment mass by ice volume, and is expressed as grams of sediment per liter of ice (g l^{-1}). This method of determining ice concentrations will be used for comparisons with other ice types in Chapter 5. Grain size distributions for seventeen of the NIC samples were determined by sieve analysis and the method of moments (Krumbein and Pettijohn 1938).

The total sediment load incorporated into the NIC during the course of the winter was determined by multiplying the average sediment concentration for each NIC ice type (grounded ice ridges, lagoonal ice and icefoot) by the calculated volume of that ice type that formed along the ML transect during the winter months.

2.4 RESULTS

The results are presented in three sections. The first section describes changes observed in the nearshore bathymetry during the 1991 winter. The second section contains observations on the growth and destruction of the NIC. The third sections discusses the amounts and characteristics of sediment found in NIC ice samples.

2.4.1 BATHYMETRY

Figure 2.3 is a series of five plates showing changes in the seven survey lines between consecutive survey dates. Each plate consists of 2 bathymetric profiles along each of the seven survey lines. Adjacent survey lines in Figure 2.3 are vertically offset by 2 m for clarity, and the zero axis (LWD55) for each line is shown along the vertical axis. "O's" on the profile lines mark the position of the inner edge of the NIC on 9 January (the position of the shoreline when the NIC formed). Once the inner edge of the NIC formed, it remained in place until the end of the ice season. For days when an NIC was present, the outer edge of the NIC is marked by a vertical line with the survey date.

The general characteristics of Gillson Beach can be seen in Figure 2.3a. The subaerial (landward of the "o's" in Figure 2.3) beach is relatively steep. The zone between the shoreline and the beginning of the longshore trough (about 100 m), here called the inner surf zone, is relatively flat. The inner and outer surf zones are separated by a 3 to 4 m deep longshore trough. Lakeward of this trough the nearshore sand fillet slopes offshore and pinches out at 450 to 600 m offshore in 5 to 6 m water depth. The average slope from the shoreline to the outer edge of the sand fillet is 0.013.

The first NIC at Gillson Beach was observed on 30 December 1990. Between the 14 December and 9 January surveys, all the profiles show sand deposition along all of the survey lines around the shoreline (Figure 2.3a). Lakeward of this small depositional feature there is net erosion along the inner surf zone of all of the profile lines. This erosion is greatest at about 90 m along lines N6 and N4, where a 50 cm high bar was destroyed. The net result is a steeper beach face right at the plunge point or shoreline and a flatter inner surf zone. On lines N6, N2, and ML there was also 10 to 20 cm of erosion in the longshore trough which exposed a cobble and boulder lag.

Between 9 January and 13 January the most visible change in the inner surf zone is the development of a shallow trough at the outer edge of the inner surf (at roughly 100 m in Figure 2.3b). This trough is best developed along lines N6 through ML just landward

of the outer edge of the 13 January NIC. Relatively little change occurred along the profiles between 13 and 18 January. The most apparent changes are the small amounts of erosion along lines S2, S4 and S6 between 95 and 125 m (Figure 2.3c). Between 18 and 22 January the outer edge of the NIC grounded ice ridge eroded back along all the lines (Figure 2.3d). This NIC erosion occurred on 20 January when waves with an estimated 0.7 to 1 m height were present at Gillson Beach. Associated with this NIC erosion is a deepening of scour depressions just lakeward of the outer NIC edge (Figure 2.3d, 22 January profiles). These scours had already appeared on 13 January but they reached their maximum extent on the 22 January surveys. On 22 January these scour depressions had depths and widths ranging from 0.3 to 0.6 m and 12 to 23 m, respectively.

Assuming the scour depressions had a simple triangular shore-normal cross section, the depressions represent a loss of 2 to 7 m³ of sand per m of beach width. In addition to the scour depressions, between 18 and 22 January is the approximately 40 cm of cut seen in the ML trough. Some of this sand may have been transported to the south, where there is about 20 cm of fill in the trough of line S2. On lines S4 and S6 there is about 10 cm of erosion and a flattening of the bottom profile at distances beyond 150 m.

The largest change in the bathymetric profiles occurs between 22 January and 15 March (Figure 2.3e). Between these dates there is aggradation along the inner surf zone along all of the lines. This aggradation has infilled all the scour depressions associated with the NIC and has formed bars at 50 to 125 m along the profile lines. In addition to the aggradation in the inner surf zone, there is a major longshore redistribution of sediment in the longshore trough between 22 January and 15 March. This redistribution is shown by the infilling of the longshore troughs on lines N6, N4, N2 and ML and the scour in the troughs along lines S2, S4 and S6.

To document the effect of the NIC on the nearshore bathymetry throughout the winter, I calculate changes in the nearshore sediment volume between 40 and 300 m along each of the survey lines (assuming a 1-m-wide strip) between 14 December and 13 January, 13 January and 15 March, and 14 December and 15 March (Table 2.2). The 13 January profiles are used for the winter comparison because this was the latest winter survey date when all of the survey lines extended to 300 m from the baseline. The 14 December/13 January surveys compare pre-NIC bathymetry with the bathymetry associated with a well developed NIC. Between these dates, all of the survey lines lost sediment as the inner surf zone was flattened (Table 2.2 and Figure 2.3). The 13 January/15 March surveys

Table 2.2. Change in volume of Gillson Beach bathymetric profiles during the 1991 winter. Positive numbers indicate fill.

Line Number	Δ Volume 14 December- 13 January (m ³)	Δ Volume 13 January- 15 March (m ³)	Δ Volume 14 December- 15 March (m ³)
N6	-12	49	37
N4	-10	10	0
N2	-2	40	38
ML	-23	0	-21
S2	-17	-3	-20
S4	-29	0	-26
S6	-28	-14	-42

compare the mid-winter bathymetry with the bathymetry five weeks after the NIC was gone. Between these surveys, some lines gained sediment and some lost sediment but there is no systematic pattern alongshore. The 14 December/15 March surveys show the net effect of the NIC five weeks after it had disappeared (Table 2.2, Figure 2.3f). This comparison shows a net sediment gain on Lines N2 and N6, no change in sediment volume on N4, and net sediment loss on Lines ML, S2, S4 and S6. Most of the change in sediment volume along lines N6, M2, S2, S4 and S6 occurs in the longshore trough. On Lines N2 and N6 there is up to 1 m of aggradation in the longshore trough. Lines S2, S4 and S6 have up to 1 m of erosion in the longshore trough. Most of this sediment redistribution in the longshore trough occurred after 22 January (Figure 2.3e). By 15 March 1991, there is no evidence of the scour depressions associated with the outer edge of the NIC (Figures 2.3e and f). Any visible effects of the NIC on the nearshore bathymetry disappear soon after the end of the ice season.

2.4.2 NIC GROWTH AND DESTRUCTION.

Figure 2.4 shows the NIC profiles. On 9 January, the NIC consisted of an icefoot that increased in width from north to south. The distance from the baseline to the inner edge of the icefoot (the shoreline) varied from 42 to 49 m. The outer edge of the icefoot ranged from 53 to 77 m from the baseline. This icefoot remained unchanged until it was destroyed in early February. By 13 January an ice lagoon and single grounded ice ridge extended the NIC out to approximately 100 m. On lines S2, S4 and S6 a second ice lagoon extended to 216 m from the baseline. Although there was a large accumulation of slush ice lakeward of the grounded ice ridge along the whole study area on 12 January, only the slush ice from line S2 south congealed into an ice lagoonal. The slush ice to the north was advected offshore. The lagoonal ice along the three southern lines disappeared by 16 January (seen in the 18 January profiles in Figure 2.4) and another series of 2+ m high grounded ice ridges grew lakeward to a distance of 110 to 128 m from the baseline along all seven survey lines. On 22 January 1991, the ice ridge had been cut back to within 90-100 m of the baseline. The reduction in ice ridge width occurred during the period of relatively large waves on 20 January. At this time, it was observed that even while the NIC was being cut back it was growing upward. This is clearly seen in the NIC profiles for lines N6, N4, ML, S2, and S6. On lines N2 and S4, the ridge was breached and a small secondary ridge formed at 80 m (Figure 2.4).

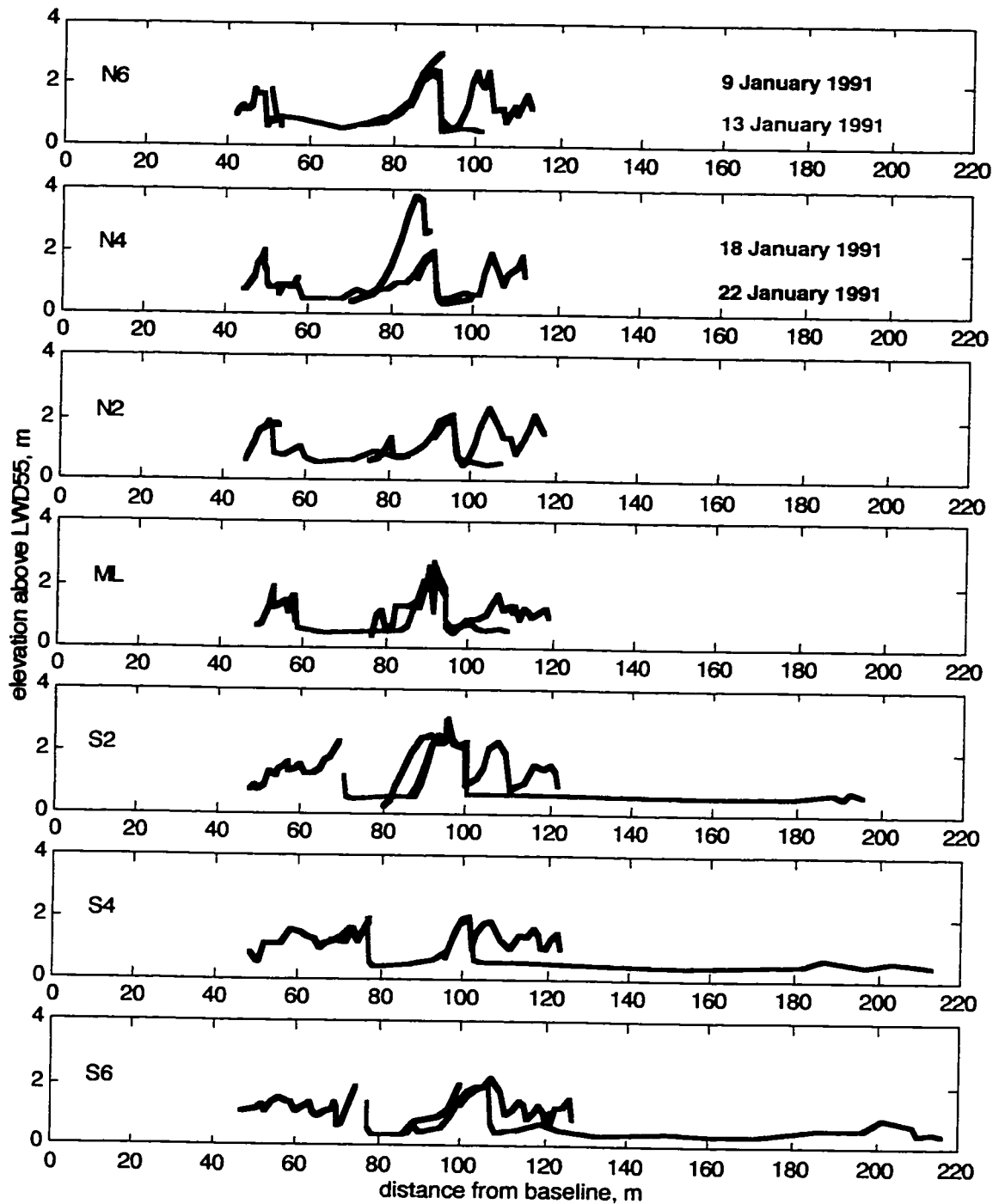


Figure 2.4. NIC profiles for lines N6 through S6 on 9, 13, 18 and 22 January 1991. Line colors are keyed to colored dates in figure. The landward edge of the NIC (the inner edge of the 9 January line) remained in the same position throughout the study period. Only changes in the NIC profile were surveyed, the inner edges of the 13, 18 and 22 January lines end where they merge with earlier profiles. Offshore is to the right.

The calculated volumes of ice of a 1-m-wide strip of NIC along each of the profile lines in Figure 2.4 are shown in Table 2.3. Grouping together all of the profiles from the same day (*c.f.* N6-S6 for 9 January) makes it possible to estimate the variability in NIC volume. The lines are spaced 30 m apart (Figure 1.3), so this variability is measured over 180 m of beach front. On 9 January the icefoot had a relatively small volume and small absolute variations in the along shore volume result in a fractional uncertainty of 62% ($= \sigma/\text{mean}$). There is also a large fractional uncertainty in the 13 January ice volume, but for a different reason. On this day the large variance results from the bimodal distribution in NIC width across the study area. Lines S2, S4, and S6 had very large ice volumes because of the ice lagoon that formed lakeward of the grounded ice ridge. On 18 and 22 January the NIC was much more uniform in volume across the study area. For the four days when the NIC was surveyed, the instantaneous NIC volume varied from 5.5 to 273 m³ of ice per m of beach, with the lowest ice volumes occurring early in the season. The fractional uncertainty in NIC volume ranged from 14% to 70%, with a mean value of $42 \pm 17\%$, where the error estimate is one standard deviation of the mean.

Measurements made at 1 to 3 day intervals show that NIC width on the Main Line varied from 5 to 121 m during the ice season (Figure 2.5). Changes in NIC width, both increases and decreases, occurred over short time periods (Figure 2.5). Growth and destruction of the NIC occurred when relatively large waves piled or eroded ice at the outer edge of the NIC. Destruction of NIC released well-indurated ice masses into the nearshore zone. This released ice formed small floating brash ice fields that dampened waves and protected the ridge from further wave erosion until they were advected away.

On 30 January 1991, a 70 m wide band of lagoonal ice formed on the lakeward side of the NIC, extending the NIC to 121 m wide (Figure 2.5). This feature was analogous to the wide band of ice seen lakeward of lines S2-S6 during the 13 January survey. Both of these ice lagoons were ephemeral features but account for a significant portion of the total lagoonal ice volume in the NIC during the winter.

The width information from Figure 2.5 is used to calculate the total volume of ice incorporated into a 1 m wide strip of the NIC along the Main Line during the winter (Table 2.4). Between 30 December and 7 February 1991, a total of 420 m³ of ice was incorporated into the Main Line NIC. Lagoonal ice makes up the largest portion of the Main Line NIC, with a total annual ice volume of 250 m³ per m of beach. However, 150 m³ of this lagoonal ice was incorporated into the NIC in one short event that built

Table 2.3. NIC ice volumes along survey lines at Gillson Beach during winter 1991. Position of survey lines is shown in Figure 1.3. All the values in the table except for the fractional uncertainties have units of m^3 of ice per m of beach. The fractional uncertainty is $(\sigma/\text{Mean Volume})$.

Line Number	Date of Survey			
	10 January	13 January	18 January	22 January
N6	10.5	68.5	97.7	59.9
N4	10.3	58.8	81.4	62.9
N2	5.5	74.2	99.4	38.0
ML	9.8	73.2	93.9	44.6
S2	26.6	273	127.3	62.1
S4	34.0	277	99.7	30.8
S6	22.1	273	92.9	47
Mean Volume	17	157	99	49
σ	11	110	14	12
Fractional Uncertainty	62%	70%	14%	24%

Table 2.4. Total ice volume and sediment load in the Main Line NIC during the 1991 winter season. The total sediment volume is calculated based on an assumed bulk sediment density of 1650 kg m^{-3} .

NIC Ice Type	Total NIC Ice Volume in 1991 ($\text{m}^3 \text{ m}^{-1}$)	Sediment Concentration mean $\pm\sigma$ (kg m^{-3})	Sediment Load in 1991 NIC Ice (kg)
Grounded Ice Ridge	160	14.2 \pm 13.7	2270
Lagoonal Ice	250	4.8 \pm 4.6	1200
Icefoot	10	13.8	140
Total	420	—	3600 (= 2.2 \pm 2.2 m^3 of sand)

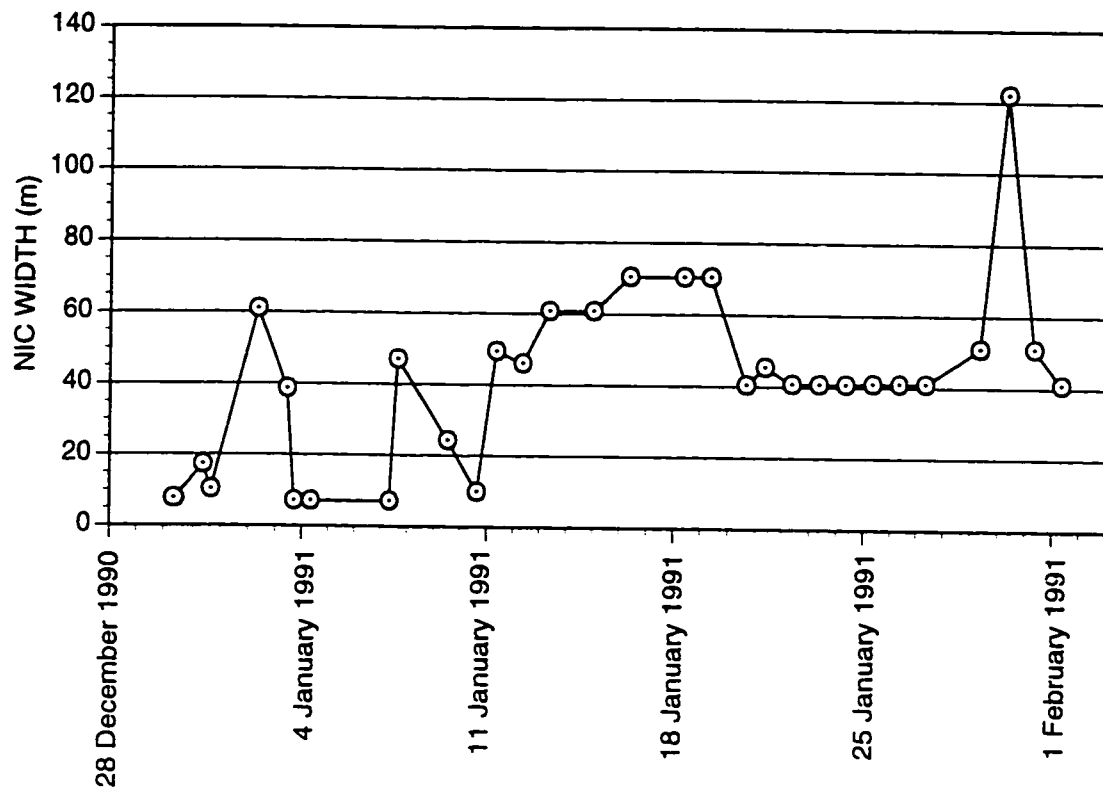


Figure 2.5. Changes in width of the Main Line NIC between 28 December 1990 and 2 February 1991. NIC growth and decay both occur over short time periods under the influence of large incident waves.

the NIC out to 120 m wide on 30 January (Figure 2.5). This ice lagoon was dispersed by 31 January (Figure 2.5). 30 January is also the day when the largest daily ice volume occurred along the Main Line, with a volume of approximately 200 m³.

2.4.3 NIC VOLUME AND SEDIMENT LOAD

Table 2.5 lists information about the sediment found in the 47 NIC samples. Statistics are given for sediment in grounded ice ridges and lagoonal ice samples. Sediment content in grounded ice ridges range from 0.3 to 55.3 g dm⁻³, with a mean value of 14.2 g dm⁻³ and a standard deviation of 13.7 g dm⁻³. Although the sediment concentration in grounded ice ridges had a high variance, the grain size was very uniform. The mean sediment grain size of fifteen grounded ice ridge samples was 2.12Ø with a range of 2.04Ø to 2.21Ø; the standard deviations for individual grain size samples ranged from 0.51 to 0.60Ø. The lagoonal ice samples have sediment concentrations ranging from 0.3 to 11.1 g dm⁻³, with a mean value of 4.8±4.6 g dm⁻³. No lagoonal ice samples were sieved; visual estimates of grain size made against a grain size distribution card showed that sediment in the lagoonal ice was fine sand (~2 Ø). The two icefoot samples have a mean concentration of 13.8 g dm⁻³, and mean grain sizes of 1.87Ø and 1.64Ø.

Estimates of sediment concentration and ice volume in the NIC allow calculation of the sediment volume incorporated into the NIC during winter. The calculated total volume of sand-sized sediment incorporated into the Main Line NIC during the winter of 1991 was 3.6×10^3 kg of sand per meter of shoreline, or 2.2 m³ of sand per meter of shoreline (assuming a bulk sediment density of 1650 kg m⁻³, Table 2.4). Nearshore ice complexes commonly extend for many kilometers along shore (Barnes *et al.* 1992, Miner and Powell 1991), so it seems reasonable to use this calculated value to extrapolate the sediment content to a regional scale of kilometers. To do this an estimate of error that includes the variability of NIC width and sediment load must be made. Concentrated sampling and surveying over a small region shows that both NIC volume and sediment concentration are highly variable over short distances (Figures 2.4 and 2.6). The fractional uncertainties (σ/mean from Table 2.4) for the sediment concentrations in the NIC are ~100%. I have no direct measure of the annual alongshore variability in NIC volume. However, the mean fractional uncertainty in ice volume along the seven NIC survey lines for the four survey dates is 42% (Table 2.3). This mean fractional uncertainty can be used as a surrogate for the fractional uncertainty in the annual ice

Table 2.5. Sediment concentration and grain size statistics for Gillson Beach NIC samples.

	Sediment in Ice g l ⁻¹	Sediment in Ice Core g dm ⁻³	Ice Conc. in Core %	Mean Sediment Grain Size (Ø)	Sediment Grain Size σ (Ø)
Gillson Beach Grounded Ice Ridges					
mean	22.3	14.2	64	2.12	0.60
maximum	80.6	55.3	96	2.21	0.66
minimum	0.8	0.3	26	2.04	0.51
std	20.6	13.7	21	0.04	0.04
Gillson Beach Lagoonal Ice Samples					
mean	5.1	4.8	92		
maximum	11.1	11.1	100		
minimum	0.3	0.3	73		
std	4.5	4.6	13		
Gillson Beach Icefoot Samples*					
	18.4	17.6	0.95	1.87	0.6
	15.6	9.9	0.63	1.64	0.63

*Only two samples were collected so individual sample information is listed

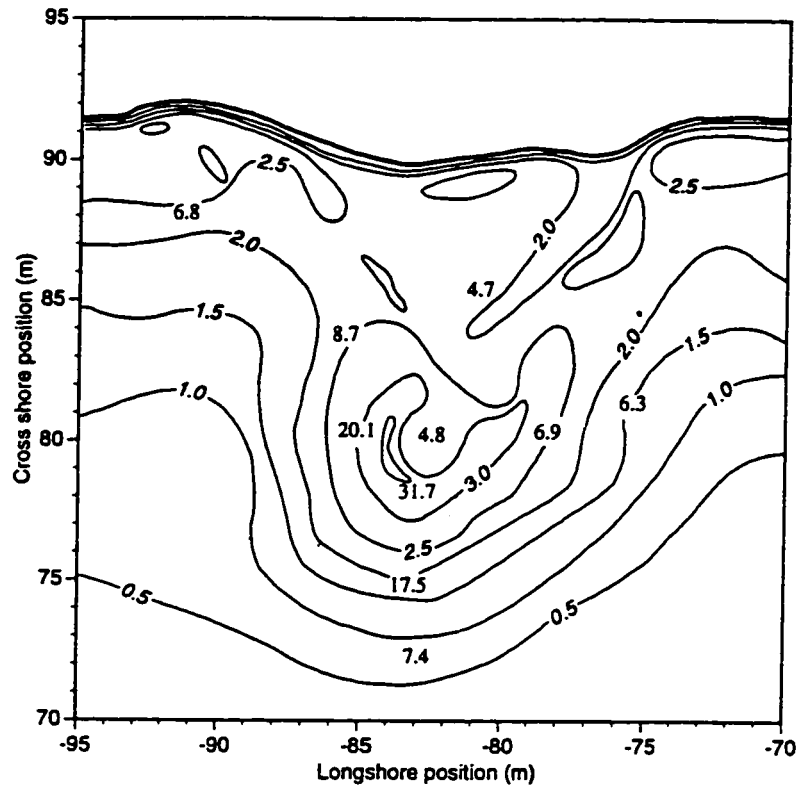


Figure 2.6. Topography of a small portion of the NIC offshore of line N6 (Figure 1.3) on 27 January 1991. Numbers mark positions of ice cores and are sediment concentrations in g dm^{-3} . Note the large variation in ridge height and sediment concentration over short lateral distances. Contour interval: 0.5 m.

volume. Taking the product of sediment concentration and ice volume and their related errors and following Taylor (1982), the best estimate for regional extrapolation is that the NIC contains $2.2 \times 10^3 \pm 140\%$ m³ of sand per km of beach. Assuming this sand was entrained from 50 m of lakebed (a typical width for the NIC, Figure 2.5), 4.4 cm of lakebed sand was entrained into the NIC during the 1991 winter.

2.5 DISCUSSION

2.5.1 NIC GROWTH AND DESTRUCTION

There was an NIC at Gillson Beach from 30 December 1990 through 7 February 1991. This was a relatively short period for the presence of an NIC in southern Lake Michigan. Assel (1983) reports that ice is present in the Great Lakes for two to four months a year. Miner and Powell (1991) report that there was an NIC at Gillson Beach for 121 days between December 1988 and March 1989. Seibel (1986) noted the presence of an NIC in southeastern Lake Michigan from December 1978 through March 1979.

In addition to a short ice season, the 1991 winter was relatively mild. Waves estimated to be 0.7 to 1 m high were observed at Gillson Beach on 7, 16, 20, and 29 January. Hubertz *et al.* (1991, see Table 1.1) hindcast waves of > 1.5 m height during 5% of the time for Lake Michigan near Gillson Beach. They also hindcast that 30 of 32 winters had an event with waves of > 3 m height, so wave conditions were not as severe during the 1991 winter as they are in most winters.

Even with the short, relatively mild winter, a well developed NIC formed at Gillson Beach. Along one survey line, an estimated 420 m³ of NIC ice formed for each m of beach. This ice had an estimated sediment load of 2.2 ± 2.2 m³ of sand per m of beach. The volume of NIC ice is highly variable over short alongshore distances. I found that the fractional uncertainty in NIC volume for four sets of surveys varied between 14% and 70% over a distance of 180 m of beach, with a mean value of 42%. This alongshore variability in NIC volume adds to the uncertainty of the sediment load in the NIC when extrapolated to regional values, resulting in an regional estimate of $(2.2 \pm 3.1) \times 10^3$ m³ of sediment per kilometer of beach. Although Miner and Powell (1991) report a much longer ice season, they report similar annual ice volumes (548 m³ per m of beach) and sediment concentrations (3.3 m³ per m of beach) at Gillson Beach during the 1989 winter. Dividing the sediment volume by the ice volume results in a bulk sediment load of

$6.0 \times 10^{-3} \text{ m}^3$ of sediment per m^3 of NIC ice for Miner and Powell and $5.2 \times 10^{-3} \text{ m}^3$ of sediment per m^3 of NIC ice for this study. These close results suggest that even though the variability in sediment concentration is high, it may be reasonable to make regional extrapolations based on a limited number of profiles.

The NIC grows when wind or waves advect a slush ice layer onto the beach. After the initial formation of an icefoot, the available wave energy determines what type of NIC ice feature forms. With relatively low wave at the outer edge of the NIC, lagoonal ice forms. It is important to note that the wave energy is not the same at the inner and outer edges of a wide slush ice zone. A thick, wide slush ice zone will dampen incident wave energy, so even during a large storm lagoonal ice will form if enough slush ice is present. Higher wave energy at the outer edge of the NIC will pile slush ice into a grounded ice ridge. Beyond this simple observation, the relationships between slush-ice-zone thickness and width, the concentration of slush ice in the nearshore zone, and incident wave energy that lead to NIC formation are not understood. These relationships are complex, as seen in the simultaneous NIC shoreward erosion and vertical growth seen on 20 January (22 January profiles, Figure 2.4).

Destruction of the NIC also occurs primarily at the lakeward edge. The NIC does not melt *in situ*. Reduction of NIC volume at the outer edge occurs by two mechanisms. First, when the outermost portion of the NIC is composed of an ice lagoon, a change in wind direction from onshore to offshore may advect the entire ice lagoon offshore *en masse*. This was seen on lines S2, S4, and S6 on 16 January (Figure 2.4, 13 and 18 January profiles) and on the Main Line on 30 to 31 January (Figure 2.5). Second, when the lakeward edge of the NIC is a grounded ice ridge, reduction in NIC volume occurs by wave erosion and calving pieces of the NIC into the slush ice zone. This is the most common type of NIC volume reduction. These observations of construction and destruction of the NIC confirm previous observations (Barnes *et al.* 1992; Dozier and Marsh 1973; Evenson and Cohn 1979; Miner and Powell 1991).

I found mean bulk sediment concentrations in grounded ice ridges, lagoonal ice, and icefoot to be 14.2 ± 13.7 , 4.8 ± 4.6 , and 13.8 g dm^{-3} , respectively. Although sediment concentrations are highly variable (Table 2.4), these values are in the same range as the few previously reported NIC sediment concentrations. Sediment concentrations in cores collected in a small area of the NIC can have sediment concentrations that vary by a factor of five (Figure 2.6) over a few meters. Although the sand content in any one type of NIC

ice (grounded ice ridge, lagoonal ice, or icefoot) varies substantially from sample to sample, it appears that there is a direct correlation between wave energy at the time of NIC formation and sediment concentration in the ice. Lagoonal ice has lowest sediment concentration. Icefoots and grounded ice ridges form in higher (wave) energy regimes, and have higher sediment concentrations. The relationship between wave energy and NIC sediment concentration is also suggested from Figure 2.6. The highest sediment concentrations seen in this small area are at the highest elevation on the grounded ice ridge. Assuming that only the largest waves deposited ice and sediment at the top of the ridge, the largest waves had the highest sediment concentrations. This relationship suggests that incident wave energy is important for incorporating sediment into the NIC. It is not clear whether wave-generated bed shear stress suspends nearshore sediment that is then directly incorporated into the NIC or if wave energy drives slush ice into the bed where the slush ice entrains bed sediment before it is incorporated into the NIC. The incorporation of sediment into the NIC needs more study.

It is clear that the sediment that is incorporated into the NIC comes from the nearshore lake bed. All of the NIC sediment samples were fine grained sand. In southern Lake Michigan the only source of sand is the thin, narrow nearshore sand file. Destruction of the NIC occurs by dispersal of NIC ice into the nearshore zone. Once this ice is released into the nearshore zone, it is readily rafted alongshore and offshore. This does not necessarily mean that all the sand incorporated into the ice is lost, because some of this ice is reincorporated into down drift NICs. Also, it is not known how efficient the released NIC ice is at retaining sediment once it calved from the NIC mass.

In 1972 O'Hara and Ayers summed up NIC formation as: ". . . Basically, the construction, maintenance, and destruction of the shore ice structure (the NIC) is continually undergoing change. It is a system that bears within itself simultaneously the means of growth and the means of destruction. What goes on at any given time is a balance between constructive and destructive forces." This statement is confirmed in the present study. It suggests that rather than looking at the NIC as a massive bulwark that protects the shoreline from the ravages of winter, the NIC can be viewed as a temporary reservoir of sediment laden ice that is stored in the nearshore zone. When ice concentrations are high, the excess ice is temporarily stored as an ice lagoon. With suitable conditions, a grounded ice ridge may form at the outer edge of this ice lagoon. Eventually, however, incident wave energy will be sufficient to break up the NIC and

release the ice back into the slush ice zone where ice rafting will occur. This ice rafting removes sand from the nearshore zone (Chapters 3, 4 and 5), so the yearly formation of a sediment-laden NIC results in a net loss of sand from the sediment starved beaches of southern Lake Michigan.

2.5.2 THE NIC AS A SEAWALL AND WINTER BATHYMETRIC CHANGES

The first NIC was observed at Gillson Beach on 30 December 1990; the first effects of the NIC on nearshore bathymetry should show up in the 9 January surveys. The initial effect of NIC formation is localized sand deposition and steepening of the beach profiles near the shoreline on all seven survey lines and net erosion and flattening of the inner surf zone between 50 and 300 m (Figure 2.3a). The aggradation seen around the shoreline is initially surprising because the normal transition from a summer profile to a winter profile results in a flattening of the beach face (Komar 1976). However, Davis (1976) notes that the subaerial beach is the first coastal feature to freeze and that rapid freezing locks the beach in a summer profile. Dillion and Conover (1965) found that finely laminated, ice-cemented sandstone blocks formed in the swash zone of a Rhode Island beach during a winter storm. These blocks formed when suspended sand settled onto the frozen beach face and froze between swash events. This process may explain the aggradation seen around the shoreline at Gillson Beach. Once the icefoot formed, this constructional feature was protected from modification by wave action until the icefoot was gone.

The net erosion seen in the 9 January surveys shows up in part as a flattening of the inner surf zone between the shoreline and 125 m (Table 2.1). The NIC built out across this region three times and eroded back twice between 28 December and 13 January (Figure 2.5). (Note that Figure 2.5 shows the width of the NIC, from the shoreline (~45 m in Figures 2.3 and 2.4) outward, so a 60-m-wide NIC (as on 2 January in Figure 2.5) would extend out to 105 m along the survey line.) It is probable that erosion of the lakebed was coincident with erosion of the NIC, because rapid NIC erosion (*e.g.* 2-4 and 7-10 January) occurred by wave action during periods when there is little or no slush ice in the nearshore zone. The same waves that destroyed the NIC flattened the inner surf zone.

The flattening of the inner surf zone suggests that the NIC acts like a seawall (Kraus and McDougal 1996, Dean 1986). However, this flattening can also be explained by a

simple increase in wave energy between summer and winter and the associated change in beach profile from a summer to a winter profile (Komar 1976). If the NIC is acting like a seawall, another feature that should form is a scour depression immediately seaward of the NIC (McDougal *et al.* 1996). Scour depressions are present along the outer edge of the inner surf zone on all of the surveys between 9 and 22 January (Figure 2.3). These depressions are best developed on the 22 January profiles (Figure 2.3d and e), when they are 12 to 23 m wide and 30 to 60 cm deep. Equation 2.1 can be used to determine if the observed scour depths are reasonable based on the studies of McDougal *et al.* (1996). Visual estimates of wave period and height were made on a daily basis at Gillson Beach. On 20 January waves were estimated to be 0.75 to 1 m high with a 5-6 s period. The grounded ridge at the outer edge of the NIC was being cut back by these relatively large waves (Figure 2.4) ; when the waves struck the vertical outer face of the NIC, they threw spray ~5 m into the air. The following two days were calm, so the scour seen in the 22 January surveys occurred on 20 January. Using Equation 2.1 with $H_b = 0.75$ and 1 m, $m = 0.013$, $h_w = 1$ m, and $D_{50} = 0.24$ mm, the predicted scour depth ranges from 24 to 32 cm. The measured ranges are from one to two times these predicted values, which is good agreement considering that the wave heights are estimates and that McDougal *et al.* point out that the scour depth is dependent on the initial profile conditions. With respect to the initial profile conditions, it is important to note that the scour depressions were not completely excavated on 20 January, instead, this event simply deepened depressions that had already begun forming before 13 January. These scour depressions were completely filled and the inner surf zone was nearing its pre-NIC profile by 15 March (Figures 2.3f), the formation of scour depressions apparently had little long term effect on nearshore bathymetry

The results from this study suggest that the NIC acts like in some ways like a seawall, and that results from seawall literature may be used to predict the amount of scour that will form lakeward of the NIC. However, the NIC and seawalls and the winter Great Lakes coastal zone and open ocean coastal zones vary in significant ways that affect how they protect the beach. Seawalls are monolithic structures; once they are placed they (hopefully) stay in place. Any scour associated with a seawall would be focused on the same spot directly offshore of the seawall. In contrast, the NIC is a dynamic feature that reacts to changing incident waves like a beach does, *i.e.* by coming to a new equilibrium. With large waves and little or no slush ice in the nearshore zone (as on 20 January) the

NIC is destroyed, so scour is spread out across a zone of the lakebed as the NIC erodes back. If the Lake Michigan nearshore zone reacts the way Chestnutt and Schiller (1971) predict, the scour at the toe of the NIC would be back filled as the NIC migrates landward. This is suggested in Figure 2.3d, on lines N2 and S4. These two lines had the greatest amount of NIC destruction on 20 January and they have the smallest scour depressions. This is also suggested by a comparison of the 22 January and 15 March profiles (Figure 2.3e). All bathymetric evidence (the scour depressions) of the NIC is gone by March 15, so in the short term the NIC has little effect on the bathymetric profile. The data collected in this study do not allow an evaluation of the long term effects of annual NIC formation on nearshore bathymetry in southern Lake Michigan.

Many researchers (Bajorunas and Duane 1967; Davis 1973; Davis *et al.* 1976; Evenson and Cohn 1979; Marsh *et al.* 1976; Marsh *et al.* 1973; Marshall 1967) studying the Great Lakes have concluded that formation of an NIC protects the beach from erosion. Implied in this conclusion is that there is little nearshore sediment transport during the winter months. This study shows that this is not the case; nearshore sediment is mobile throughout the winter. The initial formation of the NIC between 14 December and 13 January was accompanied by a flattening of the inner surf zone and a net loss of sand from the nearshore zone (Table 2.2, Figure 2.3a and b). The loss of nearshore sediment was reversed on lines N6, N4, and N2 between 13 January and 15 March, lines ML and S4 had no change in sediment volume, and lines S2 and S6 continued to loose sand. The net result for the period between 14 December and 15 March is that lines N6 and N2 had a net gain in sediment, lines ML, S2, S4 and S6 had a net loss, and line N4 retained its original volume. These net changes in volume show up in the profiles as up to 1 m of fill in the longshore trough of N6 and N2 and 1 m of cut along S2, S4 and S6 (Figure 2.3d and e). Along the ML most of the volume change occurs around the shoreline rather than at in the longshore trough. Even through the net change along N4 through the study period is zero, the sediment has been redistributed along the line with a significant volume of sediment moving out of the inner surf zone and into the longshore trough. These lines, which cover 180 m of beach front, show that profile changes vary considerably over short distances. The nearshore bathymetric surveys show that, even though the subaerial beach may be protected from wave attack by the NIC, the sediment lakeward of the NIC shifts in complex ways throughout the winter.

2.6 CONCLUSIONS

In this chapter I looked at the formation of the nearshore ice complex, and how this complex may protect the beach. The major results of this study are:

1. The total volume of ice incorporated into the NIC along one survey line at Gillson Beach during a 40 day period during the 1991 winter was 420 m^3 per m of beach.
2. Mean sand concentrations in the NIC were $14.2 \pm 13.7 \text{ g dm}^{-3}$ in grounded ice ridges, $4.8 \pm 4.6 \text{ g dm}^{-3}$ in lagoonal ice and 13.8 g dm^{-3} in the icefoot. This sand is derived from the nearshore sand file.
3. Sediment concentrations in NIC ice and NIC ice volume are highly variable over short distances. Combining estimates of NIC ice volume and the amount of sediment incorporated into the NIC, in 1991 the NIC in southern Lake Michigan contained $2.2 \times 10^3 \text{ m}^3 \pm 140\%$ of sand per km of beach.
4. NIC growth and destruction both occur rapidly when there are relatively large incident waves. Whether growth or destruction occurs depends in an unknown way on wave characteristics and the amount of slush ice present. Destruction of the NIC by waves releases sediment-laden ice into the nearshore zone where ice rafting occurs. Ice rafting of NIC ice removes sand from the sand-starved nearshore zone of southern Lake Michigan.
5. Approximately 4 cm of sand was removed from the inner 50 m of the nearshore zone at Gillson Beach if all of the ice was ice rafted out of the area when the NIC was destroyed.
6. The NIC appears to act like a seawall in two respects: the profile in front of the NIC is flattened as the NIC moves across the surf zone and scour depressions form at the lakeward edge of the NIC. Both of these features disappeared from Gillson Beach soon after the NIC was destroyed, so the NIC had little long-term effect on the overall beach profile.
7. Although sediment beneath and landward of the NIC does not move when the NIC is present, sediment lakeward of the NIC is in motion throughout the winter.

Zumberge and Wilson (1953) made preliminary studies of Lake Superior NICs between 1949 and 1953. This is one of the earliest published accounts of NICs on the Great Lakes. In their conclusions, they state:

Assuming, then, the profile is altered because of the presence of an ice-foot (the NIC), the question immediately arises as to the degree of alteration and the permanency of the change. Is the change in profile insignificant insofar as the 'normal' profile is concerned? How quickly is the altered winter profile reverted to the profile of the ice free year? Is it possible that the conditions imposed upon the regimen of the wave system by the ice-foot could have permanent effects on the general nature of the shoreline?

The results of this study indicate that, through the course of one mild winter, the formation of the NIC had little long term affect on nearshore bathymetry, but there is still much to learn about the interactions between winter waves, the NIC, nearshore bathymetric profiles and floating accumulations of slush ice.

CHAPTER 3. ANCHOR ICE FORMATION IN SOUTHERN LAKE MICHIGAN

3.1 INTRODUCTION

Anchor ice is defined as 'submerged ice anchored or attached to the bottom, irrespective of the nature of its formation' (Kivisild 1970). Early accounts of anchor-ice formation in rivers were published in 1705 (Piotrovich 1956); later observations documented anchor-ice formation in marine and lacustrine environments. The formation of anchor ice was a scientific curiosity until development of northern rivers began in the 20th century (Carstens 1966). The blockage of water intakes by anchor ice led to increased research on anchor ice formation. This research focused on determining the conditions necessary for anchor-ice formation with the goal of minimizing the effects of anchor-ice formation on municipal and industrial water supplies.

The formation of anchor ice on the bottom of a water body implies an interaction between ice and bed material. When an anchor ice mass grows to sufficiently large size, the buoyant force of the anchor ice overcomes the weight of 'anchoring' substrate, and the anchor ice, along with attached substrate, is lifted off the bottom. Lyell (1873) notes the importance of released anchor ice in transporting coarse sediment in northern, low-gradient rivers. Pebble- and gravel-sized material is often seen floating in the ice in these rivers, and Lyell (p. 363) notes that "... By the admirable provision of nature, it is in those countries where river-courses are most liable to be choked by large stones brought down from the upper country by floating ice, ground-ice (i.e. anchor ice) comes to the aid of the carrying power of running water."

Most observations of anchor-ice formation and anchor-ice induced sediment transport come from fluvial settings. Wigle (1970) and Arden and Wigle (1972) noted "great masses of white-capped, brown chunks of bottom ice (anchor ice) ... were observed floating on the surface" of the Niagara River after nights of anchor-ice formation. Although this transport of sediment by floating ice is readily apparent, Lyell (1873) suggests that the majority of sediment transport by anchor ice "... goes on unseen by us underwater" (p. 359). Osterkamp and Gosink (1982) observed slabs of near-neutrally-buoyant anchor ice with entrained sediment moving slowly along the bottom of Alaskan streams. This redistribution of anchor ice results in rapid sediment transport (Gilfilian *et al.* 1972). Benson and Osterkamp (1974) suggested this anchor ice-

induced sediment transport in Alaskan streams may result in a flux of fluvial sediment into the Arctic ocean.

Anchor-ice masses can grow to large size and can transport large amounts of sediment when released from the bottom. The ability of anchor ice to float large masses of sediment was documented by Dayton *et al.* (1969) in McMurdo Sound, Antarctica. In this region, anchor ice forms to 33 m depth and can lift portions of the bottom weighing more than 25 kg to the underside of the sea-ice cover. Tsang (1982) also reports observations of large boulders and heavy anchors being floated by anchor ice. Published observations show that anchor ice forms in rivers, lakes and oceans, and that the release of anchor ice results in sediment transport. Unfortunately, there are few published measurements of the sediment concentration in anchor ice. Consequently, it has been impossible to determine how anchor-ice induced sediment transport affects sediment dynamics in any aqueous environment.

In this chapter, I report on anchor ice formation in a small wave tank and in southern Lake Michigan. The wave tank observations are used to gain insights into anchor ice formation. Of all the aqueous environments where anchor ice forms, the formation in lacustrine settings is least well documented and understood. Field observations include meteorological and lake conditions when anchor ice formed, descriptions of anchor-ice morphology and distribution in the nearshore zone, and sediment concentrations in anchor ice samples. The sediment content data are combined with an estimate of anchor-ice concentration to determine the potential for anchor-ice induced sediment transport in southern Lake Michigan.

3.2 PREVIOUS STUDIES

In this section I review published observations of the conditions for anchor ice formation and the literature that discusses anchor ice formation in lakes.

3.2.1 CONDITIONS FOR ANCHOR ICE FORMATION

The requirements for anchor ice formation are similar to the requirements for frazil (small disks of ice suspended in the water column) formation. The prime requirement for anchor ice and frazil formation is that the water column be supercooled, *i.e.* the water must be cooled to below its freezing temperature (Michel 1972, Foulds 1977, Piotrovich 1956, Tsang 1982). Daly (1991) points out that supercooling in natural bodies tends to be less than 0.01° C and is nearly impossible to detect without laboratory grade

equipment. Tsang (1982, p.25) summarizes the conditions necessary for frazil and anchor ice formation as “. . . requires zero solar radiation heat input, and large heat losses by long wave radiation, evaporation, and convection from a small water body. In common language, one says that frazil and anchor ice are likely to form on a clear cold night when the wind is strong, the humidity of the air is low and the river is at the minimum flow, especially if such a night follows a cold, windy and cloudy day.”

In lakes and rivers, water is cooled by heat transfer to the atmosphere. Transport of cooled water from the surface downward accounts for chilling of the water at depth. As fresh water is cooled below 4°C its density decreases, so undisturbed fresh-water bodies tend to become stably stratified as they cool. The only way to mix supercooled water formed near the surface to depth is through turbulent diffusion, so turbulence is necessary for the formation of both frazil and anchor ice (Tsang 1982, Carstens 1966, Daly 1991) . Carstens (1970) states that the degree of supercooling in a water body is a function of the heat loss to the atmosphere and the turbulence of the flow. Increased turbulence increases the heat transfer, which increases supercooling. Greater supercooling of water at depth increases the potential for anchor ice formation. Tsang (1982) states that supercooled water and frazil crystals will only be transported to the bottom of lakes and rivers under highly turbulent conditions (a state he does not quantify). Figure 3.1a-d (from Svensson *et al.* 1994) shows the stages of frazil and anchor ice formation in a turbulent flow.

Carstens (1966) conducted flume experiments where he varied both the turbulence level and the amount of heat loss through the water surface. A sketch of the time history of water temperature during a typical experiment is shown in Figure 3.1e. In the turbulent flow water cooled at a constant rate through the freezing point until it reached a minimum temperature of a few hundredths of a degree below the freezing point. At this time frazil appeared in the water column and the water warmed to near 0°C. When the rate of temperature change became zero, the latent heat of frazil crystal growth exactly balanced heat loss to the atmosphere. In experiments with “strong” turbulence, relatively small levels of supercooling were seen, and the water would return to the freezing point soon after frazil started forming. “Weak” turbulence produced relatively large supercooling that persisted for long periods.

The meteorological and hydrologic conditions leading to frazil and anchor ice formation are well understood but the actual formation of anchor ice is not. Most anchor ice forms when small frazil crystals formed near the water surface are advected to the bottom in a turbulent, supercooled water column (Arden and Wigle 1972). Frazil in

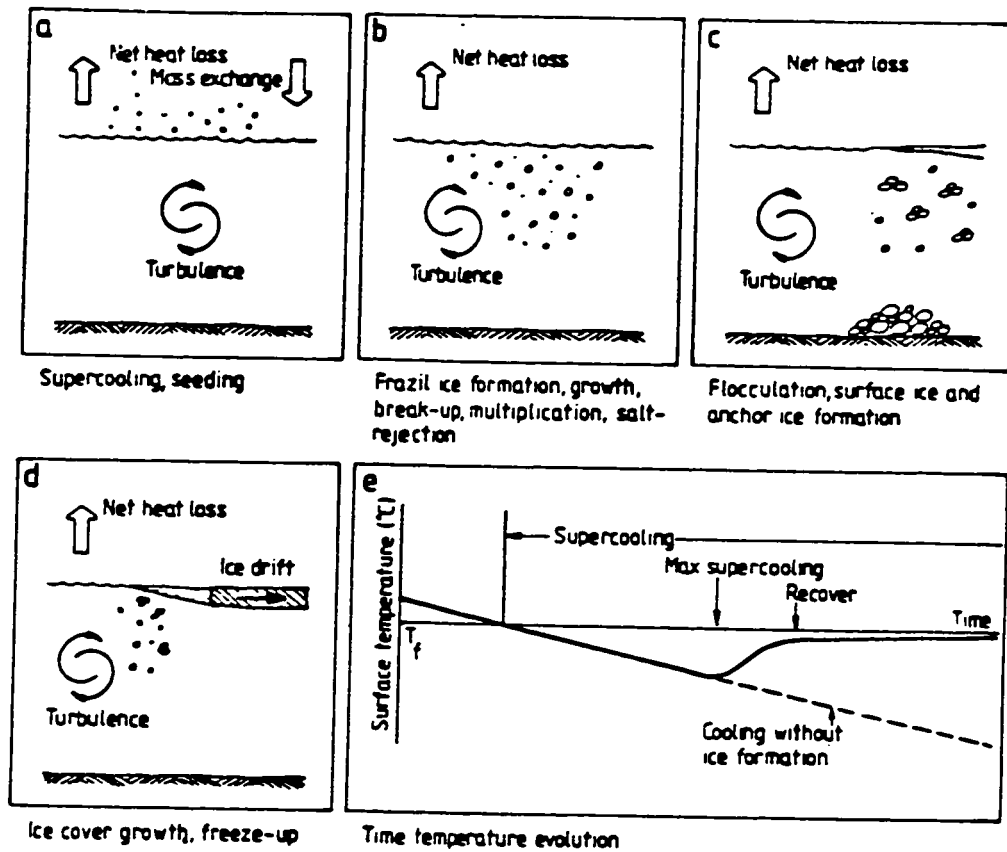


Figure 3.1. A figure modified from Svensson *et al.* (1994) showing (a-d) the steps in frazil and anchor ice formation in a turbulent flow and (e) a typical cooling curve for supercooled water when frazil and anchor ice growth occurs.

supercooled water are “sticky” and readily adhere to each other and the bottom (Arden and Wigle 1972, Tsang 1982, Daly 1991). When attached to the bottom this frazil is, by definition, anchor ice. Once attached, ice growth may increase by an order of magnitude as the anchor ice is irrigated by the flow of supercooled water (Osterkamp and Gosink 1982; Piotrovich 1956).

Anchor ice formed by frazil adhesion has a characteristic spongy texture composed of an interlocking mass of millimeter to centimeter sized, randomly oriented ice crystals. This is the most common form of reported anchor ice (Tsang 1982) but there are other morphologies. Several authors have reported that anchor ice can form large delicate crystals on submerged materials extending into the water column (Arden and Wigle 1972; Daly 1991; Dayton *et al.* 1969; Foulds and Wigle 1977; Piotrovich 1956; Reimnitz *et al.* 1987; Schaefer 1950). Anchor ice may take the form of a smooth coating over submerged objects (Tsang 1982). The formation mechanics of large anchor ice crystals or smooth anchor ice coverings at depth are poorly understood.

3.1.2 ANCHOR ICE IN LAKES

There is very little published information on anchor ice in lakes. Michel (1972), Tsang (1982) and Daly (1991) note that the main requirements for lacustrine anchor-ice formation are open water, cold air temperatures and strong winds. Strong winds produce surface turbulence that inhibits formation of a surface ice cover and mixes supercooled surface water to depth where anchor ice can form. Wind also enhances the rate of heat transfer from the water to the atmosphere.. Because the turbulence is produced in shallow water, anchor ice formation in lakes is limited to the epilimnion (Michel 1972).

The best published description of lacustrine anchor ice formation is from Foulds and Wigle (1977). They report on the formation of anchor ice on the Dunnville water intake on the north shore of Lake Erie, a crib-type intake located in 7.6 m of water. The water flow through this intake was severely reduced following a night of offshore winds of 24 km hr^{-1} , no ice cover over the intake, and temperatures below -6°C . A diver sent to investigate the flow reduction found the crib, an anchor chain and the rocky bottom surrounding the crib covered with anchor ice. This anchor ice resembled broken window glass and stuck to everything it touched. Individual ice crystals were up to 3.8 cm long by 2.5 cm wide by 0.3 cm thick. Although they lack direct visual observations, Foulds and Wigle report that similar anchor ice formation caused blockage of intakes to 17 m depth in Lake Ontario. The formation of anchor ice around water intakes may be an

anomaly. Daly (1991) points out that if the intake flow rate is high enough, the intakes themselves may entrain supercooled surface water which leads to anchor ice formation.

3.3 METHODS

3.3.1 WAVE TANK STUDIES.

A series of wave tank experiments were conducted at the University of Washington Sea Ice Laboratory. A 3.6 m long by 0.30 m wide by 0.45 m wide Plexiglas wave tank placed in a walk-in freezer was used to study anchor ice formation in a wave field. The bottom and sides of the tank were insulated so the -11° to -15°C atmosphere was the major heat sink for the water. The insulation could be removed from one wall of the tank for observations. Tap water was used in all of the experiments. A flap-type wave maker attached to one end of the tank generated 1.6 s period waves. A beach was constructed opposite the paddle with elutriated, moderately well sorted sand with a mean grain size of 2.35ϕ ($\phi = -\log_2$ (grain size in mm)). This sand was manually formed into a beach with an average slope of 0.07 before each experiment.

The wave tank experiments consisted of planing the beach smooth and starting the wave generator. The wave generator was run for 2 to 9 hours with the room temperature held at about 2°C so that the beach could approach an equilibrium profile. When there was little observed change in the profile, the air temperature was lowered and ice was allowed to form in the tank. A total of 14 wave tank experiments were run; in this study I report on the qualitative results of those experiments.

Wave heights at the break point were measured with a pressure transducer resting on the sand bed. Breakers of 1.6 s period and 7 cm wave height were used in all experiments. These spilling breakers broke at 8.2 cm water depth at a position 78 cm from the beach end of the tank. Suspended sediment concentrations at the break point were measured with an Optical Backscatter Sensor (OBSTM, D&A Instruments, Port Townsend, WA). The OBS is a miniature nephelometer that measures backscattering of infrared radiation by suspended particles. Because scattering is a strong function of both particle concentration and size the OBS must be calibrated with the actual sediment used in the experiment (D&A Technote, 1988). The OBS is small, has a wide observational range, and a linear response to changing sediment concentrations (Downing *et al.* 1981).

This sensor was mounted perpendicular to the wave direction at the break point and 5 cm above the bed. Pressure and OBS data were recorded at 5 Hz during experiments.

The OBS sensor was calibrated in two separate ways. For the case when no ice was present, the OBS sensor was calibrated in a recirculating tank using the experimental sand. Calibration for sediment concentration when ice was present was done by placing the OBS sensor in a slurry of frazil, water, and sediment in a bucket. The ice concentration in this slurry varied from 42% to 64%. This ice concentration held the sand in suspension, so the slurry was not agitated during calibration. After the voltage output for a given sediment concentration was determined, the slurry directly in front of the OBS sensor was collected and analyzed for sediment and ice concentration. Figure 3.2 shows the calibration curves for the water and the slurry. When no sediment is present, the voltage offset is nearly identical for ice and water. As sediment concentration increases, the calibration curves quickly diverge, with the slurry mixture having a lower voltage for a given sediment concentration. Based on these calibrations, I use the calibration constants for ice-free water to calculate all sediment concentrations, resulting in conservative sediment concentration estimates when ice is present.

There may be some question about the validity of using an optical sensor to determine sediment concentrations in the presence of ice. Pegau *et al.* (1992) tested optical sensors in an attempt to detect frazil in the water column. They report that frazil ice crystals tend to scatter light in forward directions, so backscatter devices like OBS's do not see the frazil. However, they did not attempt to measure sediment concentrations when ice was present. Their report, combined with our observations that there is no offset when clean frazil is added to clean water, and the OBS's linear response to increasing sediment concentration when frazil is present suggests that the OBS's is a valid instrument for determining sediment concentrations in the presence of frazil.

3.3.2 FIELD STUDIES .

Anchor ice observations were made at four locations in southern Lake Michigan between February 1989 and March 1991. The sites and times of observations are listed in Table 3.1. Limited observations were made at the City of Chicago water intake cribs, Illinois Beach State Park and Kohler-Andrae State Park during reconnaissance studies of the winter ice regime during 1989 and 1990. Detailed observations of anchor ice were made at Gillson Beach during the 1990-91 winter as part of a study of the effects of the winter ice regime on nearshore sediment transport. Three of these sites are beaches along

Water: Voltage = $0.0219(\text{concentration}) + 0.124$; $R^2 = .995$
 Ice: Voltage = $0.0151(\text{concentration}) + 0.078$; $R^2 = .972$

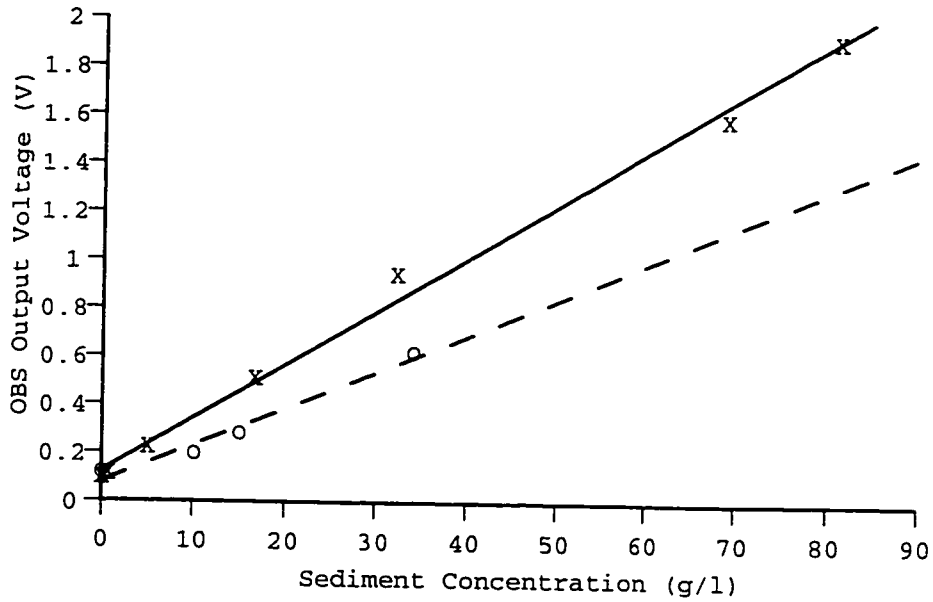


Figure 3.2. Wave tank calibration curves for OBS sensor in water and water/ice slurry. The calibration constants for water were used for the entire experiment, resulting in conservative estimates for sediment concentration when ice was present. Solid line and dots: water; dotted lines and circles: ice.

Table 3.1. Anchor ice observation sites in southern Lake Michigan.

Location	Dates
City of Chicago Cribbs	9 February 1989
Illinois Beach State Park	12 February 1989
Kohler-Andrae State Park, WI	19-20 February 1990
Gillson Beach, Illinois	1 January - 1 February 1991

the Wisconsin and Illinois shoreline of the lake. The fourth site, the City of Chicago water intake cribs, are located some distance offshore (Figure 3.3).

3.3.2.1 Weather

Weather observations for the 1989 and 1990 studies were recorded with hand-held analog thermometers and anemometers. These data are essentially instantaneous readings taken at the time anchor ice observations were made. For the thirty-two day study of ice processes at Gillson Beach in January 1991 weather information was obtained from the NOAA Marine Coastal Weather Log - Coastal Station. This weather station is at the Wilmette Harbor Coast Guard Station located 450 m southeast of the study site. The coastal weather station data were collected daily at 0200 hours and at two-hour intervals between 0600 and 2200 hours. The wind speed, wind direction, and air temperatures from the Weather Logs were digitized for this report.

3.3.2.2 Nearshore Water Conditions

Ice is a potential hazard to any instruments positioned in the nearshore zone during the winter. To gather data on nearshore hydrodynamics and suspended sediment concentrations, a Backpack/Staff Instrument Package (BSIP) that can be used when ice is present was developed. The BSIP consists of an instrumented staff and a backpack worn by an operator. The 2.5 m long by 5 cm diameter staff has sensors for measuring wave heights, current speeds and suspended sediment concentrations in the nearshore zone. The staff has a 10 cm base diameter plate to keep it from sinking into the sand bottom. Sensor electronics are mounted on a backpack. The backpack also contains a Tattletale IV data logger that is used to control the sensors and record the data. The data logger has a remote on/off switch, so data logging can begin when the staff is in the correct position. In use, an operator in a dry suit would enter the water with the backpack and staff; after positioning the staff the operator would turn on the data logger to record data at 5 Hz. Data collection runs lasted from 2 to 5 minutes at several positions across the surf zone. The BSIP could be used in water depths of up to 1.5 m.

Wave heights were measured with a 0 to 5 psi pressure transducer mounted 30 cm above the bed. Current measurements were made with a Marsh-McBirney Model 512 electromagnetic current meter mounted on a cantilevered arm 25 cm above the bed. The current meter has a 4.5 cm sensor which measures orthogonal flow components in a

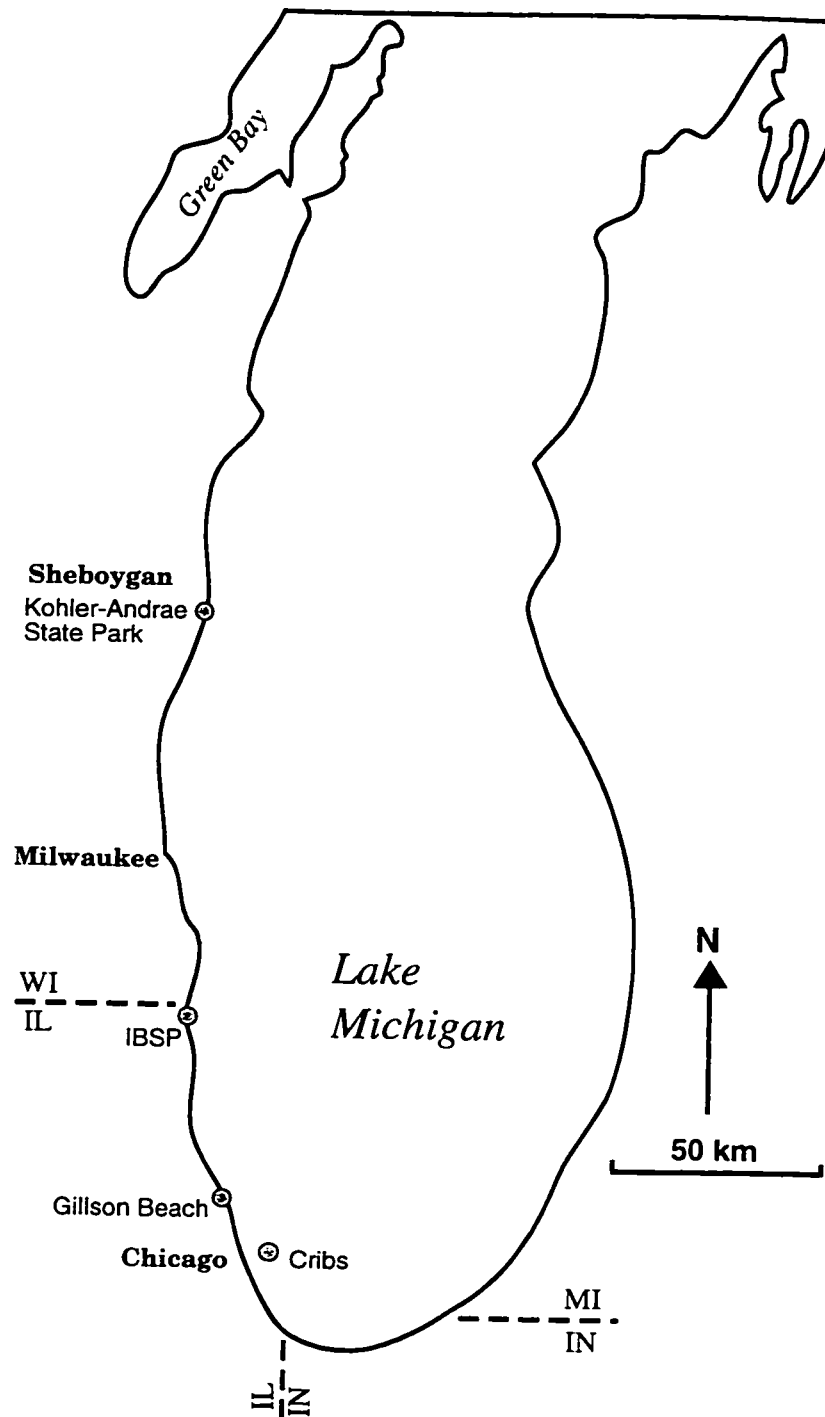


Figure 3.3. Lake Michigan map showing the four areas (shaded dots) where anchor ice was observed during the winters of 1989, 1990 and 1991. Anchor ice was observed during reconnaissance studies at Kohler-Andrae State Park, Illinois Beach State Park (IBSP) and the City of Chicago Water Intake Cribs (Cribs). Daily observations of nearshore ice were made at Gillson Beach between 1 January and 1 February 1991.

horizontal plane over a flow range of -3 to 3 m s^{-1} . An OBS, calibrated with local beach sand, was used to measure suspended sediment concentration 25 cm above the bed.

3.3.2.3 Anchor Ice Observations and Analysis.

All of the anchor ice samples in this study were collected by divers either wading or diving in the nearshore zone. Samples were collected by hand using two different methods. In some cases, anchor ice masses were simply picked up and carried to the outer edge of the NIC where they were transferred to a bucket. This was possible when individual ice crystals in a mass were strongly frozen together. Buoyant anchor ice that has been released from the bottom was common in the nearshore zone of southern Lake Michigan on mornings following anchor ice formation events (Figure 3.4). These floating anchor ice masses were often beginning to disaggregate and were collected with a nylon 2 mm mesh dip net. Dip net samples had volumes of 0.5 to 5 l. After collection, the net was shaken to drain interstitial water before the sample was transferred to a bucket for melting. Collecting samples with a dip net resulted in an integrated sample: ice crystals from several different anchor ice masses would be aggregated into a single sample. For convenience, in this report I divide the anchor ice samples on the basis of whether they were on the bottom or floating when they were collected when discussing sediment concentrations and grain size distributions.

Anchor ice samples were either melted in a microwave or melted naturally as they warmed to room temperature. After melting, the melt water was decanted off and the volume was measured, and sediment was packed in plastic containers for transport back to the laboratory. In the lab, samples were oven dried and weighed to the nearest 0.01 g. The melt water volume was converted into an ice volume based on an ice density of 917 g l^{-1} , and the concentration of sediment in ice was calculated. For samples with sediment concentrations less than 100 g l^{-1} , it was assumed that the sediment volume in the sample was insignificant compared to the total volume of ice plus sediment. When samples had more than 100 g l^{-1} of sediment, I calculated the sediment volume by assuming a sediment density of 2.65 g cm^{-3} and added the calculated sediment volume to the ice volume to get the total sample volume.

Determination of sediment concentration in this way has a number of built-in inaccuracies. When an ice sample is drained it retains some interstitial water; there is no easy way to remove interstitial water from the ice crystals. For sand samples in the 3.25 to -0.25ϕ size range Kraus and Nakashima (1986) found that in the "no drip" condition

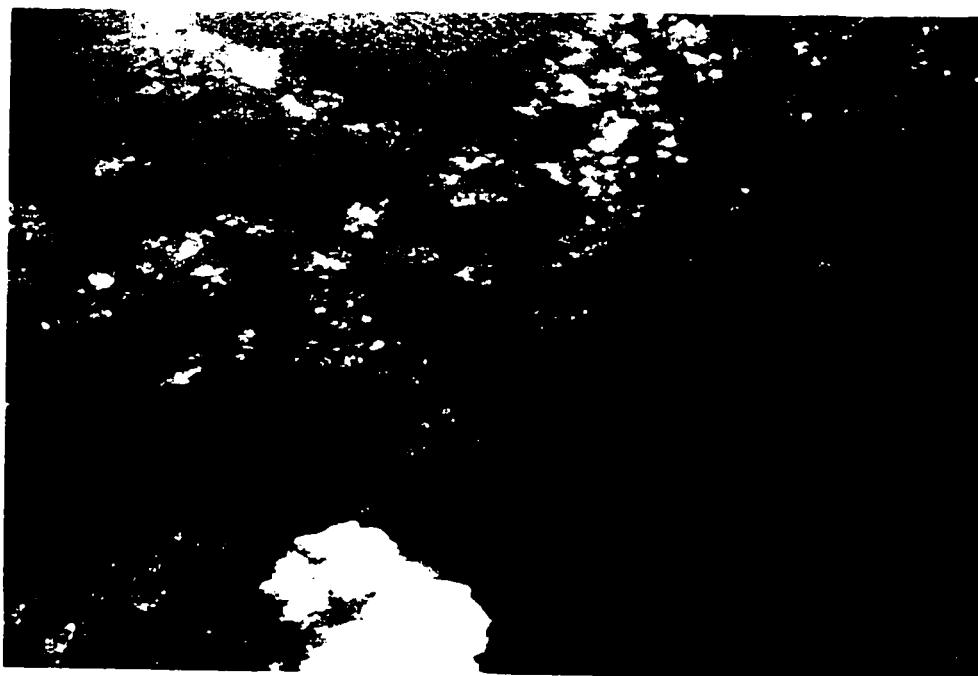


Figure 3.4. Floating anchor ice masses released from the lakebed at Gillson Beach on 23 January 1991. The dirty-looking anchor ice mass in the center of the photograph is 40 cm in diameter.

the sand retained between 21% and 10% water. Water content decreased with increasing grain size. Anchor ice samples retain water in a similar fashion. However, anchor ice crystals are usually much larger than sand sized sediment and so retain less interstitial water but it is impossible to determine the amount of water retained. This water is included in the melt water measurement and the ice volume calculation resulting in an underestimate of the sediment concentration. Individual crystals in different anchor ice masses vary in diameter from a 1 mm to > 40 cm; anchor ice masses made up of different size ice crystals would retain differing amounts of water.

There is a difference between anchor ice samples and bulk water samples which must be kept in mind. A water sample can be thought of as a cube in the water column filled with water and sediment to give a sediment concentration of "g l⁻¹". This mental image cannot be carried over to sediment concentrations in anchor ice samples. Anchor ice samples consist of an open framework of ice crystals and sediment surrounded by water. When anchor ice is sampled the surrounding water is lost. For example one anchor ice sample in this study was composed of interlocking, large, delicate ice crystals and had dimensions of 20 cm x 20 cm x 25 cm (Figure 3.5). The total volume encompassed by this sample was 10 liters, but there was only 1.1 liter of ice in the sample. The ice accounted for only 11% of the total "volume" encompassed by the anchor ice mass, the other 89% was water which was not sampled.

In addition to anchor ice samples, on four days when anchor ice was present at Gillson Beach water samples were also collected. Water samples were collected by placing a 2 liter plastic sample jar mouth down into the water and inverting it when it was 20 to 50 cm above the bottom and screwing on the lid. Suspended sediment concentrations in water samples were determined by vacuum filtration through pre-weighed 0.45 micron Millipore filters. These water samples had very low sediment concentrations, so no grain size distributions were determined.

Raw sediment grain size distributions for some samples collected in 1989 and 1990 were determined by Rapid Sediment Analyzer (RSA). A detailed description of the analysis is available in McCormick *et al.* (1990). Selected 1991 samples were sieved to determine the grain size (Folk 1974). The raw size data from RSA or sieve analysis was analyzed by the method of moments (Krumbein and Pettijohn 1938) to determine the grain size statistics.



Figure 3.5. An anchor ice sample collected on the surface 15 m lakeward of the NIC edge on 26 January 1991. Individual ice crystals in the mass are up to 10 cm in diameter and 1 mm thick. All of the sand in this sample adhered to ice crystal faces. The sediment concentration in this sample is 1.2 g l^{-1} .

3.4 RESULTS

3.4.1 WAVE TANK RESULTS

In the wave tank experiments the sand in the middle 2/3 of the tank formed vortex ripples that had characteristic wavelengths and heights of 3.4 to 5.5 cm and 0.8 to 1.5 cm, respectively. These vortex ripples extended both onshore and offshore of the breakpoint. In the inner surf zone, the beach was planed smooth for a distance of 30 cm. For 40 cm landward of the wave generator, the bottom was swept clear of sand, then there was a steep sand slope where the water shoaled from 25 to 17.5 cm over a distance of 20 cm. The vortex ripples started at this 17.5 m depth. This made the active part of the wave tank extend from the beach end of the tank, where the sand elevation was +8 cm to 300 cm from the beach end of the tank, where the water depth was 17.5 cm. The still water line was 40 cm from the beach end of the tank, although swash extended to within 10 cm of the back of the tank.

As waves traveled down the tank before ice began forming, they generated sediment-laden near-bed vortices in the x-z plane. Near the bed, these cylindrical vortices had diameters approximately equal to the local ripple height. The circular motion of the vortices could be clearly seen by the rotary motion of the entrained sand. As a wave crest passed over a ripple crest, these current vortices were separated from the bed and advected up into the water column. As the vortices rose into the water column, their diameter increased to about 2 cm and they dissipated. Eventually, the circular currents were no longer strong enough to keep the entrained sediment in suspension, and the sand settled back to the bottom.

Frazil was the first ice to form in the water column. Frazil formed first in the swash zone and propagated through surf zone. When waves broke, frazil was advected down into the water column. This entrained frazil passed through the sediment-rich vortices ejected from the bed and entrained sediment. At the same time, it formed roughly cylindrical flocs with cylinder axes oriented perpendicular to the direction of wave approach. These cylindrical flocs had diameters of the same order as the vortices in the water column, so when a vortex's path intersected a floc, the vortex was destroyed and sediment was entrained in to the floc.

As flocs grew and entrained sediment, they would take one of two paths. If large sediment concentrations were incorporated into flocs, they sank to the bed and formed

anchor ice masses. When these flocs were just slightly negatively buoyant, they would plane the sand ripples off the bed while entraining more sediment. These anchor ice masses had an offshore drift, and usually came to rest just lakeward of the break point. The anchor ice masses were composed of mm-sized ice particles and sand. If flocs did not collect enough sediment to become negatively buoyant and form anchor ice, they rose to the surface where they were advected onshore and incorporated into a lakeward-growing NIC complex.

Observations during the early stages of ice formation showed that frazil ice characteristics were different inside and outside of the surf zone. During the first few minutes of ice formation, the frazil ice concentration appeared to be higher inside the surf zone than outside the surf zone. Outside the surf zone, frazil appeared as perfect disks about 1 mm in diameter; they remained suspended in the water column and did not flocculate. Inside the surf zone, frazil disks were often fragmented and readily formed flocs which rose to the surface or picked up sediment and formed anchor-ice masses.

Visual observations suggest that sediment concentration increased and that the settling rate decreased when frazil first appeared in the water column. Use of the OBS in four experiments confirmed these visual observations. Figure 3.6 is a plot of the raw and filtered OBS-measured sediment concentrations 5 cm above the bed at the break point during an experiment. The raw data is filtered through a 20 s low pass filter applied in the frequency domain. The plot starts at the time when the first frazil crystals appear in the upper swash zone. At 'A' the first frazil was observed in the water column at the OBS and the sediment concentration rises. 'B' is when the frazil at the OBS started agglomerating into flocs. At time 'C' the entire surf zone was filled with flocs and the mean sediment concentration has dropped. The high sediment concentrations between 'B' and 'C' probably result from supercooling during that time. Frazil in supercooled water is sticky (Carstens 1966), so more sand is held in the ice when the water is supercooled. As supercooling and stickiness decrease the sediment concentration also decreases. Similar time histories of sediment concentrations were seen in four experiments where the OBS was used.

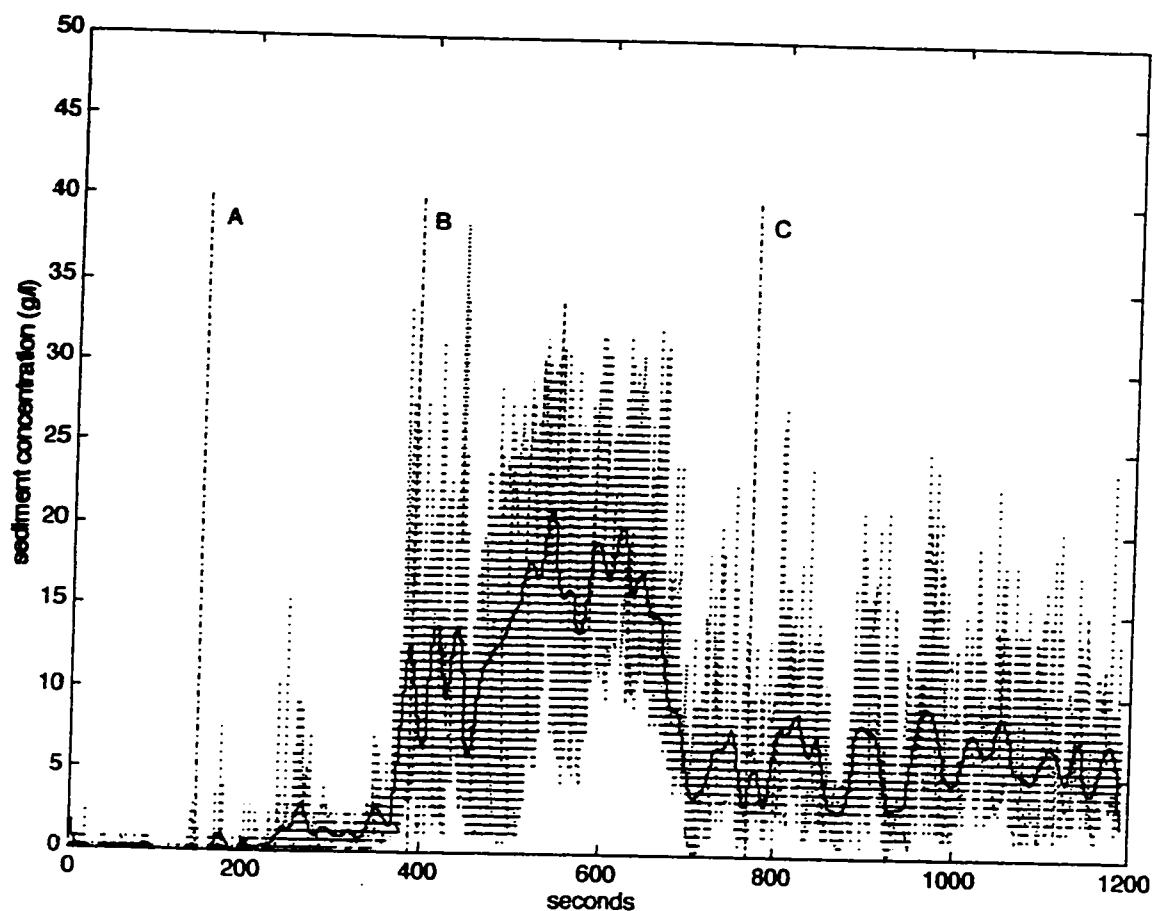


Figure 3.6. Sediment concentration measured in a wave tank experiment with an OBS. The dotted line is the raw data, sampled at 5 Hz and the solid line is the data filtered through a 20 s low pass filter. 'A' is the time when frazil crystals first appeared in the water column. 'B' is the time when frazil crystals at the OBS position started forming flocs. 'C' is the time when the OBS was completely surrounded by frazil flocs. The high sediment concentrations between 'B' and 'C' are probably due to frazil in supercooled water actively sticking to sediment crystals during that time.

3.4.2 SOUTHERN LAKE MICHIGAN OBSERVATIONS

3.4.2.1 Chicago Cribs.

The City of Chicago Dunne/68th Street crib and the Harrison/Dever crib were visited on 9 February 1989. These two structures are the water intakes for the City of Chicago municipal water system. The Dunne/68th Street Crib is located 3.2 km from the southwestern shore of Lake Michigan in 9.75 m of water (Figure 3.3). The crib is built of wood, steel, and stone, and has an outside diameter of 34 m and inside diameter of 18.3 m (City of Chicago Department of Water). This crib has eight water intakes 2.1 m above the bottom arranged around its perimeter. The Harrison/Dever Crib is located 4 km from the southwestern shore in 11 m of water. It is constructed of steel with an inside diameter of 12.2 m. Lake water enters the cribs through intake ports located near the bottom and rises around a central shaft until it reaches the center shaft ports. The water flows through screens into the center shafts and flows downward to supply tunnels located 15.2 to 61 m below the lake floor. These tunnels transport the water to purification plants on shore (City of Chicago Department of Water) .

On the night of 8 February the air temperature dropped to -18°C with southwest winds of 9 m s^{-1} . On the trip out to the cribs the lake surface was almost completely covered by a sheet of ice 10 cm thick. When we arrived, anchor ice was forming in the cribs and City Water employees were using dynamite to release the anchor ice from the crib walls. One sample of this anchor ice was collected from the Harrison Crib, and two samples were collected from the Dunne Crib after they floated to the surface inside the crib following dynamiting. These three samples were collected with a dip net and drained. They were all turbid, 'spongy' looking masses composed of small ice crystals. The sample from Harrison Crib contained 0.1 g l^{-1} of sediment; the two samples from the Dunne Crib contained 0.25 and 6.0 g l^{-1} of sediment. Grain size was not determined for the crib samples, but field logs note that the samples were predominately sand with at least one pebble.

3.4.2.2 Illinois Beach State Park.

Anchor ice was observed south of the North Point Marina at Illinois Beach State Park on February 12, 1989 (Figure 3.3). In the morning there was a layer of slush ice that extended out to 150 m offshore. Offshore winds soon blew the floating slush

offshore and a diver got into the water to act as a rod man for a nearshore bathymetric survey. The diver reported that he occasionally stepped on lumps on an otherwise sandy bottom and he was finally able to retrieve one of these fist-sized lumps after it bumped into his ankle at a distance of 15 m from the outer edge of the NIC. The lump consisted of ice-cemented sand with bands of interstitial ice. The sediment concentration in this sample was 1042 g l⁻¹ (Table 3.2). This high sediment concentration suggests that the sample might be better characterized as an ice-cemented sandstone than an anchor ice sample. In addition to stepping on 'lumps' on the bottom, the diver also reported seeing many 20-cm-diameter masses of sand-laden ice that were barely afloat.

3.4.3.3 Kohler-Andrae State Park.

Anchor ice observations were made in Wisconsin at Kohler-Andrae State Park (Figure 3.3) on 19 and 20 February 1990 (Table 3.1). On the 19th there were light offshore winds. The lake bed immediately lakeward of the outer edge of the NIC on the afternoon of the 19th was covered by a mass of interlocking, sediment-laden ice up to 30 cm thick that was firmly attached to the bed. When this ice was dislodged it floated to the surface and drifted offshore. During the night of 19 February, the air temperature reached a low of -7°C and winds remained light and offshore. A thin layer of congelation ice was on the water surface on the morning of 20 February. At 8 A.M. on 20 February, fluffy rounded masses of anchor ice covered 30 to 50% of the lake bed within 2 m of the outer edge of the NIC in water depths to 60 cm. These masses extended up to 10 cm above the bed, and contained sand in the interstices between the ice crystals. This was not the same as the ice seen on the 19th. It had a much more open structure and was not as firmly attached to the bed. Lakeward, the anchor ice concentration on the bed decreased until at 8 m from the outer edge of the NIC no more anchor ice was seen. At 30 m from the NIC, in 75 cm water depth on the crest of a bar, anchor ice was again observed, but in much lower concentrations than immediately adjacent to the NIC edge. No ice had been observed on the bar crest on the afternoon of 19 February.

As the morning of 20 February progressed, the fluffy, rounded anchor ice masses that formed during the night were spontaneously released from the bottom and floated to the surface. When on the surface, the ice crystals had very little adhesion: they readily broke apart when agitated, and sand entrained in the masses settled to the bottom. By 10 A.M., no more of the large anchor ice crystals were observed on the lake bed. Floating anchor ice samples collected on 19 February had sediment concentrations of 69.0

Table 3.2. Sediment concentration and grain size characteristics of southern Lake Michigan anchor ice samples collected from the lake bottom.

Location	Date	Sample Number	Ice Sediment Concentration (g l ⁻¹)	Mean Grain Size (Ø)	Std. (Ø)
Illinois Beach State Park	12 Jan 1989	9	1140		
Kohler-Andrae	20 Feb 1990	73	50.9		
Gillson Beach	14 Jan 1991	39	217	2.26	0.68
Gillson Beach	23 Jan 1991	86	512	2.06	0.51
Gillson Beach	25 Jan 1991	94	192	2.37	0.47
Gillson Beach	28 Jan 1991	133	207	0.38	1.52

and 23.0 g l^{-1} (Table 3.3). A single floating anchor ice sample collected on 20 February had 28.2 g l^{-1} of sediment; an anchor ice sample collected from the lake bed had 50.9 g l^{-1} of sediment. A water sample collected at the same time as the floating anchor ice sample on 20 February had a sediment concentration of 10^{-2} g l^{-1} (Table 3.3).

After these masses of relatively large anchor ice crystals that formed during the night of 19-20 February rose to the surface, the ice observed on the afternoon of the 19th was still present on the lakebed. This ice was in the form of randomly oriented, roughly equidimensional crystals less than 5 mm in diameter that formed 'underwater snowdrifts'. In places this ice was buried by rippled sand. This ice was restricted to the region near the NIC, where it formed vertical scarps up to 15 cm high. The ice was very strong: in many places it would support the weight of a wading diver, and it took a fair amount of kicking to break up the ice masses. When this anchor ice was broken from the bottom, it floated to the surface in barely buoyant masses less than 10 cm in diameter.

3.4.3.4 Gillson Beach.

Daily ice observations were made at Gillson Beach (Figure 3.3) from January 1 through February 1, 1991. During this thirty-two day period, there was evidence of anchor ice formation on fourteen days. There were three different kinds as evidence of anchor ice formation: (1) direct visual observations of anchor ice attached to the bottom or to instruments, lines and cables (which were resting on the bottom) mounted in the nearshore zone to 4 m water depth; (2) anchor ice rising to the surface in the nearshore zone in the wake of wading divers, or the divers 'feeling' the anchor ice on the bed with their feet; (3) spontaneously released anchor ice masses floating on the surface in the morning (Figure 3.4). In the case of (2) and (3) it was easy to distinguish floating anchor ice from slush ice by the large crystal size and dirty appearance of anchor ice.

Figure 3.7 shows the wind speed and air temperature at the Wilmette Harbor Coast Guard Station for January 1991 along with periods of anchor ice formation. The coordinate system for the wind vector diagram has been rotated 32° east so that the horizontal axis corresponds to the direction of the shoreline at Gillson Beach, with offshore to the top. No observations were made at night, so the boxes outlining anchor ice periods are based on morning observations and backward extrapolations. Many researchers (Arden and Wigle 1972; Daly 1991; Furguson and Cork 1972; Michel 1971; Schaefer 1950; Tsang 1982; Wigle 1970) working in rivers and lakes have noted that anchor ice commonly forms on clear cold nights several hours after sundown and is

Table 3.3. Sediment concentration and grain size in floating anchor ice samples and sediment concentration in lake water.

Location	Date	Sample Number	Ice Sediment Concentration (g l ⁻¹)	Water Sediment Concentration (g l ⁻¹)	Mean Grain Size (Ø)	Std. (Ø)
Kohler-Andrae	20 Feb 1990	66	69.0			
		67	23.0			
Kohler-Andrae	20 Feb 1990	74	28.2	0.010		
Gillson Beach	18 Jan 1991	63	1.5	0.017	1.97	0.82
		64	13.6			
Gillson Beach	19 Jan 1991	65	2.5		2.22	0.47
		66	50.2		2.19	0.50
		67	13.8			
Gillson Beach	22 Jan 1991	74	21.3	0.081	1.67	0.92
		75	25.7	0.68*	1.64	0.89
		76	51.3		1.55	0.99
		77	65.3			
		80	49.5		1.81	0.62
Gillson Beach	23 Jan 1991	81	17.9	0.048	2.28	0.57
		87	13.6	0.084 0.52*		
Gillson Beach	26 Jan 1991	105	1.2			
		108	6.6			
Gillson Beach	27 Jan 1991	119	102.0	0.13*	1.72	1.07
		120	10.5			
		121	5.2			
		122	3.7		1.91	0.60
		123	33.7		1.94	0.76
		124	1.4			
Gillson Beach	91/1/2 8.	134	6.2	0.010		

Mean concentration measured with OBS on BSIP. These readings were in the late morning and afternoon, when the conditions in the nearshore zone had changed compared to the early morning.

*Mean concentration measured with OBS on BSIP at 1025

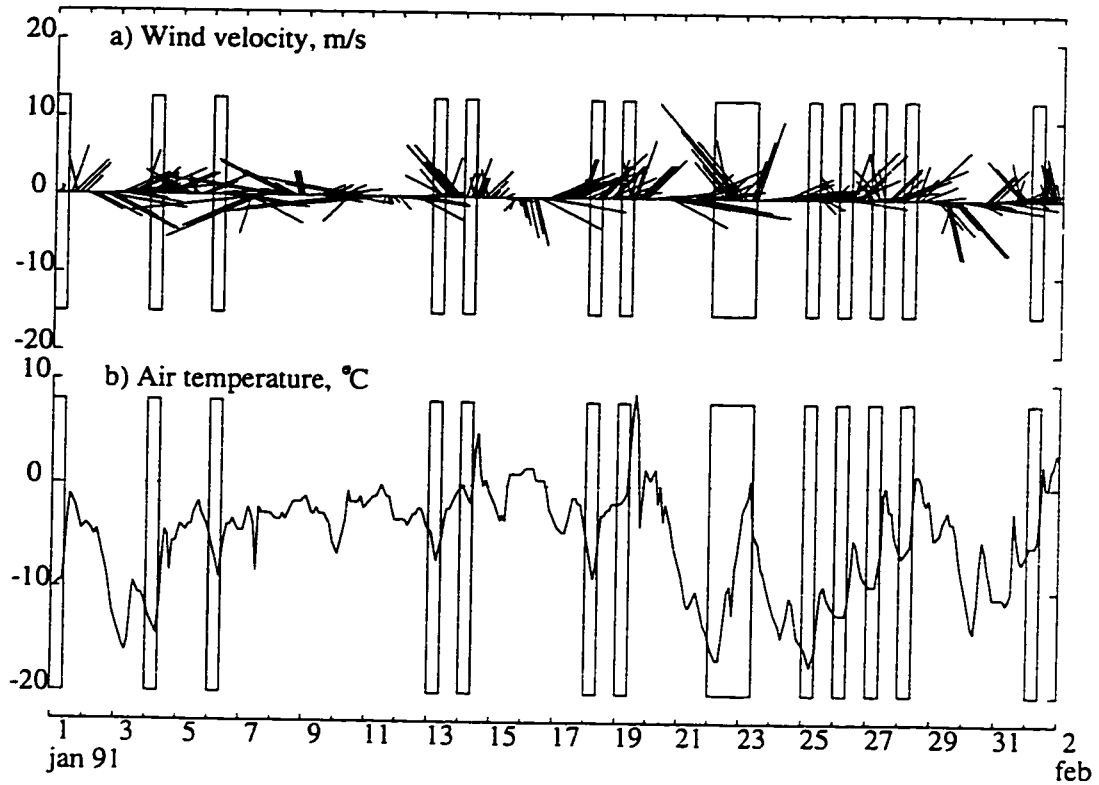


Figure 3.7. Weather conditions during periods of anchor ice formation. The coordinate system on the wind vector diagram has been rotated 32° E so that the top of the figure is offshore and the bottom is onshore (sticks pointing towards the top of the page are blowing offshore). The rectangles outline inferred periods of anchor ice growth. Evidence of anchor ice formation at Gillson Beach was seen on 14 nights in 1991. Anchor ice formed predominately on clear, cold nights with offshore winds and no slush ice cover.

released from the bottom on the following morning. Based on these observations, midnight is used as the starting time for anchor ice growth in this figure. Diving and wading observations show that, with the exception of 22 January, anchor ice was consistently released from the bottom during the mornings following formation events. The anchor ice at Gillson Beach was usually gone by 10 AM, so this time was chosen as the end of all anchor ice events except for 22 January.

Anchor ice formation occurred predominately at night, with low air temperatures during formation events ranging from -1.7°C to -17.2°C (Figure 3.7). Wind speeds ranged from $<1 \text{ m s}^{-1}$ to 17 m s^{-1} . There was consistently an offshore wind component on the nights anchor ice formed. These offshore winds often resulted in very quiet nearshore conditions with either wind ripples moving offshore or very low amplitude, non-breaking swell in the nearshore zone. On five mornings following anchor ice formation events (4, 25, 26, 27 and 28 January), conditions were so calm that 1-3 cm of congelation ice had formed on the surface in the nearshore zone. On 26 and 28 January, divers reported that frazil crystals were suspended in the water column during morning dives, an indication that the water column was still supercooled. The offshore winds also tended to advect any slush ice accumulations out of the nearshore zone. Most mornings when anchor ice was observed there was little or no slush ice in the nearshore zone.

Anchor ice was observed under a thick nearshore slush ice accumulation only on 6 January. On this day, a diver observed that instrument packages mounted on pipes jetted into the bottom were covered with large anchor ice crystals. The only occurrence of day-time anchor ice formation was seen was on 21 January 1991. This was one of the coldest days of the study period (Figure 3.7) with offshore winds and small, non-breaking waves.

3.4.3.5 Turbulence and Anchor Ice Formation

On 22, 23 and 27 January 1991 the BSIP was used to collect wave data in the nearshore zone at Gillson Beach. Several data sets (2 to 4 minute duration), were collected at varying distances from the outer edge of the NIC. Power spectra for these data sets were calculated using a 128 point window, 4π prolate filter, and 70% overlap. An estimate of the significant wave height (H_s) can be retrieved from the power spectra using the relationship of Guza and Thornton (1980) :

$$H_s = 4\sqrt{\text{variance}} \quad (3.1)$$

where the variance is found by summing the area under the wave power spectrum. Figure 3.8 is an example of a wave record for the 22nd and its associated power spectrum. This power spectrum shows energy concentrated in the low frequency range and at an incident frequency of at 0.312 Hz, corresponding to a wave period of 3.2 s. Table 3.4 lists the measured and calculated nearshore wave data collected on these days.

Most mornings when anchor ice was observed at Gillson Beach and Kohler-Andrae State Park were characterized by very calm conditions in the nearshore zone. The water was also usually calm on the evenings before anchor ice formation occurred, so the morning conditions are assumed to be representative of the conditions during formation of the anchor ice. The BSIP data collected on 22, 23, 27 January allow a quantitative assessment of the wave and turbulence conditions when anchor ice formed. Wave periods for 22 and 23 January BSIP data runs are 3.2 and 2.5 s, respectively (Table 3.4). Wave energy on 27 January was concentrated at very low frequencies, and no period can be determined from the power spectra (Figure 3.9b). For the 27th BSIP data, wave periods of 32 to 40 s were estimated using a zero-point crossing method on the raw data records (Figure 3.9a).

A commonly stated condition for anchor ice formation is a turbulent water column (Tsang 1982). In the nearshore zone, turbulence is generated by waves; the criteria for a laminar or turbulent wave boundary layer depends on the Reynolds number and the roughness of the bed. Dyer (1986, p.102) quotes Jonnson's (1966) two criteria for a laminar wave boundary layer:

$$Re_w < 1.26 \times 10^4 \quad \text{and} \quad A_b/k_s > 1.8(Re_w)^{0.5} \quad (3.2)$$

where Re_w is the wave Reynolds number, A_b is the amplitude of near-bed oscillatory motion and k_s is a measure of bed roughness. The quantity (A_b/k_s) is a measure of bed roughness. For a rippled sand bed, $k_s = 4H_r$, where H_r is the ripple height (Dyer 1986). At Gillson Beach the ripple height was 4 cm. The wave Reynolds number is defined as

$$Re_w = \frac{u_m A_b}{\nu} \quad (3.3)$$

Table 3.4. Wave characteristics during periods of anchor ice formation determined with the BSIP at Gillson Beach.

Date	Run	Distance from NIC edge (m)	Wave Type *	h (m)	T (s)	H _s (m)	λ (m)	u _m (m s ⁻¹)	u _t (m s ⁻¹)	Re _w	A _b /k _s
22 Jan	22.1	1	S	1	6.3	0.11	19.0	0.17	0.18	15900	1.4
3:30 PM	22.2	10	I	0.9	2.8	0.11	8.0	0.16	0.14	6400	0.6
	22.3	25	S	0.6	3.2	0.14	7.5	0.29	0.14	24000	1.2
	22.4	40	I	1.2	3.2	0.11	10.0	0.13	0.14	5200	0.6
23 Jan	23.3	0.5	I	1.2	2.6	0.27	8.0	0.29	0.13	19500	1.0
10:25 AM	23.4	10	I	1	2.6	0.25	7	0.31	0.13	22300	1.0
	23.5	25	I	0.95	2.3	0.25	6.5	0.30	0.13	19300	0.9
	23.6	40	I	1.25	2.4	0.22	7	0.21	0.13	9400	0.7
27 Jan	27.1	1	S	1.1	36	0.07	118	0.11	0.32	39700	5.3
10:30 AM	27.2	5	S	0.86	40	0.07	116	0.11	0.33	44000	5.9
	27.3	15	S	0.77	40	0.07	104	0.12	0.33	55500	6.6
	27.4	25	S	0.66	32	0.05	81	0.11	0.30	29800	4.4

*Wave type: S: Shallow water wave; I: Intermediate water wave

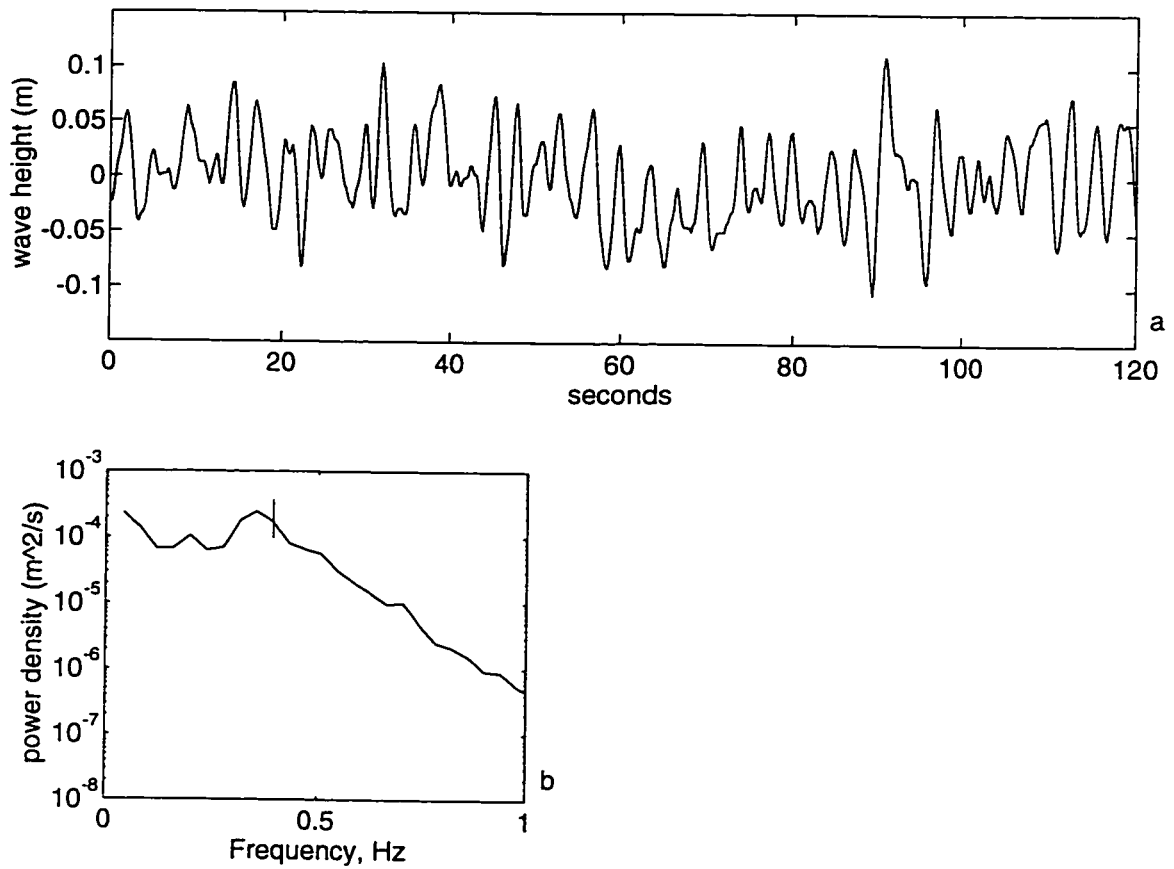


Figure 3.8. (a) Wave heights 25 m from the NIC edge at 3:30 PM on 22 January 1991. Sampled at 5 Hz. (b) Power spectra of (a), 17 degrees of freedom; the peak at 0.32 Hz is used to determine a characteristic wave period of 3.2 s. The bar on the power spectra is the 95% confidence interval.

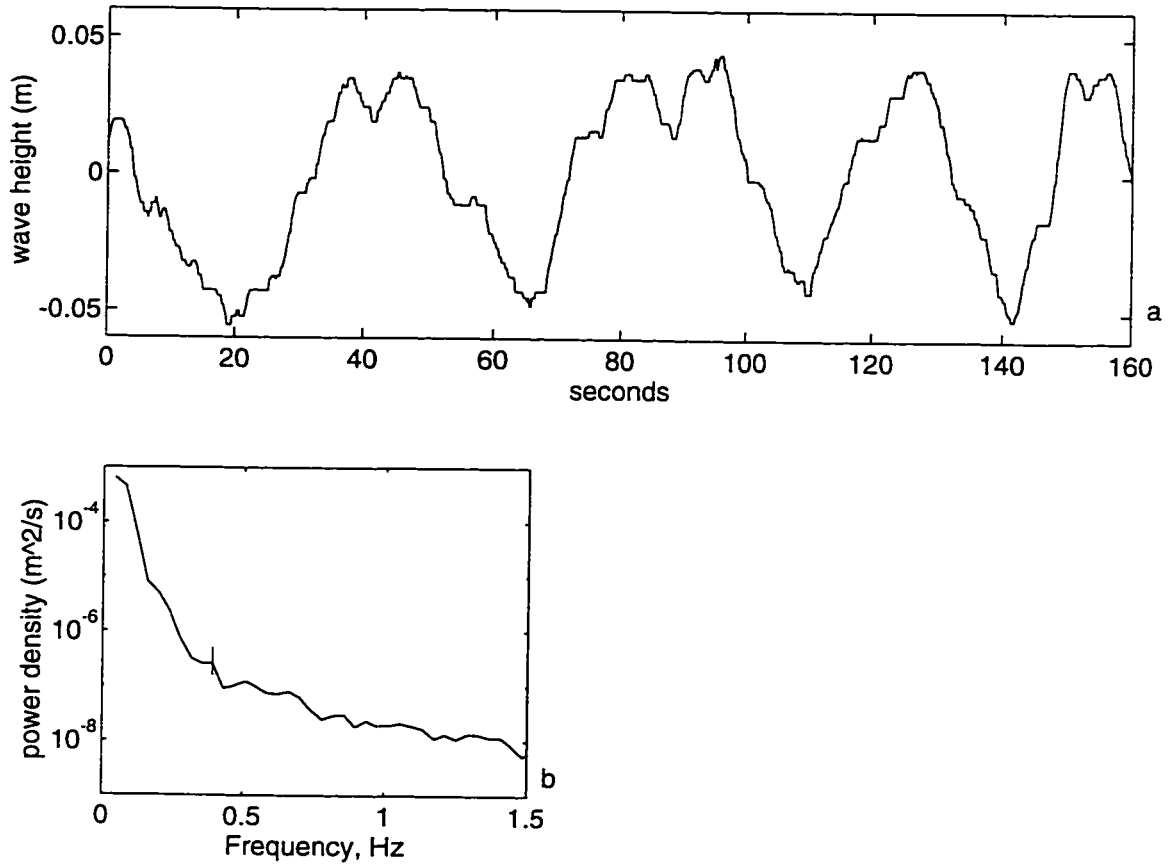


Figure 3.9. (a) Wave heights 15 m from the NIC edge at Gillson Beach on 27 January 1991. Sampled at 5 Hz. (b) The wave spectra for (a). For this day, energy was in very long period waves, and no peaks can be seen in the power spectra. Wave periods for 27 January were determined by a zero-crossing method on the raw wave heights. The bar on the power spectra is the 95% confidence interval.

where u_m is the maximum near-bed orbital velocity and ν is the kinematic viscosity (at 0°C , $\nu = 0.0179 \text{ cm}^2 \text{ s}^{-1}$).

Table 3.4 shows the wave characteristics generated with equations 3.1 to 3.3. In all but three of the data runs (runs 22.2, 22.4 and 23.6) Re_w is greater than 1.26×10^4 , indicating a turbulent wave boundary layer. For the three cases when Re_w is less than 1.26×10^4 , the A_b/k_s criteria (equation 3.2) is not met, so these runs are also turbulent. The data from all the runs on for these three days indicates that there was a turbulent wave boundary layer, even though visually the nearshore zone appeared to be very calm.

In addition to wave characteristics, the threshold velocity for grain motion under waves (u_t) was been calculated using the relationship of Komar and Miller (1973; 1975):





$$\frac{\rho u_t^2}{(\rho_s - \rho)gD} = 0.21 \sqrt{\frac{d}{D}} \quad (3.4)$$

where ρ_s is the density of sediment (assumed to be 2.65 g cm^{-3}), ρ is the density of water, D is the sediment grain diameter (I use the mean grain diameter on the inner bar in the nearshore zone = 0.024 cm , see figure 1.4), and d is the near bed orbital diameter. On 22 January, $u_m \approx u_t$, so sediment was just moving when anchor ice formed. On 23 January, $u_m > u_t$, so sediment was in motion when anchor ice formed. Finally, on 27 January, $u_m < u_t$, so no sand was in motion when the anchor ice formed.

3.4.3.6 Anchor Ice Morphologies

The anchor ice at Gillson Beach had four distinct morphologies (Table 3.5). The first type of anchor ice consisted of large masses of interlocking, randomly oriented crystals (Figure 3.5). These masses were up to 50 cm in diameter and 40 cm wide. Individual crystals in the masses were up to 25 cm in diameter and $\sim 1 \text{ mm}$ thick. These crystals were characterized by their large size and delicate scalloped edges. These masses were observed attached to boulders exposed in a longshore trough at 3.6 m water depth (Figure 1.4). The largest masses of crystals appeared to be attached to the largest boulders. These large coherent masses were seen on 19, 26, 27 and 28 January, days which were characterized by the calmest conditions (Figure 3.9, Table 3.3) in the nearshore zone. Three floating samples of this type of anchor ice were collected to

Table 3.5. A continuum of anchor ice types. Ice crystal size and morphology, and the amount of sediment incorporated into the anchor ice mass are functions of the incident wave energy when the anchor ice forms. High wave energy will move bottom material, low wave energy will not. Relative transport potential is speculative.

Anchor Ice Morphology	Crystal Size (mm)	Sediment Conc. (g l ⁻¹)	Substrate Size	Relative Wave Energy	Relative Transport Potential*
 Dense, fine grained	1	100 to 1500	sand - pebble	High	Intermediate f ¹ = low d ¹ = low c _s ¹ = high
 Clusters of small crystals	1 to 10	10 to 500 sediment gradient	sand	High - Transitional	High f = low d = inter c _s = high
 Individual large crystals	25 to 400	1 to 100	sand - boulders	Low	High f = high d = high c _s = inter
 Clusters of large crystals	50 to 400	1 to 10	sand - boulders	Low	Low f = low d = low c _s = low

*f = frequency of occurrence
d = distribution in the nearshore zone
c_s = sediment concentration

determine the sediment concentration in the ice (Samples 65, 66 and 105, Table 3.3). Sediment concentrations in these samples were 2.5, 50.8 and 1.2 g l⁻¹. In the sample with the highest sediment concentration there was a strong concentration gradient, with most of the sediment found near the base. The sand (Table 3.3, Sample 91-66) in these samples was scattered across the ice crystal faces.

These large, interlocking masses of anchor ice crystals were the predominate type of anchor ice seen on instrument packages, cables, and ropes in the nearshore zone. On some days these ice masses grew to 50 cm diameter on ropes and electrical cables resting on the lake bed and lifted them off the bed. These masses were never firmly attached to equipment or rocks during morning dives; they could always be dislodged with a sweep of the hand.

The second, most common type of anchor ice seen at Gillson Beach consisted of 5 to 10 cm diameter by 1-2 mm thick ice crystals that were individually attached to the bottom in boulder, pebble, and sand substrates. On some days this ice covered up to 50% of the sand bottom in the nearshore zone. The ice crystals in this type of anchor ice are similar to individual crystals in the interlocking masses, the difference between the first and second anchor ice types is that ice crystals in the second type were individually attached to the lakebed. Figure 3.10 (Sample 91-119) shows one of these ice crystals recovered floating on the surface in the nearshore zone. The jagged right hand side of the crystal probably marks the line where the ice crystal was attached to the lakebed. The sediment in 91-119 consists of a few sand grains attached to the crystal face and one 7 x 3 mm granule. The sediment concentration is 102 g l⁻¹ (Table 3.3). This ice crystal is typical of released anchor ice crystals that were drifting off shore on 20, 26, 27, 28 and 30 January. These individual crystals were often nearly neutrally buoyant, so they were not easily observed unless the observer was in the water. The largest pebble seen in a floating individual anchor ice crystal was 1 cm in diameter.

Figures 3.11 and 3.12 are underwater photographs taken on 27 January, 1991. Figure 3.11 shows large anchor ice plates attached to the boulder lag in ~3.5 m water depth. This figure is a good representation of anchor ice observed in the boulder lag. On the four days I observed ice in the boulder lag, I estimated that individual anchor ice crystals covered up to 50% of the boulders, and up to 10% of the bottom was covered by the large, interlocking anchor ice masses (Figure 3.5). Figure 3.12 is a photograph taken on the rippled sand bottom of the nearshore bar crest at 80 cm water depth. Although no anchor ice was present on the bottom when this photograph was taken, the imprints of

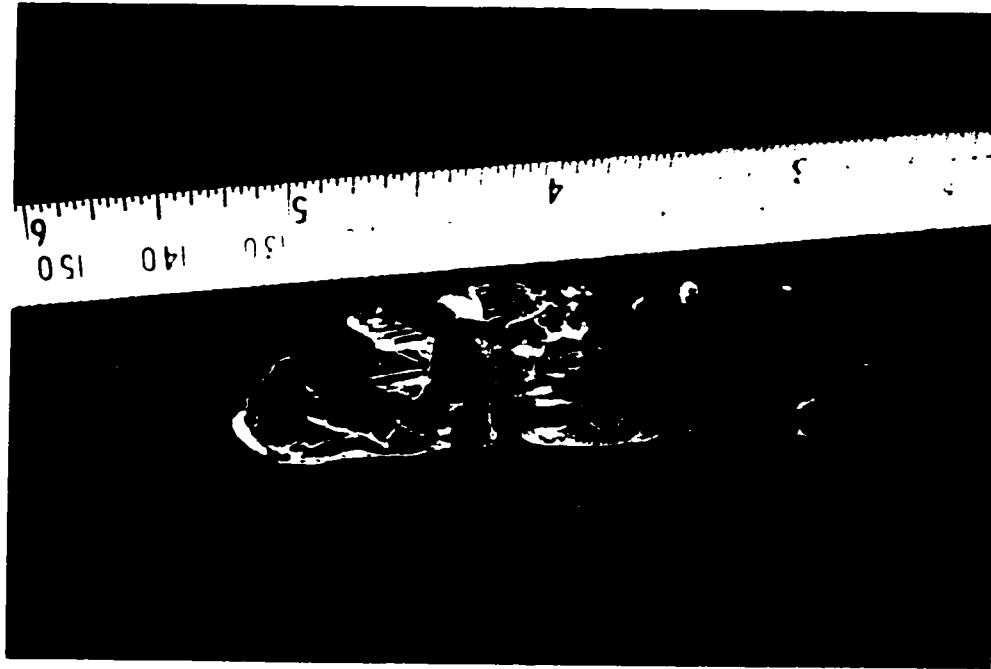


Figure 3.10. Anchor ice sample 91-119, collected 27 January 1991. This single anchor ice crystal is 7 cm x 3 cm by 2 mm thick. The crystal was collected at the surface; the entrained pebble is 7 mm x 3 mm. Sediment concentration is 102 g l^{-1} .



Figure 3.11 Bottom photograph taken at Gillson Beach on 27 January 1991 in the boulder lag at ~3.5 m water depth. Anchor ice crystals cover many of the boulders in the photograph. The prominent boulder in the right center of the photograph is 20 cm in diameter.

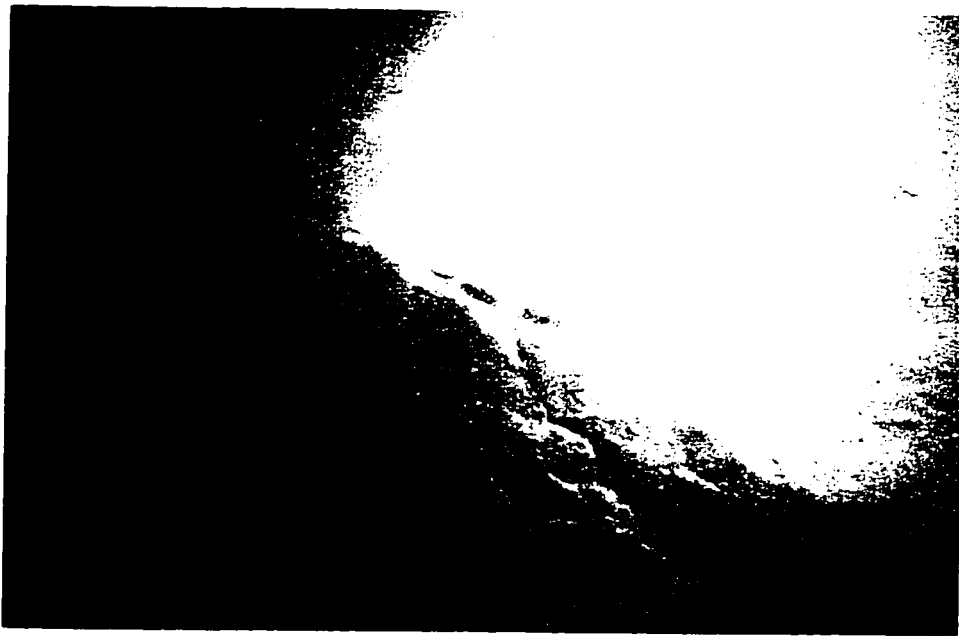


Figure 3.12. Bottom photograph taken at Gillson Beach on the morning of 27 January 1991 in 80 cm water depth. The crest of a sand ripple runs obliquely across the photograph from lower right to upper left. The distinctive imprints of released anchor ice crystals are clearly visible on the sand bottom. This is evidence that no sand was in motion at the time the anchor ice released from the bed. Width of photograph is 30 cm.

individual large anchor ice crystals similar to Figure 3.10 can be seen. The distribution of anchor ice imprints in this photograph is typical of what was observed on the sand bottom between 0.6 m and 3.3 m on days when the large, individual anchor ice crystals were present. This photograph is also striking evidence that no sediment was moving in the nearshore zone when the anchor ice was formed and released.

A third type of anchor ice (Figure 3.13) is composed of dense masses of ice crystals up to 2.5 cm in diameter. This anchor ice formed small mounds on the lake bed of up to 15 cm in diameter. These mounds often coalesced into low-relief sheets that covered areas of up to several square meters. On 18 January, this type of anchor ice covered up to 30% of the sand bottom too 2 m water depth. This anchor ice differs from the two previously described anchor ice types in a number of ways. The most apparent difference is in the size and structure of the ice crystals in different types of anchor ice. For example, in sample 91-86 (Figure 3.13), ice crystals ranged from 1 cm in diameter at the base to 2.5 cm diameter at the top. The edges of individual ice crystals were much more rounded and the crystal faces have much less visible structure than the larger anchor ice crystals (compare Figures 3.5, 3.10, and 3.13). This third type of anchor ice was attached to the bed differently than the first two anchor ice types. It appeared to grow into the bed or to be buried under sand ripples. This resulted in a dense ice masses with high sand concentrations. In dive notes for 18 January, I note that I tried to collect samples of this anchor ice but "... could not separate the ice from the substrate, so [I] threw the two samples out." Similarly, for the sample shown in Figure 3.13 I note "... I was very careful (actually discarded) the bottom part of the mass, because I was not sure if the sand at the base was the result of anchor ice or just free material I picked up." These observations suggest that there was not a clear demarcation between the anchor ice and the surrounding sand bottom. On the bottom, these anchor ice masses were sometimes almost completely covered by sand. This results in sand concentrations of up to 512 g l^{-1} (Table 3.2, sample 91-86) inhomogenously distributed throughout the anchor-ice mass. In sample 91-86 the highest concentrations were found near the base of the sample, where the ice crystals were smallest and concentration decreased as crystal size increased. In the largest crystals at the top of the anchor ice mass, sediment adhered to crystal faces and was found in the interstices between crystals (Figure 3.13). On 22 January, floating anchor ice was composed of 10 to 50 cm diameter masses composed of small ice crystals. The five floating anchor ice samples collected on this day had sediment concentrations ranging from 21.3 to 65 g l^{-1} .



Figure 3.13. An anchor ice sample retrieved from the bottom at the bar crest 25 m from the NIC edge on 23 January 1991 (Sample 81-86, $h=80$ cm). The ice mass this sample came from covered several square meters of the bottom. Individual ice crystals in this sample vary from 1 cm diameter at the base to 2.5 cm diameter at the top. The sediment concentration in the sample is highest at the base. The bulk sediment concentration is 512 g l^{-1} .

The fourth type of anchor ice consisted of equi-dimensional, 1-2 mm diameter ice crystals mixed with high concentrations of sand (Figure 3.14). This type was seen at Illinois Beach State Park in 1989, at Kohler-Andrae State Park in 89, and at Gillson Beach on 13, 14, 25 and 28 January 1991. In some cases this anchor ice was buried in a sand bottom (*i.e.* Kohler-Andrae State Park in 1990 and Gillson Beach on 28 January 1991) and at other times the masses were resting or moving along the lake floor (*i.e.* the Illinois Beach State Park 1989). When buried in the bottom, this type of ice was often surrounded by rippled sand, as if sand waves had migrated over the anchor ice mass. These masses were negatively buoyant, extremely dense or compact, and usually rounded as if they had been weathered. These dense, negatively buoyant anchor ice masses acted as substrate for relatively large anchor ice crystals described earlier to adhere to as they grew into the water column. These larger crystals were never firmly attached, and would break off when the sample was disturbed.

Figure 3.14 is an example of this fourth type of anchor ice (sample 91-133, 28 January 1991, Table 3.2). This 92 x 63 x 15 cm slab of ice was found in the granular material at 3.5 m depth in the longshore trough at Gillson Beach. This mass was buried nearly flush with the bed and had a dense covering of 10 cm diameter anchor ice crystals on its top side when found. These large crystals broke from the mass and floated off as soon as I began excavating the mass from the bed. Figure 3.14b is a cross section through the center of this sample, and shows a stratigraphy of roughly banded sediment-rich layers separated by bands of relatively clean, dense ice.

This sample had both the largest mean grain size (Tables 3.2 and 3.3) and the largest single clast of any anchor ice sample collected at Gillson Beach. The sediment in this sample has a mean grain size of 0.38 ϕ with a standard deviation of 1.52 ϕ . The largest clast in the sample measured 5 x 3 x 1 cm and weighed 31 g. The grain size distribution in this sample matched the grain size distribution in the longshore trough where the sample was collected (Figure 1.3), suggesting that this anchor ice formed locally.

3.4.3.7. Sediment in Anchor Ice.

Anchor ice is important because its formation on granular material and its subsequent release results in sediment transport. The ice buoyancy lifts sediment up into the water column where it can be transported by currents. This is analogous to the idea that waves in the nearshore zone suspend sediment and weak longshore currents result in



Figure 3.14. Massive anchor ice sample collected 28 January 1991 (sample 91-133). This 90 x 63 x 15 cm ice mass was buried flush with the granular bed at 3.5 m water depth when found. This cross section of the sample shows the stratified coarse sediment and the clean, dense ice layers. A diver's gloved hand is visible on the right side for scale. Sediment concentration is 207 g l⁻¹.

a net sediment transport (i.e. Komar 1976). The difference from the analogy is that longshore currents are restricted to a narrow band near the coastline while ice-suspended sediment can be advected any distance offshore by very weak surface currents. This was observed repeatedly at Kohler-Andrae State Park and at Gillson Beach when morning winds blew surface masses of anchor ice directly offshore. The common drift of anchor ice offshore is shown in Figure 3.15. This figure shows the average daily drift velocity of released, floating anchor ice as measured with a video system at Gillson Beach. The system is described in Chapter 4. All six days with drift velocities in Figure 3.15 are days when anchor ice formed. All of the anchor ice formed on these days was advected offshore.

Table 3.2 shows sediment concentrations and grain size data for anchor ice samples collected from the lake bottom. Sediment concentrations in bottom anchor ice samples range from 50.9 to 1140 g l⁻¹. Three of the Gillson Beach samples analyzed for grain size were moderately well sorted, fine grained sands (samples 91-39, 91-23 and 91-94, Table 3.2) even though they were collected on different days. The fourth sample (91-133) has a mean grain size of 0.38 Ø with a standard deviation of 1.52 Ø. Although all these samples were collected from the lake floor, they all had the potential to be transported as coherent masses under the action of waves and currents. The bottom anchor ice sample with the highest sediment concentration (89-9, 1140 g l⁻¹) was collected after it bounced into a wading diver's leg. The rounded nature of these negatively-buoyant anchor ice masses also suggests that they may have been rounded during transport (Figure 3.13a).

Table 3.3 gives sediment concentrations and grain size analysis data for floating anchor ice samples. Sediment concentrations in floating anchor ice samples range from 1.2 to 102 g l⁻¹. The mean sediment concentration in floating anchor ice samples was 25.7±26.3 g l⁻¹. In every sample except 91-119 (Figure 3.10) the entrained sediment was medium to fine grained sand. The sediment concentrations in these floating samples vary by two orders of magnitude for samples that were collected within a few minutes and meters of each other (27 January 1991 in Table 3.3).

Floating anchor ice samples collected on 18, 19, 22, 26, 27 and 28 January 1991 indicate a possible inverse relationship between ice crystal size and sediment concentration. Floating anchor ice crystals on 18 and 19 January were 5-10 cm in diameter and had sediment concentrations ranging from 2.5 to 50.2 g l⁻¹. The sample with the highest sediment concentration (91-66) had a visible sediment gradient. Floating anchor ice samples collected on 22 January were fine grained and had sediment

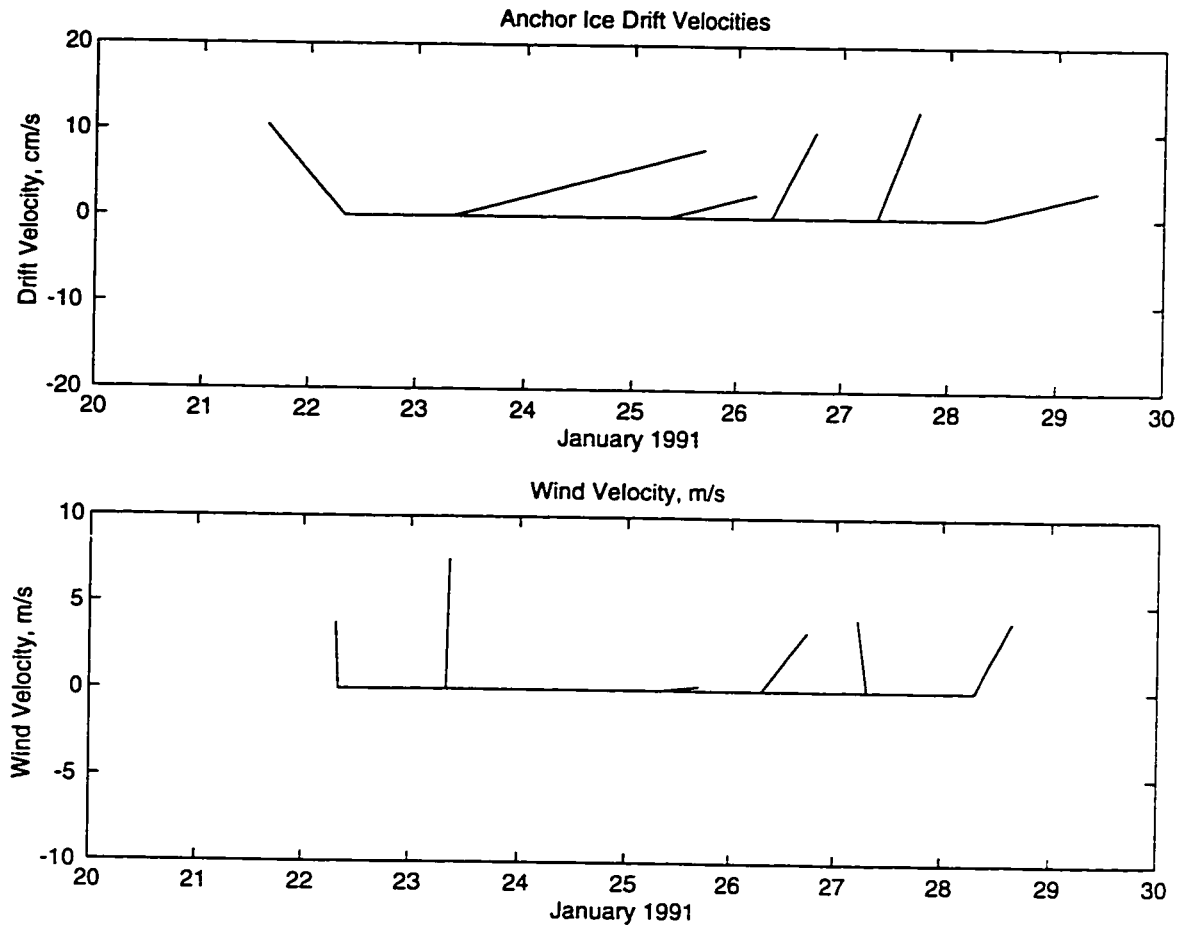


Figure 3.15. (a) Average daily drift velocities for floating anchor ice at Gillson Beach. The drift velocities were measured with a video system (described in Chapter 4). (b) Average wind velocities during periods when anchor ice was present. Anchor ice masses rose the water surface on 22, 23, 25, 26, 27 and 28 January when the video system was operational. On all these days there was a strong offshore component to the ice drift, so the floating anchor ice, along with any entrained sediment, was quickly advected offshore. The figure is oriented so that the horizontal axis is parallel to the beach, so vectors pointing to the top of the page show offshore drift.

concentrations ranging from 21.3 to 65.3 g l⁻¹. Sample 91-119 (Figure 3.10), a large single anchor ice crystal, had the largest sediment concentration, and the largest grain size of any of the floating anchor ice samples, but the sediment consisted of essentially one pebble, so this sample may be an anomaly. Samples 91-120 and 91-123, with concentrations of 10.5 and 33.7 g l⁻¹ of sand, came from floating anchor ice masses with ice crystals less than 2 cm in diameter. Samples 91-121, 91-122, 91-124 and 91-128 came from floating masses of large crystals and had concentrations ranging from 1.4 to 6.2 g l⁻¹.

In addition to sediment concentrations in anchor ice, on several days we measured suspended sediment concentrations at Gillson Beach. Suspended sediment concentrations in the water are from 2 sources: bulk water samples collected in 2 liter bottles and the mean values from the OBS mounted 25 cm above the bed on the BSIP staff. For 22 and 23 January when both methods were used to measure suspended sediment, the two sampling systems do not agree very well (Table 3.3). On 22 January several hours passed between measurements made with the two sampling systems. Bulk water samples were collected in the morning, and BSIP measurements were made in the afternoon when new anchor ice was forming in the nearshore zone. On 23 January, bulk samples and BSIP measurements were made within an hour of each other, so changing conditions cannot be invoked to explain the difference in concentration. Measured suspended sediment concentrations in the water on the days when anchor ice formed were as much as 3 orders of magnitude less than sediment seen in anchor ice samples (Table 3.3).

On 27 January 1991 the entire lake surface visible from Gillson Beach was covered by a 2-to-3-cm-thick layer of solid ice. By the time divers entered the water, most of this ice had drifted offshore, but there was still a 40-m-wide solid ice plate held in place by a pipe in the nearshore zone. When viewed from above or in cross section, individual anchor ice crystals incorporated into the solid ice plate were outlined by entrained sand grains. These outlined anchor ice crystals indicate the history of the previous night's freezing: anchor ice formed on and was released from the lake bed before any congelation ice formed on the surface. After anchor ice was released from the lake bed, it floated up to the surface where it was incorporated into the solid surface ice cover. This shows that anchor ice forms and is continuously released throughout the night. In southern Lake Michigan the formation and release of anchor ice are contemporaneous and continuous on some nights.

More important than what the solid ice cover revealed about the freezing history is the fact that once it formed it captured all of the anchor ice that was subsequently released from the lakebed. Diving traverses under the 40-m-wide ice plate showed that released anchor ice masses consisting of large, individual crystals formed a layer 10 to 50 cm thick under the solid ice cover. Assuming that the anchor ice originally extended 200 m offshore and had an average depth of 20 cm under the ice cover; that the average amount of anchor ice was 10% (based on sample 91-105) and that the average sediment concentration was 25.7 g l^{-1} , the amount of sediment incorporated into the water column by anchor ice was 100 kg per m of coastline. Assuming a bulk density of 1650 kg m^{-3} for sand sized sediment, this is $6.2 \times 10^{-2} \text{ m}^3$ of sand per meter of coast. This is equivalent to 62 m^3 sand per km of coastline, and may have occurred along tens to hundreds of kilometers of the west coast of Lake Michigan on this day. All of this sediment laden ice was advected offshore on 27 January (Figure 3.15).

3.5 DISCUSSION

3.5.1 WAVE TANK EXPERIMENTS AND INSIGHTS INTO ANCHOR ICE FORMATION AND MORPHOLOGY

One of the surprising things about the wave tank experiments was that even with spilling breakers in a relatively small tank, the water was not well mixed. This is seen in the progression of frazil formation down the tank from the swash zone out past the surf zone. Frazil always formed first in the swash zone, a shallow, high energy zone. It took 2-3 minutes from the time frazil was first seen in the swash zone until it propagated out horizontally 50 cm to the break. This 'lakeward' progression of frazil formation indicates that not all of the water was supercooled and/or seeded at the same time, and that conditions favoring frazil and anchor ice formation may vary over very short distances.

Frazil ice also behaved differently inside and outside of the surf zone. Outside the surf zone frazil disks tended to stay suspended in the water column. Inside the surf zone, frazil ice flocculated. Once formed, these flocs entrained sediment by striking the bed or by trapping sediment suspended in the water column. These wave tank observations show that energetic conditions are necessary to form sediment-rich masses of floating ice or anchor ice. Anchor ice formed in this manner had a characteristic fine-grained (mm-sized) morphology with sediment dispersed throughout the anchor ice mass.

Figure 3.6 shows that the sediment concentration at inside the surf zone increased rapidly as frazil and anchor ice are formed. Before frazil is observed at the OBS ('A' in figure) the mean sediment concentration was 0.19 g l^{-1} . As soon as the first frazil appears in the water column, the suspended sediment concentration increased by an order of magnitude to 1.7 g l^{-1} . The sediment concentration continued to increase as the frazil agglomerated into flocs, reaching mean concentrations of 17.2 g l^{-1} (between 'B' and 'C'). Beyond 'C' the mean sediment concentration decreases to 6.5 g l^{-1} . I interpret the rise in sediment concentration between 'B' and 'C' to represent the period of maximum supercooling and the formation of 'sticky' frazil and anchor ice. By 'C', supercooling had probably been reduced to a very low residual level (Tsang 1982), and the anchor ice was no longer sticky, resulting in a lower sediment concentration in the water column. The time period of increased sediment concentration corresponds to the period typical of supercooling in a flume or wave tank reported by Carstens (1966).

These wave tank experiments show that it is relatively easy to make sediment laden slush ice and anchor ice in a very small wave field. However, even with the small waves used in these experiments, the anchor ice that formed is fine-grained and compact. This anchor ice is similar to pieces of sediment rich anchor ice found on the lake bottom at Illinois Beach State Park and at Gillson Beach (Figures 3.12 and 3.13), and to the 'underwater snowdrifts' seen at Kohler-Andrae State Park. This suggests that blocks of fine-grained, sediment-rich anchor ice form under energetic conditions. The high sediment concentrations in some anchor ice and observations of anchor ice buried by sand suggests that conditions at the time of anchor ice formation were turbulent enough to move sediment in suspension and/or as bedload when the anchor ice formed.

This suggestion is supported by the observation that at Kohler-Andrae State Park and Gillson Beach where fine-grained anchor ice samples were found surrounded by or buried by non-ice bonded sediment. High sediment concentrations in anchor ice and anchor ice buried by sediment suggest that conditions were energetic enough to suspend high concentrations of sand when the anchor ice was formed. High sediment content, fine grained anchor ice samples found in southern Lake Michigan probably form in the same way as the wave tank samples: frazil suspended in supercooled water interacts with suspended sediment or strikes the bed and entrains sediment until it becomes dense enough to sink to the lake floor. Once on the lake floor, suspended sediment continues to settle onto the anchor ice mass or ripples migrate over the ice mass (Kempema *et al.* 1993). The weight of the overlying sediment compresses the ice and sediment into a

more compact mass, making a relatively hard, dense block. This explains the Kohler-Andrae observations and anchor ice masses similar to the core of 91-86 (Figure 3.13), but it does not explain the formation of masses like sample 91-133 (Figure 3.14). When sample 91-133 was collected it was buried almost flush with the sediment surface; it is hard to imagine that bedload transport of the coarse material in the area could account for 15 cm of local aggradation.

Although wave tank observations give insights into the formation of fine grained, high sediment concentration anchor ice masses, they give no insights into the formation of the large-crystal-size anchor ice that predominates in the nearshore zone of southern Lake Michigan. These large crystals formed on the calmest nights. A relationship between crystal size and calm conditions is implied in published anchor ice observations. Dayton *et al.* (1969) and Piotrovich (1956) noted that anchor ice crystals in the Antarctic grow to large sizes under the permanent ice cover, which implies relatively calm conditions. Foulds and Wigle (1977) noted that anchor ice crystals on a crib at 7.6 m water depth in Lake Ontario ranged up to 3.8 cm in diameter. Daly (1991) notes that anchor ice crystals blocking intakes in lakes are usually much larger than anchor ice found in rivers and speculates that it may result from a lower concentration of frazil crystals in suspension because of the lower level of turbulence in lakes. Shaefer (1950) reports that large anchor ice crystals formed on flats in the Mohawk River following a sudden water level rise. Flooded flats would be a zone of relatively low speed flow and low turbulence.

The relationship between turbulence level (or energy level) and anchor ice crystal size probably, as Daly (1991) speculates, results in part from lower frazil concentrations in the water column. With lower frazil concentrations, each ice crystal has a larger supercooled water volume in which to release the latent heat of fusion into, allowing the ice to grow to a larger size. However, there is probably more at work than just frazil concentration. As Carstens (1966) noted, 'weak' turbulence produces a relatively large supercooling. Carstens also noted that with 'weak' turbulence supercooling could exist for a long time below a surface ice cover. These are exactly the conditions found at Gillson Beach when the large anchor ice crystals formed. Even when conditions appeared calm, there was a rough turbulent wave boundary layer (for example, on 27 January, Table 3.4), but the turbulence was so 'weak' that a solid ice cover formed over the water surface, and large anchor ice crystals grew beneath this ice cover. That the water was supercooled was illustrated by the diver's observations of frazil in the water

column on 26 and 28 January. The perfect disk shape of these suspended crystals indicates low turbulence levels on these mornings.

Weak turbulence also contributes to large anchor ice crystals because it exerts relatively small shear stresses across the ice crystal face. With strong turbulence, formation of large anchor ice crystals is inhibited because they are broken up by shear in the flow or the crystals are lifted off the bottom before they can grow to large sizes. Research in rivers (Arden 1970; Arden and Wigle 1972; Tsang 1982; Wigle 1970) has shown this phenomena with frazil flocs: large frazil flocs may settle to a sand bed momentarily but they are soon lifted off by the force of the flow. Also, anchor ice masses in rivers tends to consist of shingles of small crystals (Wigle 1970, Arden and Wigle 1972, Arden 1970, Tsang 1982, Osterkamp 1983, Benson and Osterkamp 1974) rather than individual large crystals, presumably because shear stresses inhibit formation of large ice crystals.

In this report I have described four different anchor ice morphologies that represent a continuum. This continuum reflects the balance between the dynamic conditions in the nearshore zone and the morphology of the anchor ice masses formed there.

3.5.2 ANCHOR ICE AND SEDIMENT TRANSPORT

To evaluate the importance of floating ice as a sediment transport agent, it is necessary to know how much sediment the ice can carry. The maximum amount of sediment a volume of ice can carry in the water column is limited to the amount that brings the bulk density of sediment and ice mixture to bulk density of water at 0°C, that is:

$$\rho V_{i+s} = \rho_s V_s + \rho_i V_i \quad (3.5)$$

where ρ is density and V is volume and the subscripts w , i , s , and $i+s$ refer to water, ice, sediment, and ice plus sediment, respectively. V_{i+s} is the volume of ice plus sediment in a neutrally buoyant ice mass and is composed of fractional volumes of sediment (f_s) and ice (f_i) such that

$$V_s = f_s V_{i+s} \quad (3.6)$$

and

$$V_i = V_{i+s} - f_s V_{i+s} \quad (3.7)$$

or

$$V_i = V_{\text{tot}} (1 - f_s) \quad (3.8)$$

Substituting into equation 3.4 and simplifying gives

$$\rho_w = \rho_s f_s + \rho_i + \rho_i f_s \quad (3.9)$$

Substituting $\rho_w = 1.00 \text{ g cm}^{-3}$, $\rho_i = 0.917 \text{ g cm}^{-3}$, and $\rho_s = 2.65 \text{ g cm}^{-3}$ into equation 3.9 results in $f_s = 4.79\%$.

The volume of sediment in a neutrally buoyant ice/sediment block in fresh water is 4.79% of the total volume of the block. This value can be translated into the more common units of mass of sediment per unit volume by considering a neutrally buoyant block that has a volume of 1 liter. The mass of this block is 1000 g, and the mass of sediment in the block is equal to its volume times its density, or 127 g, so the sediment concentration is 127 g l^{-1} . Any ice with a sediment concentration of less than 127 g l^{-1} should float, and ice with greater sediment concentrations should sink in still, fresh water.

Sample 90-73, collected from the lake floor at Kohler-Andrae State Park on 20 February 1990 (Table 3.2) is an apparent contradiction to this calculation. This anchor ice sample collected from the bed had a sediment concentration of 50.9 g l^{-1} . The low sediment concentration measured in this sample must result from not sampling the entire anchor ice mass; only the top of an anchor ice mass with an inhomogenous sediment distribution was sampled.

Most of the floating anchor ice samples collected in this study carry well below their maximum sediment capacity (Table 3.4). There are three possible reasons for these low sediment concentrations in ice. First, sediment may wash out of a sample during collection. Divers observed this on several occasions; it indicates that the sediment was not firmly attached to the ice. Second low sediment concentrations may occur when anchor ice breaks free from the substrate and leaves most of the entrained sediment behind. This happens when there is a strong concentration gradient in the anchor ice, and only the most buoyant ice breaks free. This mechanism occurs when anchor ice has formed over boulders (Figures 3.5, 3.11) and the anchor ice mass never grows to a size where it will lift the boulder off the bottom. As the water warms in the morning, the bond between the ice and the boulder weakens and the whole mass of anchor ice with some amount of sediment breaks free of the bottom. This mechanism may also work in the

sand substrate, where some sand grains are firmly attached to the ice and other grains are only weakly attached. When the buoyancy of the ice becomes too great, the crystal breaks near the ice/sediment interface or between the strongly-bonded and weakly-bonded sand and lifts only a relatively small amount of sand to the surface.

The third possible reason for the low sediment concentrations seen in floating anchor ice samples may be a bias in the sampling technique. Anchor ice with high sediment concentrations will never rise to the surface where it can be collected. It is probable that anchor ice with high sediment concentrations were suspended in the water column where they were never seen and sampled (Benson and Osterkamp 1974; Gilfilian *et al.* 1972; Osterkamp and Gosink 1982). Divers occasionally saw large ice crystals suspended in the water column during diving traverses. Sample 91-119 (Figure 3.10), for example, had a sediment concentration of 102 g l^{-1} and was barely floating when found. Other nearly neutrally buoyant anchor ice crystals were occasionally observed. The logical end point is that ice which is negatively buoyant and is resting on the lake bed (as opposed to attached to the lake bed). This anchor ice was occasionally sampled (Table 3.2), and could have very high sediment concentrations. Sample 89-9, from Illinois Beach State Park, had a sediment concentration of 1140 g l^{-1} , but was still moving in the incident wave field at the time it was collected. This is an extreme example, and shows that ice buoyancy combined with waves and currents may move sediment that could not be moved by either mechanism alone.

Anchor ice also has the potential to lift large boulders off the bed into the water column. Dayton *et al.* (1969) report that anchor ice lifted masses of substrate estimated to weigh 25 kg from the bottom of McMurdo Sound, Antarctica. Martin (1981) reports that boulders weighing up to 30 kg are transported into the trash racks of water intakes of Swedish power plants. Nothing this large was observed in floating anchor ice in this study, but there is no reason southern Lake Michigan anchor ice could not lift boulders. Fahnestock *et al.* (1973) report finding a 20 kg shale block in a Lake Erie NIC. These authors suggest that the block was transported to an ice ridge by locally intense hydraulic forces at the outer edge of the NIC. An alternative explanation is that anchor ice buoyed the shale block up to the water surface before the block was incorporated into the NIC.

Anchor ice formation is common in the southern Lake Michigan nearshore zone. This ice, with attached sediment, is released from the lake bed on mornings following formation events. Incorporation of sediment-laden anchor ice into the water column results in ice rafting. At Gillson Beach and Kohler-Andrae State Park this sediment

transport is often offshore (Figure 3.15), so anchor ice results in a net loss of sand from the nearshore zone. Based on the Gillson Beach observations, an estimate of the amount of sand-sized sediment anchor ice carries into the water column can be made. Assuming 27 January 1991 represents a typical day and that January 1991 represents a typical year with 14 anchor ice producing events, the amount of sand carried to the surface by anchor ice is:

$$14 \text{ days} \times 100 \text{ kg per m of coastline day}^{-1} = 1400 \text{ kg per m of coastline year}^{-1}$$

Assuming a bulk sediment density of 1650 kg m^{-3} , this is 0.85 m^3 of sand per meter of coastline per year. Shabica and Pranchke (1994) estimate that there is 899 m^3 of sand per meter of beach at Gillson Beach. If anchor ice is removing this sand at the rate of $0.85 \text{ m}^3 \text{ year}^{-1}$, all of the sand would be removed from the beach in 1000 years. The Illinois beaches of Lake Michigan are sand starved (Chrzastowski and Trask 1995 ; Shabica and Pranschke 1994), so this loss of nearshore sediment by anchor ice processes may play a significant role in the total nearshore sand budget for southern Lake Michigan. Colman and Foster (1994) note that 25% of the recent surficial sediment in the southern Lake Michigan basin is sand. Much of this sand is removed from the nearshore zone and transported offshore by anchor ice formation, release, and subsequent melting in the warm center of the lake (Figure 1.1, Figure 3.15).

3.5.3 ANCHOR ICE DISTRIBUTION: DEPTHS

Anchor ice was a common phenomena in the nearshore zone at Gillson Beach. To evaluate the importance of anchor ice formation and release as a sediment transport mechanism, it is necessary to know the maximum depth of anchor ice formation. Observations at the Chicago cribs show that anchor ice forms to at least 11 m depth in southern Lake Michigan. The anchor ice samples at the cribs consisted of relatively small ice crystals suggesting that it formed under relatively turbulent conditions. Observations from Lake Ontario (Foulds and Wigle 1977) show that anchor ice consisting of large 'window glass' ice pieces formed in 7.6 m water around a crib intake. Foulds and Wigle also present indirect evidence that anchor ice can form to 17 m depth. Daly (1994) notes that blockages of water intakes has occurred to 20 m depths in lakes. He suggests that the large intake flow of the cribs may entrain supercooled flow from the surface and induce anchor ice growth at greater depths than under normal conditions.

Diving observations in this study show that anchor ice extends out to at least 4 m depth; indirect observations indicate anchor ice formation at greater deeper depths. On 28 January 1991 the lake surface at Gillson Beach was covered by solid ice all the way to the horizon. This ice had an specular reflection pattern. In the nearshore zone this pattern was caused by differential reflection of sunlight off of anchor ice crystals oriented at various angles, so I assume that the solid ice offshore was also congealed anchor ice. Nearshore bathymetric surveys show that the water is 7 m deep m 600 m offshore at Gillson Beach, so anchor ice had probably formed out to at least that depth on the night of the 27-28 January.

Another method of constraining the maximum depth of anchor ice formation is to determine the conditions of anchor ice formation, and then examine the local wave fields to determine how deep these conditions extend. Assuming that 27 January 1991 represents the calmest conditions that can initiate anchor ice formation and growth, a minimum near-bed maximum orbital velocity (u_m) of 0.11 m s^{-1} is required to form anchor ice. Table 1.1 summarizes the wave hindcast conditions of Hubertz *et al.* (1991). This table shows that waves with 1 -1.5 m amplitude and 4 to 4.9 s median wave period occur 10% of the time in southern Lake Michigan and that 2 to 2.5 m amplitude waves with 6 to 6.9 s periods occur 1% of the time. Assuming 1.25 m waves with 4.5 s period and 2.25 m waves with 6.5 period, and using the technique outlined by Clifton and Dingler (1984), conditions for anchor ice formation exist to 17 m depth 15% of the time (the sum of wave occurrences greater than 1.0 m, Table 1.1) and there is potential for anchor ice formation to 38 m depth 2% of the time. Of course, anchor ice would only occur when atmospheric conditions were favorable to extract sufficient heat from the water column to supercool the water to these depths. These calculated depths, particularly for 4.5 s period, 1.25 m amplitude waves are similar to reported depths of crib fouling from other large lakes (Daly 1991; Foulds and Wigle 1977) and suggest that waves have the potential to produce anchor ice formation at depths far beyond the nearshore zone.

3.5.4 ANCHOR ICE DISTRIBUTION: SUBSTRATES

Most published accounts indicate that anchor ice does not form on sand bottoms. Wigle (1970) states that anchor ice forms only on rock bottoms because of the lack of anchoring effects of sand. Arden and Wigle (1972) note that in the Niagara River ice will momentarily adhere to a sandy bottom before being swept away by the flow, but anchor ice does not normally form on sand. Gilfilian *et al.* (1972) report that in small Alaskan

streams anchor ice forms on rocks, but not on sand bottoms. They attribute the lack of anchor ice formation on sand to the dynamics of frazil ice particle motion and laminar flow layers at the stream bed, but do not present any details. Tsang (1982) states that anchor ice forms on boulders, stones, gravel, and coarse sand, but almost never forms on fine sand, silt, and clay substrates. Tsang gives two reasons for this: (1) Sand, silt, and clay particles are small, so they are easily lifted off the bed by the buoyancy of anchor ice before it can grow to large size and (2) Fine-grained bottoms are more under the influence of terrestrial heat because of a laminar sublayer. This laminar sublayer apparently reduces the heat flux from the bed, making fine grained beds slightly warmer than coarse-grained beds that extend into the turbulent flow. Anchor ice will only form on supercooled materials (Benedicks and Sederholm 1943; Piotrovich 1956; Tsang 1982), so if the bottom is not supercooled anchor ice will not form. Reimnitz *et al.* (1987) studied anchor ice formation in the nearshore zone in the Arctic Ocean near Prudhoe Bay, Alaska and report that anchor ice formed on sand substrates. However, most of the anchor ice they observed had a dense, sediment rich ice core surrounded by large ice crystals (similar to Sample 91-86, Figure 3.13 in this report). They suggest that anchor ice formed on sand in this location because the sand bed froze before anchor ice crystals grew out from it. They conjectured that the sand bed froze because interstitial water had a lower salinity than the overlying water column. Once the sand bed froze, it acted as a substrate for growth of ice crystals into the water column. In this scenario, anchor ice does not form on a sand substrate unless it is previously frozen.

Diving observations in this study show that anchor ice formed regularly on the sand bottom at Gillson Beach when conditions were favorable. Ice crystals were seen attached to non-ice-bonded bottom on the mornings of 18-19 and 25-28 January 1991. Grain size analysis (Tables 3.1 and 3.2) shows that the sediment entrained into anchor ice is predominately sand, indicating that most anchor ice in southern Lake Michigan formed on sand substrates. This study shows that there is no inherent reason why anchor ice cannot form on sand substrates. The most probable reason that most studies dismiss anchor ice formation on sand is that these studies focused on ice formation in turbulent rivers. In these conditions, anchor ice is unlikely to form on sand.

Another anchor ice fact that is commonly stated in the literature (Arden and Wigle 1972; Tsang 1985; Wigle 1970, Piotrovich, 1956) is that anchor ice remains attached to the substrate for as long as the water is supercooled and is released from the bottom as the water is warmed by the morning sun. This was observed at Gillson Beach: sediment rich

anchor ice masses rose to the surface on mornings following formation events (Figure 3.4). Usually these masses were not observed after 10 A.M. When multiple dives were made on a given day, large anchor ice crystals were often observed on the bed during the first dive of the day but later in the day these crystals would be gone. Large anchor ice crystals were never observed on the lakebed in the afternoon. The only time evidence for anchor ice was seen in the afternoon was on 22 January 1991, one of the coldest days of the study period (Figure 3.7); the evidence consisted of sediment-laden ice masses rising to the surface. These 22 January observations show that anchor ice can form during the day under some conditions.

The dense, sediment-rich anchor ice masses seen in southern Lake Michigan have the potential to last more than a single day at the lakebed. This was seen at Kohler-Andrae State Park in 1990 when sediment covered ice masses seen just lakeward of outer edge of the NIC on the afternoon of 19 February lasted through the night and formed a substrate for anchor ice crystal growth on the night of 19-20 February. The large anchor ice crystals that formed on this night rose from the bottom during the morning of the 20th, but the dense, sediment rich anchor ice masses lasted throughout the day. The rounded anchor ice mass collected at Illinois Beach State Park in 1989 and sample 91-133 from Gillson Beach (Figure 3.14) were also probably more than 1 day old, based on their size and density. On 23 January, there were large expanses of sediment-laden anchor ice on the nearshore lakebed at Gillson Beach. This sediment-laden ice potentially lasted for several days. No dives were made on January 24 or 25, so I cannot confirm that any of this anchor ice lasted for more than one day. When anchor ice blocks with high sand concentrations are exposed to water at the freezing point they do not necessarily separate from the substrate like large anchor ice crystals do because they are too thoroughly mixed with or buried by the substrate. Likewise, when these dense masses are exposed to current flow, they do not break off at the contact with the substrate like large, delicate anchor ice crystals do, instead, if a critical threshold velocity is exceeded, the whole sediment-rich block will be transported *en masse*. When these sediment rich anchor ice masses do last for more than one day, they make excellent substrates for the nightly growth of large, delicate crystals, as observed on several occasions at Gillson Beach and Kohler-Andrae State Park.

3.5.5 ANCHOR ICE MORPHOLOGY AND SEDIMENT CONCENTRATION: A CONTINUUM

The results and discussion sections of this chapter describe four different anchor ice morphologies. These four morphologies are summarized in Table 3.5. The four morphologic divisions are based on ice crystal size and sand content in the anchor ice. In this section, I argue that these four morphologies represent a continuum in anchor ice that occurs because of differing wave energy and substrate conditions. The continuum goes from fine-grained anchor ice with high sediment concentrations that form in high energy conditions to large, intertwined masses of ice delicate crystals that form in very quiet conditions. The wave tank studies showed that frazil will interact with suspended sediment to form dense masses of fine-grained anchor ice. Ackerman and Shen's tank studies (1994) show that suspended frazil is very efficient at entraining sediment from the water column. 23 January 1991 was the day with the most widespread occurrence of dense, sediment laden anchor ice masses on the lake bed at Gillson Beach (Figure 3.13), and the BSIP wave measurements made on that day indicate that the threshold of grain motion was far exceeded (Table 3.4), so this anchor ice was present when sediment was suspended in the water column. However, I suggest that the dense, sediment rich cores in samples like Figure 3.13 probably formed on the 21 January, a very cold day (Figure 3.7) with large waves. This suggestion is based on the observations of Reimnitz *et al.* (1987) who reported very similar anchor ice masses on the seaward side of a barrier island in the Alaskan Beaufort Sea after a storm. Reimnitz *et al.* speculate that the sediment rich masses formed because differential salinities caused freezing of interstitial water at the bed. However, the sediment-rich anchor ice sample they collected and melted had 25% excess water; an indication that the mass could not have formed simply by freezing of interstitial water. I propose that the dense, sediment rich anchor ice masses like those reported by Reimnitz *et al.* in the arctic nearshore and those observed at Gillson Beach and Kohler-Andrae State Park form by interactions of frazil and suspended sediment in the water column. Once the ice becomes heavy enough to sink to the lake bed, it is buried by sand settling from suspension or by migrating bedforms. The sediment burying this dense anchor ice firmly anchors it to the bed so it cannot rise to the surface. Once formed, this anchor ice may survive on the bottom for several days if the water temperature does not rise much above the freezing point. For this type of anchor ice to form, bottom material must be fine enough to be suspended by waves. This is what is represented in the "Substrate Size" column of Table 3.5: the top values in this column are the substrate size and the bottom are the size of material found in anchor ice samples.

Once a core of fine grained, negatively buoyant anchor ice forms, it can act as a substrate for large anchor ice crystal growth into the water column. The maximum size of the large ice crystals depends on the wave conditions at the time the anchor ice forms; in relatively large waves crystal of order 1 cm form (Figure 3.10), while in more quiet conditions ice crystals of order 10^1 - 10^2 cm form (Figure 3.5). If waves are decreasing during anchor ice growth, crystal size will increase upward in the anchor ice mass (Figure 3.10). A relationship between large crystal size and quiet conditions is supported in the literature (Daly 1984; Dayton *et al.* 1969; Foulds and Wigle 1977; Osterkamp and Gosink 1982; Piotrovich 1956; Schaefer 1950). However, for large masses of crystals as shown in Figure 3.5 to grow, there has to be a suitable substrate consisting of either heavy anchor ice (Figure 3.14) or boulders (Figure 3.10). These large masses of crystals are attached to the bed rather than growing into the bed and form during periods when there is little sand suspended in the water column, so they contain very low concentrations of entrained sediment. These crystals appear similar to large crystal masses reported from the Antarctic (Dayton 1989; Dayton *et al.* 1969) and have the potential to transport boulder-sized sediment.

I suggest that it is possible to go from the top row to the bottom row of Table 3.5 (fine-grained heavy anchor ice to large, low concentration anchor ice masses) as conditions in the nearshore zone abate following a cold storm. The Gillson Beach observations show that highly turbulent conditions are not necessary to form the individual large anchor ice crystals (Figure 3.10) on sand or boulder substrates or to form large masses of large anchor ice crystals (Figure 3.5) on boulders or heavy, fine grained anchor ice masses. These types of anchor ice formed on several cold, clear nights with offshore winds and essentially no waves.

The final column in Table 3.5 is a largely speculative attempt to determine how important the different anchor ice morphologies are for sediment transport. I base the relative transport potential on three factors: the frequency of formation of a particular anchor ice type, the percentage of anchor ice cover seen in the nearshore zone, and the sediment concentration ranges seen in the different types of samples. None of these parameters is well constrained, so I present these transport potentials as a hypothesis to be tested rather than as an observational fact. In particular, the dense, fine grained anchor ice forms in conditions that make it difficult to observe during formation. These conditions of large waves also offer the best potential for hydraulically induced or enhanced transport of large amounts of negatively buoyant ice that would never be observed on the water

surface. So, what Lyell (1873) suggested for the rivers in England and Scotland '... the principal transfer from place to place of pebbles and stones adhering to ice goes on unseen by us underwater' may also apply to sand, gravel and boulders (?) in southern Lake Michigan.

3.6 CONCLUSIONS

In the middle of the 19th century Lyell (1873, p. 360) wrote about the capacity for anchor ice to transport sediment in rivers:

"Pebbles and small pieces of rock may be seen intangled in ice, and floating annually down the Tay in Scotland, as far as the mouth of the river. Similar observations might doubtless be made respecting almost all of the larger rivers of England and Scotland; but there seems reason to suspect that the principal transfer from place to place of pebbles and stones adhering to ice goes on unseen by us under water. For although the specific gravity of the compound mass may cause it to sink, it may still be very buoyant, and easily borne along by a feeble current."

Since Lyell's observations there has been very little progress on the effects of anchor ice on sediment transport. There have been numerous observations of anchor ice transporting sediment (Arden 1970; Arden and Wigle 1972; Benson and Osterkamp 1974; Dayton *et al.* 1969; Gilfilian *et al.* 1972; Michel 1971; Osterkamp *et al.* 1983; Reimnitz *et al.* 1987; Tsang 1982; Wigle 1970), but none of these published accounts made any attempt to quantify the sediment concentration or size distribution found in anchor ice samples.

In this report, I document the occurrence of anchor ice in southern Lake Michigan. Anchor ice is very common in southern Lake Michigan: at Gillson Beach it formed on fourteen nights between 1 January and 1 February 1. This anchor ice formed on sand, pebble, cobble and boulder substrates, and was released from the bed on mornings following formation events.

This formation and release of anchor ice results in sand transport that is not restricted to the nearshore zone. Twenty-four floating anchor ice samples were collected for this study. These samples had sand concentrations ranging from 1.2 to 102 g l⁻¹, with a mean concentration of 25.7 g l⁻¹. Six negatively buoyant anchor ice samples were also collected from the lake bed. Sand concentrations in these samples ranged from 51 to 1140 g l⁻¹. The largest sedimentary clast recovered from anchor ice at Gillson Beach was

5 cm x 3 cm x 1 cm with a mass of 30 g. This is a fairly modest clast, anchor ice has the potential to lift much larger material from the bed. All of the samples collected were potentially mobile, and had the ability to transport sediment out of the nearshore zone.

One of the most surprising results of this study is that the "highly turbulent conditions" of Tsang (1982) or "the intensive wind mixing" of Piotrovich (1956) may not be necessary for anchor ice growth. These terms conjure up images of rock-studded rapids or breaking waves and boiling eddies producing anchor ice. At Gillson Beach and Kohler-Andrae State Park anchor ice formed during calm conditions. Surf zone wave measurements show that there was a rough turbulent wave boundary layer on even the calmest night when anchor ice formed, but the water surface appeared 'calm as a mill pond.' Anchor ice was never observed when conditions were extremely rough because *in situ* observations could not be made at those times. We do not know what happens during storms, but I suggest that large amounts of fine-grained, negatively buoyant, sediment rich anchor ice masses form in the nearshore zone under storm conditions. This is an area where more work needs to be done; there should be an effort to quantify the relationship between turbulence conditions and anchor ice formation. This effort should include study of the relationships between turbulence level and anchor ice crystal size, turbulence level and sediment concentration in anchor ice samples, and turbulence level and the size of bed material that anchor ice forms on.

What is clear from this study is that anchor ice is common in southern Lake Michigan, forming on 40% of the nights at Gillson Beach during January 1991. This anchor ice entrains sand into the water column, where it is transported alongshore and offshore. The regular formation of anchor ice in the nearshore zone is slowly removing sand from the sand-starved southwestern shoreline of southern Lake Michigan.

CHAPTER 4: THE SLUSH ICE ZONE

4.1 INTRODUCTION

The nearshore zone of the Great Lakes is ice covered for two to four months each year. This ice consists of a combination of stable and mobile ice types. The relatively stable ice, known as the nearshore ice complex (the NIC, discussed in Chapter 2) remains attached to the coast for periods of days to months. Lakeward of the NIC there is an zone of mobile, intermittent ice consisting of a combination of brash ice (fragments of ice less than 2 m across, the wreckage of other forms of ice) and slush ice (an accumulation of water-saturated ice crystals that may or may not be slightly frozen together, U.S. Navy 1952). Slush ice consists of floating frazil crystals, water-saturated snow, floating anchor ice, or some other ice morphology. In this report I call the mobile ice *slush ice*, and the zone where it is found the *slush ice zone* (Figure 1.2)

Because slush ice is unconsolidated and mobile, its width, depth, and concentration tend to be highly variable in time and space. When present, the width of the slush ice zone can vary from a few meters up to 17 kilometers or more (O'Hara and Ayers 1972). Near the shoreline, the floating slush ice tends to form a lakeward-thinning wedge (Figure 1.2) but is often thick enough to be in contact with the lakebed at depths of a meter or more (Marsh *et al.* 1973). Slush ice distributions change quickly with changes in wind and incident wave directions. Often, a band of slush ice will be advected onshore from over the horizon shortly after the change to an onshore wind. Conversely, the change to offshore wind can advect nearshore slush ice out to the center of the lake. Floating slush ice is extremely important because it is responsible for any ice rafting (*i.e.* ice induced sediment transport) which occurs in southern Lake Michigan.

Early studies of Great Lakes ice focused on the importance of the NIC in shoreline protection. Many of these studies recognized that slush ice is a necessary component for formation of the NIC (Evenson and Cohn 1979; Marsh *et al.* 1976; Marsh *et al.* 1973), but did not explicitly state the importance of slush ice for sediment transport. Evenson and Cohn (1979) state that sediment incorporated into the NIC can be transported offshore when the NIC is destroyed, but say nothing about sediment transport by the unincorporated slush ice. O'Hara and Ayers (1972) note that brash ice masses

incorporated into the NIC had 'considerable sand' entrained in them during their initial formation 'at a distant site', but say nothing more about sediment transport by mobile ice.

Miner and Powell (1991) directly address the question of how NIC formation and destruction at Gillson Beach could contribute to ice rafting. They determine that the NIC is mainly destroyed through wave action rather than by melting, so sediment-laden ice is released into the nearshore zone for ice rafting. They were able to establish the amount of sediment incorporated into the NIC during the winter of 1989, but could not determine the importance of ice rafting to the overall littoral budget. There are two curious facets of the Miner and Powell study. First, like previous studies, they deal with sediment incorporation into the NIC and say nothing about potential sediment transport by other ice in the slush ice zone. Second, they recognize that destruction of the NIC can lead to longshore ice rafting, but do not recognize the potential for direct offshore ice rafting.

Reimnitz *et al.* (1991) note the importance of slush ice for ice rafting. They used three methods to study ice rafting by slush ice in southern Lake Michigan: (1) aerial reconnaissance flights along Lake Michigan's western shore to map the distribution of slush ice; (2) an ice sampling cruise in February 1990 to determine the characteristics of sediment in offshore ice; and (3) satellite imagery to determine ice drift patterns. They found that slush ice drifting along the southwest shore of Lake Michigan is deflected offshore at promontories. The aerial reconnaissance showed that these offshore ice streamers dissipate 5 km offshore. Satellite imagery showed that ice streamers sometimes cross the entire lake. Reimnitz *et al.* (1991) collected sixteen offshore ice samples between Milwaukee and Sheboygan Wisconsin. Fifteen of these samples contained sand and gravel. Sediment concentrations were determined for only two samples, these samples had 19.6 g l^{-1} and 21.0 g l^{-1} of entrained sand.

Barnes *et al.* (1992, 1994) studied ice formation in southern Lake Michigan and collected a number of slush ice samples in the coastal zone. Barnes *et al.* estimate for a three year period that ice rafting transports to 0.35 to $2.7 \times 10^3 \text{ kg}$ of sediment day^{-1} along the southwest shore of Lake Michigan during the ice season. They state that more sediment is transported alongshore than offshore. Barnes *et al.* (1992) note that sediment is ubiquitous in slush ice, and that this 'nearly submerged, often visually inconspicuous ice zone, which is easily overlooked' is the major contributor to ice rafting. Barnes *et al.* (1994) note that once sediment is entrained into the slush ice layer, it is easily transported

long distances and that jetties and groins do not stop littoral transport of slush ice but rather deflect the slush-ice stream offshore.

To evaluate the importance of slush ice for ice rafting, it is necessary to determine a number of parameters for the slush ice zone including (1) thickness (depth), (2) width, (3) sediment concentration, (4) ice concentration and (5) direction of ice drift. In this chapter I present the following potpourri of field observations of slush ice from southern Lake Michigan: (1) Measurements of the vertical distribution of sediment in the water column when slush ice was present at Kohler-Andrae State Park in February 1989; (2) A comparison of ice rafting to longshore sediment transport at Gillson Beach in December 1989; (3) Slush ice observations and ice rafting estimates at Gillson Beach during January 1991; and (4) Results of drifter studies that suggest the direction of ice rafting in southern Lake Michigan. Together these observations illustrate the importance of ice rafting on the nearshore sand budget for southwestern Lake Michigan.

4.2 THE VERTICAL DISTRIBUTION OF SEDIMENT IN THE SLUSH ICE ZONE

The slush ice zone is basically a surf zone with the addition of a layer of floating, mobile, fine-grained, unconsolidated ice. One of the goals of this study was to determine the vertical distribution of sediment in the slush ice zone and compare it to published observations of sediment distribution in an ice-free surf zone. Kana (1976) developed a mechanical sampler (here called the *Kana sampler*) that simultaneously collects several water samples in a vertical array. Kana samplers were used in southern Lake Michigan in an attempt to determine the vertical sediment distribution in the nearshore slush ice zone.

The Kana sampler consists of a two-meter-long vertical mounting pole which holds several Van Dorn-type sample bottles in a horizontal position (Kana 1976). The Van Dorn-type samplers are cylinders with doors on both ends. These doors are held open by a trigger mechanism when the sampler is deployed. When a trigger on the bottom of the mounting pole is jammed into the lakebed, the doors slam shut and a sample is retained. Two types of sample bottles were used with the Kana samplers in southern Lake Michigan. One type of bottle was the original two-liter bottle designed by Kana (1976). This bottle was made of 20 cm long by 12.7 cm diameter acrylic with doors machined from sheet PVC and sealed with an O-ring. The second bottle type was made from 30 cm long by 8 cm diameter acrylic with doors made of foam rubber balls.

Both types of Kana samplers were tried on a number of occasions at different locations around southern Lake Michigan. Generally, the Kana samplers performed very poorly in the slush-ice covered nearshore zone. The major problem with these samplers was that ice often kept the samplers from closing properly. This problem was especially severe with the O-ring sealed bottles. A small amount of ice fouling the O-ring would allow the sample volume to drain before the sampler could be returned to the beach for processing. Bottles with the foam-rubber-ball caps worked better because the balls could be pushed into the sample cylinder after the Kana sampler was tripped, which usually resulted in a good seal. Even when the samplers worked, samples were often spilled during transfer from sampling jars to storage containers. Draining the samplers required a level of manual dexterity that was difficult to achieve with cold, wet hands. The result is that only one good set of samples was collected with the Kana samplers in the slush ice zone.

The one good Kana-sampler set was collected at Kohler-Andrae State Park, Wisconsin (Figure 1.1), on 17 February 1990 with the 8 cm diameter bottles. On this day there was an eleven meter wide nearshore ice complex at Kohler-Andrae State Park (Figures 4.1 and 4.2a). Lakeward of the NIC, a twenty meter wide band of slush ice was drifting southward at 4 cm s^{-1} . Spilling breakers at the outer edge of the slush ice zone were estimated to be less than 30 cm high (Figure 4.1). Four sample arrays were collected across the slush-ice zone, at distances of 12 m, 16.5 m, 23.5 m, and 29.5 m from shore (Figure 4.2). An array consists of a set of vertical samples that are simultaneously collected. Samples were collected at 10, 44.5, and 84 cm above the bed at the outer stations. At the inner station (S1 in Figure 4.2) the water was 60 cm deep so only two samples were collected. All sample sets were collected when the crest of a bore passed by to minimize suspended sediment load variation associated with position relative to the wave crest (Zampol and Inman 1989).

Figure 4.2b shows the vertical sediment distributions at the four sampling stations. Sediment concentrations in the eleven samples range from 0.5 to 4.8 g l^{-1} . Visual examination of the samples show that they were predominately sand. Note that the y-axis in each plot of Figure 4.2b varies. At station S1, the sediment concentration decreases with increasing height above the bed. Stations S2, S3 and S4 have sediment concentration inversions, with higher sediment concentrations near the top of the water



Figure 4.1. Photograph of the slush ice zone at Kohler-Andrae State Park on 17 February 1990. A set of samples showing the vertical distribution of sediment in the slush ice zone was collected on this day. The man in the water on the far right is holding a Kana sampler.

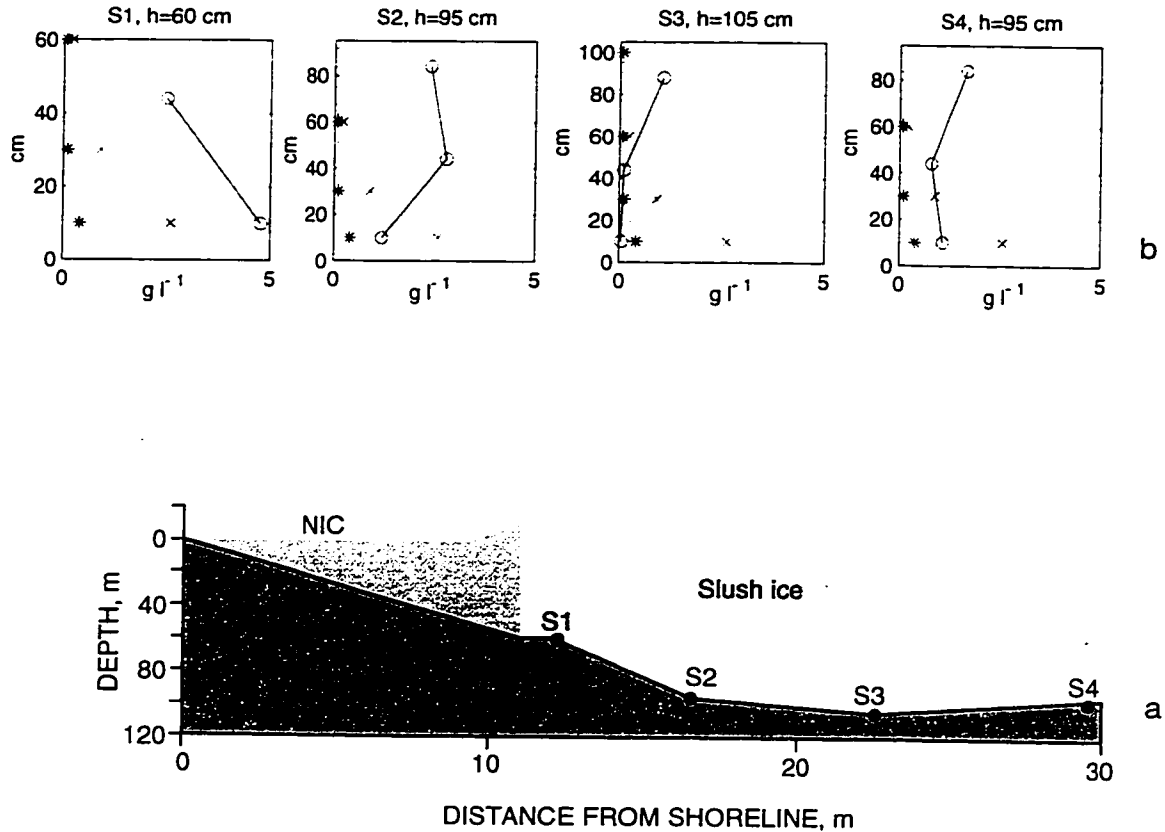


Figure 4.2. a. Sketch of nearshore zone at Kohler-Andre State Park on 17 February 1990 showing the NIC, the slush ice zone and positions where Kana samplers were used to collect sediment and slush ice samples. b. Vertical sediment concentration profiles in the water column and slush ice at Kohler-Andre State Park on 17 February 1990 (solid lines) along with average data for ice-free conditions at a South Carolina ocean beach from Kana (1979, Figure 31). Solid/circle: array data from slush ice zone at Kohler-Andrae State Park; dotted/asterick: Kana's data for spilling waves; dotted/x's: Kana's data for plunging waves. Note differences in vertical scale for the four plots.

column. At station S1 slush ice was present in the 10-cm-elevation sample, so I assume that slush ice extended all the way to the lake bed. At the other three sampling stations slush ice was present in the upper two sample bottles, but not in the 10-cm bottles.

For an ice free nearshore zone, the suspended sediment concentrations decrease exponentially with height above the bed (Downing 1983). For a rippled sand bottom in a wave field, sediment concentrations can decrease by a factor of 100 in 25 cm (Neilsen 1984). In a study of an ice free ocean beach in South Carolina, Kana (1979) found that, in general, sediment concentration decreased with height above the bed for both spilling and plunging breakers, although plunging breakers suspended up to an order of magnitude more sediment than spilling breakers. Kana's curves of average sediment concentration with height above the bed (Figure 31 of Kana 1979) are plotted along with the array data from Kohler-Andrae State Park slush ice zone (Figure 4.2b).

Concentration profiles in slush ice do not show an exponential decrease in height above the bed, which shows that slush ice has a large affect on the sediment concentration profile. Only S1 from Kohler-Andrae has decreasing sediment concentration with increasing height above the bed (Figure 4.2b). This is also the only array where slush ice was found in the 10-cm-elevation sample. S2, S3 and S4 all had their highest sediment concentrations near the top of the water column (Figure 4.2b) where slush ice was also present.

The inverted concentration profiles in these outer arrays is explained by slush ice buoyantly holding the 'suspended' sediment near the top of the water column. The slush ice is also 'suspending' sediment at S1, but at this location the slush ice extends all the way to the bed resulting in a normal (*i.e.* not inverted) concentration gradient. This sample set, comprised of four arrays with eleven total samples is very small, so the results must not be viewed as the definitive work on vertical sediment distributions when slush ice is present in the nearshore zone. Many more samples, in different wave regimes, must be collected to confirm this result. However, the data suggests that the method of sediment 'suspension' is fundamentally different in the slush ice zone compared to an ice-free nearshore zone. When slush ice is present, no turbulence is necessary to keep sediment in suspension, instead, the buoyant force of the ice keeps the entrained sediment near the top of the water column. Note that this says nothing about the necessity of turbulence for entraining sediment into the floating slush ice. The specific

interactions that lead to sediment incorporation into slush ice is an area that needs more study.

4.3 ICE RAFTING AT GILLSON BEACH, DECEMBER 1989

On 11 and 12 December 1989 it was possible to estimate ice rafting at Gillson Beach (Figure 1.1). Twelve slush ice and four brash ice samples were collected at Gillson Beach on these days. The samples and surf zone measurements made during these two days allow estimation of the amount of ice rafting that occurred during this time. At this time there was a 40 m wide NIC at Gillson Beach that terminated in water 70 cm deep. For several days prior to sampling, air temperatures had been below freezing. On 11 and 12 December, divers estimated that the slush ice zone varied in width from 5 to 20 m and in depth from 0.25 to 0.60 m. There were two distinct ice types in the slush ice zone: unconsolidated slush ice and well indurated, sediment-laden brash ice pieces with diameters of 10 to 100 cm. Brash ice was estimated to be 2 to 5% of the total ice in the slush ice zone.

Ice samples were collected by dipping a bucket into the slush ice and collecting a sample of ice and interstitial water. In eight of the slush ice samples, ice was separated from interstitial water by draining through a sieve before melting. The ice concentration for these samples was determined by melting the ice, measuring the melt water volume, converting the melt volume to an ice volume by assuming an ice density of 0.917 g cm^{-3} , and dividing the ice volume by the volume of ice plus water. After decanting the melt water and oven-drying, sediment concentrations were determined by dividing sediment mass by the volume of ice plus water. The grain size distributions in four of the 1989 slush ice samples were determined by settling tube analysis, and grain size statistics were calculated using the method of moments (Krumbein and Pettijohn 1938). Table 4.1 gives the average sediment concentrations for the brash and slush ice samples collected in December 1989. The four samples that were analyzed for grain size had mean sizes range from 2.04 to 2.41 ϕ , with a mean of 2.19 ϕ ; all of the samples were moderately well sorted, fine grained sand.

Two methods were used to measure longshore drift rates. On 11 December the drift rates of 17 different pieces of brash ice were timed over a measured distance. The average drift rate of these ice pieces was $30 \pm 13 \text{ cm s}^{-1}$ to the southeast. On 12 December

Table 4.1. Sediment concentrations in Gillson Beach slush ice samples.

Year	Ice Type	Number of Samples	Sediment Concentration Range (g l ⁻¹)	Sediment Concentration Mean (Std) (g l ⁻¹)
1989	Slush ice	11	0.6 - 3.3	1.6 (0.7)
	Brash ice	5	7.5 - 53.8	23.4 (18.7)
1991	Combined Brash + Slush	40	0.03 - 42.8*	4.3 (7.8)*

*1991 bulk sediment concentrations are based on a mean ice concentration of 0.56

longshore currents were measured for three-minute sampling periods at three locations across the slush ice zone with a General Oceanics Flow Meter suspended at 20 cm depth. The average measured longshore current was 30 ± 6 cm s⁻¹ for these three measurements. Wave periods of 5 s were estimated for both days. Breaker heights were independently estimated by two observers, the average for the two observers was 85 cm.

Based on the observations made on 11 and 12 December, it is possible to estimate the amount of ice rafting in the slush ice zone on these two days. I assume that for the two day period, the slush ice band was on average 10 m wide and 0.35 m thick. I assume that 98% of the ice in the band was slush ice with a mean sediment concentration of 1.6 kg m⁻³. The remaining 2% of the ice was brash ice with a mean sediment concentration of 23.4 kg m⁻³ (Table 4.1). The longshore drift rate was 30 cm s⁻¹ and the sediment is assumed to have a bulk density of 1650 kg m⁻³. Based on these values, the slush ice transported 110 m³ day⁻¹ of sand sized sediment to the southeast.

This estimate of 110 m³ day⁻¹ of longshore ice rafting at Gillson Beach in December 1989 is hard to evaluate without something for comparison. A fundamental equation for longshore sand transport is given by Komar (1983):

$$Q_s = 2.5(EN)_b \frac{v_l}{u_m} \quad (4.1)$$

where Q_s is the longshore sand transport rate (m³ day⁻¹), $(EN)_b$ is the wave energy flux at the breakpoint, v_l is the mean longshore current velocity and u_m is the maximum near

bed wave orbital velocity. To solve this equation for the observed wave conditions a correction must be made. Komar (1976, p. 78) notes that visually observed or estimated wave heights correspond roughly to the significant wave height, which is 1.41 times greater than the root-mean-square wave height normally used in this equation. Thus, in solving this equation, the observed (significant) wave height of 85 cm was reduced to an (rms) wave height of 60 cm. To determine the wave speed (C) and orbital velocity used to solve this equation, it is necessary to know the water depth at the breaking wave. This depth was calculated based on the widely accepted (Komar 1976) critical breaking criteria of

$$\left(\frac{H}{h}\right)_{\max} = 0.78 \quad (4.2)$$

where H is the wave height and h is water depth.

For the wave conditions observed at Gillson Beach, equation 4.1 predicts a longshore sand transport rate of 860 m³ day⁻¹. Thus, the amount of sand carried in a relatively small slush ice band is about 13% of the total predicted sand transport for the given nearshore conditions. Considering that the slush ice band was relatively narrow and thin during the observation period (the mobile ice band can often be several hundred meters wide and extend all the way to the bed), these observations show that ice can account for a significant portion of the sand transport along Great Lakes shorelines.

4.4 GILLSON BEACH OBSERVATIONS JANUARY 1991

The dynamic nature of ice in the nearshore zone requires frequent observations to document changes. This requirement, combined with the difficulty of working in an ice-covered nearshore zone, led to installation of a time-lapse video system at Gillson Beach during January 1991. This system was used to determine the width and drift rate of the slush ice which are two of the parameters necessary for determining the amount of ice rafting. Similar systems have been useful for studying open-water nearshore processes (Lippmann and Holman 1989; Lippmann and Holman 1990). Time-lapse photography has been used by Seibel *et al.* (1976) and Seibel (1986) to monitor changes in the NIC at a site in southeastern Lake Michigan. In this section, video-determined ice-drift rates and

ice-zone widths are combined with data on sediment content and ice thickness to estimate ice rafting.

The video system consisted of a single lakeward-looking black-and-white video camera mounted on a 10-m tower. The camera/lens combination imaged the entire cross shore from the upper beach to the horizon (Figures 2.1 and 4.3). The tower was located 1 m lakeward and 6.6 m to the southeast of the origin of a beach survey reference grid system established by McCormick *et al.* (1991) and was approximately 50 m from the shoreline (Figure 1.3). The video system was operational between 16 January and 1 February 1991, but data for 31 January were lost. The data set covers daylight hours for a 16-day period. Information on the stability of the video imaging system can be found in Kempema and Holman (1994).

In addition to the video record, 40 slush ice samples were collected at Gillson Beach in January 1991. All of these samples were collected with a mesh 2 mm dip net, so they differ from the 1989 samples because only the ice and sediment was retained and calculated sediment concentrations are for a given volume of drained ice, not a given volume of ice plus water in the water column. In order to determine the bulk sediment concentration in a given volume of ice and water, I used the average ice concentration (56%) determined for the 1989 Gillson Beach slush ice samples. The bulk sediment concentrations in the slush ice are given in Table 4.1. Sediment grain size analysis was performed on six of the 1991 samples, using sieves and the method of moments to determine sediment size characteristics (Krumbein and Pettijohn 1938). The range and mean values of the bulk sediment concentrations for the 40 slush ice samples collected in 1991 are given in Table 4.1. The mean grain sizes for seven of these samples ranged from 1.82 to 2.65 ϕ , with the mean of the means falling at 2.13 ϕ .

An obvious characteristic of a video system is that it cannot see through obstructions. At Gillson Beach, a grounded ice ridge up to 4 m high formed 90 m from the camera tower in 1991 (Figure 2.5). With the geometry used at Gillson Beach, a three to four meter high ridge in this position projects onto the lake surface 130 to 150 m from the tower. Everything between the ridge and its projection on the lake surface is in a "shadow zone" and is hidden from the camera view. Thus, the inner portion of the slush ice zone adjacent to the NIC was not visible to the video system. Analysis of the video record shows the dynamic nature of the slush ice zone. A total of 140 hours of video

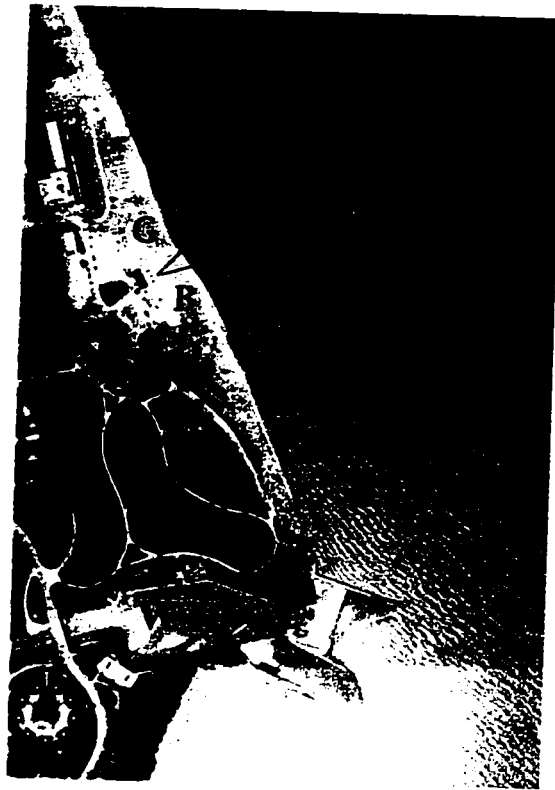


Figure 4.3. Aerial view of Gillson Beach during ice-free conditions (24 March 1991). The large, tilted 'V' marks the field of view of the video camera; the apex marks the position of the 10 m camera tower. WH: Wilmette Harbor. GB: Gillson Beach. Photo from the Illinois Department of Transportation.

records were obtained; of that brash and slush ice were visible for 75 hours, or 54% of the time. Slush ice was present for at least part of the day on 12 of the 16 study days. Brash and slush ice were usually present in the morning but often dissipated by noon. The slush ice zone consisted of a relatively dense band against the outer edge of the NIC for 39 hours; for another 36 hours the ice was widely dispersed, with areas of open water between ice masses or with a wide band of open water between the slush ice zone and the outer edge of the NIC.

On eleven of the twelve days when ice was present it was possible to measure ice-drift velocities from the video records. The number of ice-drift measurements made on a given day varied from 3 to 101; these measurements covered an offshore distance of 106 to 672 m from the camera tower (Table 4.2). A total of 315 individual ice-drift measurements were made. Ice-drift velocities were measured by digitizing the position of a piece of ice at two different times. The number of drift rates determined for a day depended on the number of suitable targets in the video record. To be a suitable target, a piece of ice had to be recognizable so that it could be tracked in the moving slush ice field; therefore, drift rates were determined by tracking pieces of brash ice. Trackable brash was not always present in the slush ice zone. On 29 January there was a very uniform band of slush ice with no trackable targets, so no ice-drift measurements could be made, even though the video record qualitatively shows longshore drift to the southeast.

Figure 4.4 shows a typical set of daily ice drift vectors, collected on 23 January. The field of view of the camera and the outer edge of the NIC are also shown. The wind direction during the period when ice-drift measurements were made was constant from 257° (relative to the reference grid, with 0° pointing offshore, the geographic wind direction was 225°T ; Figure 1.3), and the mean wind speed was 7.7 m s^{-1} . The mean ice-drift rate on 23 January was 0.293 m s^{-1} at a reference grid direction of 74° . The gap of 30 m between the outer edge of the NIC and the innermost ice drift vector is the shadow zone formed by NIC ridges.

Table 4.2 lists the daily mean longshore and cross shore ice drift velocity components, the number of drift measurements made each day and the time periods over which measurements were made. Longshore ice drift rates varied between 0.05 and 0.38 m s^{-1} . Longshore drift was predominately to the southeast, northwesterly drift occurred only on 22 January, a day when the cross shore component of ice drift

Table 4.2: Mean video ice-drift rate measurements made at Gillson Beach in January 1991.

Date Jan. 1991	Time	# of Drift Measure- ments	Video Mean Cross Shore Velocity (m s ⁻¹)	σ (m s ⁻¹)	Video Mean Longshore Velocity (m s ⁻¹)	σ (m s ⁻¹)
16	0935- 1035	3	0.03	0.05	0.11	0.07
17	0757- 1059	29	0.04	0.07	0.19	0.05
20	0815- 0855	9	0.01	0.07	0.27	0.05
21	0808- 1657	54	0.05	0.14	0.38	0.08
22	1015- 1230	13	0.11	0.03	-0.09	0.05
23	0812- 0915	13	0.08	0.15	0.28	0.06
25	0831- 1705	101	0.02	0.06	0.11	0.04
26	0810- 1037	16	0.10	0.05	0.05	0.02
27	0757- 1144	11	0.13	0.07	0.05	0.04
28	0753- 1120	32	0.03	0.14	0.12	0.04
30	0836- 1610	34	0.03	0.14	0.12	0.05

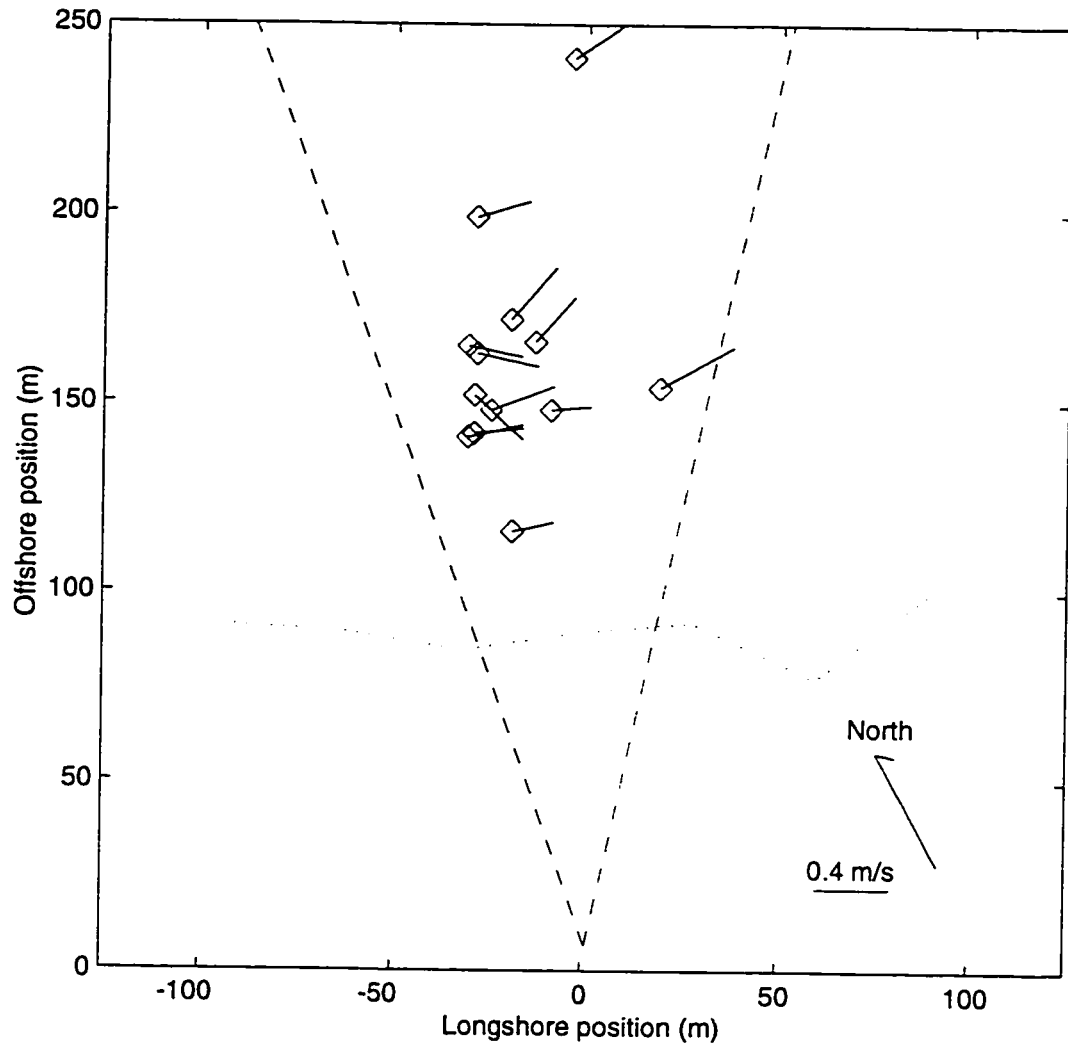


Figure 4.4. Vector plot of ice drift measurements made on 23 January 1991. The diamonds mark the mean position of a single ice drift measurement, barbs point in the direction of drift. The length of the barbs is proportional to the drift rate; a scale bar for drift rate is in the lower right corner of the figure. The shore parallel dotted line marks the position of the outer edge of the NIC; the dashed lines mark the field of view of the camera (Figure 4.3).

dominated. Daily mean cross-shore ice-drift velocities varied from 0.01 to 0.13 m s⁻¹ (Table 4.2). Daily mean cross-shore components of ice drift were consistently offshore, although individual ice drift measurements often had an onshore component (Figure 4.4). Days when cross-shore drift velocities were highest (22, 23, 26, 27 and 28 January 1991) were characterized by widely dispersed anchor ice which was released from the lake bottom in the morning. These mornings were also characterized by strong offshore wind components.

The U.S. Coast Guard Station at Wilmette Harbor (Figure 4.3) maintains a marine coastal weather log. Wind speed and direction are recorded daily at 2-hour intervals beginning at 0600 local time. These data recorded no major storm events during the study period; the strongest winds blew offshore so that no large waves developed at the study site. These consistent offshore winds, combined with mild temperatures during the winter of 1990-91, may account for the relatively small amount of slush ice seen during the study period. Weather data were used to check for correlation between the daily mean components of ice drift and wind stress. Mean winds were calculated by averaging wind speed and direction from 0600 through the time when ice was present (for example, on 17 January, when ice was present from 0757 to 1059, wind components were calculated by using wind values measured at 0600, 0800, 1000, and 1200). Mean longshore and cross shore components of wind stress, proportional to velocity squared, were calculated from the wind data. The correlation coefficients between the longshore and cross-shore wind stresses and ice-drift rates are $r = 0.64$ and $r = 0.87$, respectively. The high correlation between the cross-shore components confirmed visual observations made at the inner edge of the slush ice zone. On days when ice concentrations were low and offshore winds were strong, ice was rapidly advected offshore. This combination of conditions explains the morning disappearance of the slush ice zone on many days (Table 4.2).

Recent research has documented sediment transport by nearshore ice (Reimnitz *et al.* 1991, Miner and Powell 1991, Barnes *et al.* 1992 and 1994). The ice-rafted sediment flux, defined as the volume of sediment passing over a meter of bottom in either the longshore or cross shore direction, can be found by:

$$Q_{si} = C_s * T_i * U \quad (4.3)$$

where Q_{si} is the sediment flux, C_s is the sediment concentration in a volume of ice and water, T_i is the thickness of the slush ice, and U is the vector mean ice drift velocity. Each of these parameters is difficult to measure, primarily because of the necessity of working in a freezing, wet environment. Video monitoring of the slush ice zone provides a relatively simple method of determining the components of the drift velocity.

To determine the total longshore sediment transport rate, the longshore component of flux must be multiplied by the width of the slush ice zone. To determine this width with the video system it is necessary to have a relatively continuous band of slush ice whose inner edge is in contact with the NIC. On 22, 23, 26, 27 and 28 January, floating anchor ice was widely dispersed in the nearshore zone and surrounded by large areas of open water. For this situation it is not possible to estimate the ice concentration so fluxes and sediment transport rates cannot be calculated. However, for six days it is possible to calculate longshore and cross shore fluxes and longshore ice rafting rates (Table 4.3). The width of the slush ice zone could not be directly determined from the video record because the inner edge of the continuous slush ice zone fell in the video shadow zone created by NIC ridges. For periods when the nearshore slush ice coverage on the video record is continuous, I assume that the inner edge of the slush zone corresponds to the outer edge of the NIC. The slush ice band often varied in width throughout the day but average daily width values were determined by analyzing the video records. C_s for 16, 17, 20 and 21 January is the mean sediment concentration of the 40 slush ice samples collected at Gillson Beach in 1991 (Table 4.1). Slush ice thickness (T_i) for these days is an average value based on divers' observations.

On both 25 and 30 January the slush ice zone was atypical, so average values of C_s and T_i were not used to calculate ice rafting. On 25 January, the ice cover consisted of a thin, solid sheet underlain by a slush ice layer 0.05 m thick. The sediment concentration used for this day's calculation is the average of two samples collected within 20 m of the NIC edge. On 30 January, divers observed pancake ice more than 5 m in diameter and up to 2.5 m thick filling the slush ice zone. The pancakes consisted of brash and slush ice with highly variable sediment concentrations. The sediment concentration used to calculate transport rates on this day is the weighted average of three samples collected about 300 m from shore. A weighted average is used because divers who sampled the slush ice estimated that 95 percent of the ice had low sediment concentrations (mean value

Table 4.3. Calculated longshore and cross shore ice-rafted sediment transport at Gillson Beach in January 1991.

Date January 1991	Time of Continuous Slush Ice Band (hr)	Width of Continuous Slush Ice Band (m)	Slush Ice Depth (m)	Bulk Sediment Conc. (kg m ⁻³)	Cross Shore Sediment Flux (m ³ m ⁻¹ hr ⁻¹)	Longshore Sediment Flux (m ³ m ⁻¹ hr ⁻¹)	Longshore Sediment Transport Rate (m ³ hr ⁻¹)
16	1	72	0.30	4.3	0.08	0.31	22
17	3	60	0.30	4.3	0.11	0.53	32
20	1	50	0.30	4.3	0.03	0.76	38
21	9	110	0.30	4.3	0.14	1.06	120
25	9	210	0.05	0.4	0.001	0.004	0.8
30	8	300	2.50	0.2	0.03	0.13	40

of two samples); the remaining 5 percent consisted of ice with much higher sediment concentrations.

Table 4.3 gives the calculated longshore and cross shore components of ice-rafted sediment flux and longshore sediment transport rates. These estimated fluxes and longshore transport rates offer insights into the amount of sediment transported by ice. However, they severely underestimate the total amount of sediment transported during the study period for three reasons: (1) Estimates of ice-induced sediment transport could be made for only 31 of the 75 hours when ice was present. (2) Even on days when a continuous ice band was present there were also bands of dispersed ice further offshore. This widely scattered ice was not included in sediment transport calculations. (3) Only daylight hours were considered when sediment transport rates were calculated, even though ice was often present at night.

In summary, deployment of the video system at Gillson Beach showed that video monitoring of the winter nearshore zone can supply important information on nearshore ice characteristics. Brash and slush ice were easily discernible in the video record. The video system showed that brash and slush were common in the morning but often dissipated in the afternoon. When this mobile ice was present, the longshore and cross-shore components of ice drift could often be determined. During the study, daily mean longshore components of ice drift varied from 0.05 to 0.38 m s⁻¹; mean drift to the south occurred on 10 of the 11 days when drift direction could be determined. The daily mean cross-shore component of ice drift was consistently offshore and ranged from 0.01 to 0.13 m s⁻¹. This offshore drift component accounts for the disappearance of ice from the nearshore zone during many mornings when brash and slush ice were present (Table 4.2). This net offshore drift also results in a net loss of sand from the nearshore zone of southwestern Lake Michigan during the ice season.

Although the video system makes it relatively easy to determine drift rates and ice widths, these measurements cannot always be made when ice is visible in the video record. When the slush ice zone is uniform, no drift-rate measurements can be made because there are no trackable targets. When slush ice is widely dispersed, drift rates can be determined but it is impossible to estimate the volume of ice rafting. During this study, widely dispersed ice was much more common than uniform ice containing no trackable targets. In addition, video data can be collected only during daylight hours, so there are

large periods each day when no measurements can be obtained. Even with these limitations, video measurements of ice drift rate and ice width are of much higher spatial and temporal resolution than measurements of ice thickness, ice concentration, or sediment concentration made in the slush ice zone to date. The next step in improving estimates of ice-induced sediment transport must be to refine our ability to measure these last three parameters.

4.5 1991 AND 1992 DRIFTERS

During the winters of 1991 and 1992 'Woodhead Seabed Drifters' ('drifters') were deployed along the southwest shore of Lake Michigan. drifters consists of an eighteen centimeter diameter yellow perforated plastic disk mounted on a 55 cm long red plastic tail (Lee *et al.* 1965). A five-gram weight may be attached to the lower end of the stem to make the drifter negatively buoyant. When deployed, the drifter rests with its tail on the bottom looking somewhat like an open umbrella, and is easily moved by near-bed currents. With no weight attached, the drifter floats at the surface and can be used to track surface currents.

One component of slush ice is NIC ice that is eroded by wave action. This eroded NIC ice is usually well indurated and forms the pieces of brash ice found in the slush ice zone. In January 1991, 102 weighted bottom drifters were buried 50 cm deep in the NIC at Gillson Beach (Figure 4.5). I reasoned that the bottom drifters would be transported by ice as long as they remained trapped in large NIC blocks. If the bottom drifters melted out of the ice over deep water, they would settle to the bottom of the lake and not be recovered. Drifters that came out of the ice in shallow water near the coast would have a chance of being advected onto the beach by waves and currents.

During 11-12 February 1992, 304 additional drifters were deployed in the ice in southwestern Lake Michigan. Based on 1991 returns, several changes were made in the deployment program. A major change for 1992 was that the standard drifter was modified to withstand the rigors of ice. The modification consisted of shortening the tail to 20 cm and riveting a 5 g weight to the surface of the disk rather than adding weight to the stem. These two changes resulted in the drifters lying on the bottom in a slightly different orientation than a normal drifter. Flume calibrations (unpublished data) show that these modifications result in a threshold velocity of 5 cm s^{-1} as compared to a

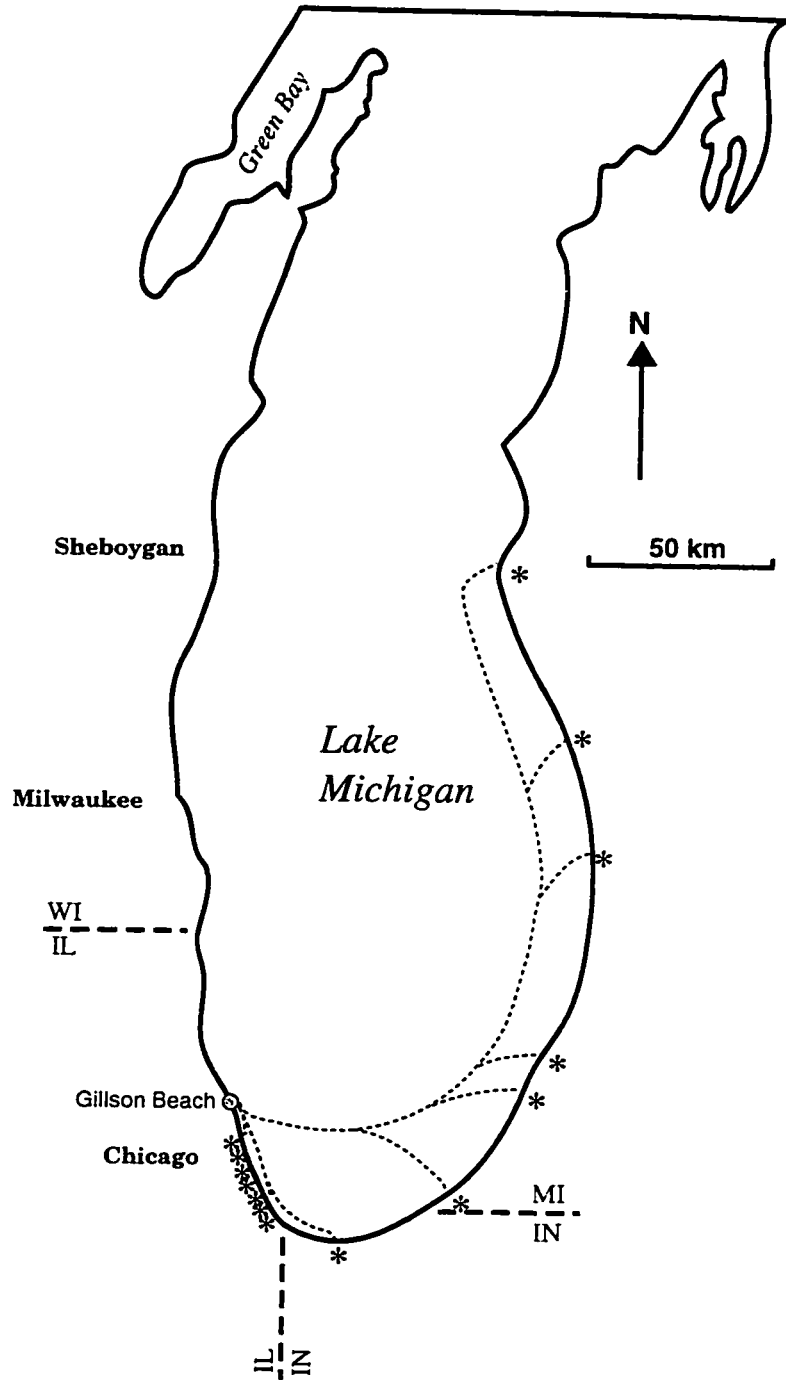


Figure 4.5. 1991 drifter returns. Asterisks (*) are recovery locations. All 1991 drifters were weighted (bottom) drifters that were buried in the NIC at Gillson Beach. None of the recovered drifters had the weights attached when found. Possible drift paths (dashed lines) are based on Harrington (1894) and Allender (1977).

Table 4.4. February 1992 drifter release locations in southern Lake Michigan.

Release Location	Latitude Longitude	Drifter Type		
		Weighted, Buried in NIC	Weighted, Released in slush ice	Surface Drifters
North Point Marina	42.4833° N 87.8013° W	35	26	24
Lake Bluff/ Sunrise Beach	42.2800° N 87.8292° W	0	25	25
Kenilworth Water Plant	42.0900° N 87.7025° w	0	19	0
Gillson Beach	42.0800° N 87.6850° W	50	50	50

threshold velocity of 4 cm s^{-1} for the unmodified drifter in a unidirectional flow. The drifters were also deployed differently in 1992. In addition to burying drifters in the NIC, bottom and surface (i.e. unweighted) drifters were released into the slush ice zone adjacent to the NIC edge. Drifters were deployed at four separate locations along the southwestern shoreline of Lake Michigan (Table 4.4 and Figure 4.6).

Sixteen of the 102 drifters that were deployed in January of 1991 were recovered between 10 March 1991 and 28 January 1992. 1991 drifter recoveries are listed in Table 4.5 and shown in Figure 4.5. Unfortunately, 15 of the drifters were recovered without their stems and weights attached, so I assume they acted as surface drifters. However, as surface drifters their trajectories would mimic floating ice during the winter months.

Table 4.6 lists the recovery location of the twenty-one 1992 drifters recovered between 24 February 1992 and 29 October 1993. Fifteen of these drifters were recovered before the end of March 1992, so ice could have been transported along the same drift paths as the drifters. Figure 4.6 shows the approximate drifter recovery locations. Four bottom drifters and 17 surface drifters were recovered from the 1992 deployment. Of the four bottom drifters recovered, three still had the weights attached, and one was returned without information about the weight. The recovery positions listed in Tables 4.5 and 4.6 are approximate because the people reporting the recovery usually just note where the drifter was found. For example, drifter #22197 is simply reported as being found at

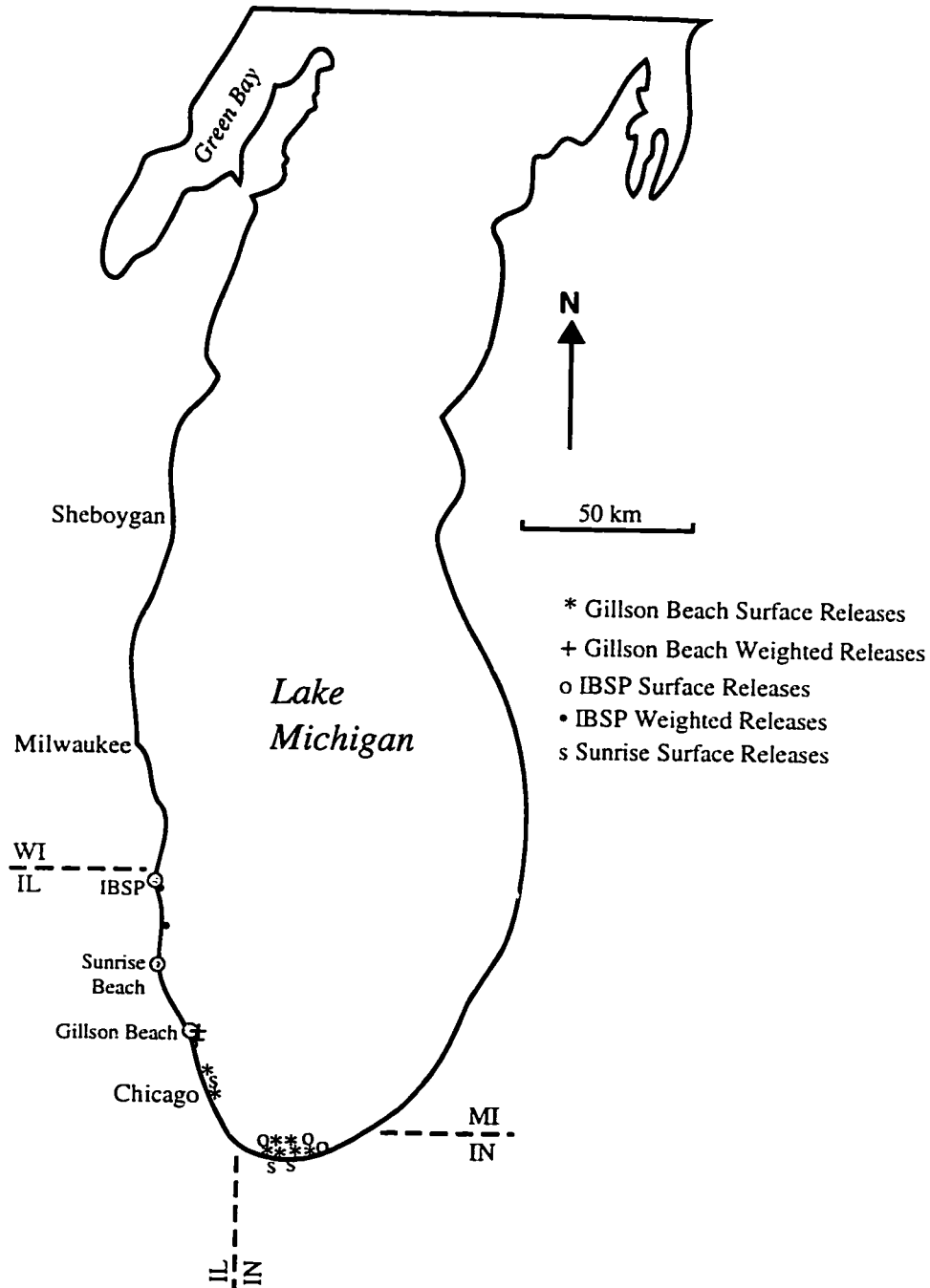


Figure 4.6. 1992 drifter returns. All returned drifters moved south along the southwest shore of Lake Michigan this year.

Table 4.5. 1991 drifter recoveries in southern Lake Michigan.

Drifter Number	Release Latitude (°)	Release Longitude (°)	Release Date	Type ¹	Recovery Latitude (°)	Recovery Longitude (°)	Recovery Date	Recovery Status ²	Recovery Location
21876	42.0800	-87.6850	1/11/91	BB	43.1500	-86.1800	4/10/91		10 mi. S of Muskegon Harbor
21878	42.0800	-87.6850	1/11/91	BB	41.9650	-87.6333	3/10/91		Montrose Beach, Chicago
21887	42.0800	-87.6850	1/11/91	BB	42.3833	-86.2883	11/23/91		South Haven, MI
21891	42.0800	-87.6850	1/11/91	BB	41.9420	-86.5820	3/30/91		Bridgeman, MI
21892	42.0800	-87.6850	1/11/91	BB	41.9000	-87.6200	5/91		Chicago
21895	42.0800	-87.6850	1/11/91	BB	43.6900	-86.5200	3/30/91		N of Little Sable Point
21897	42.0800	-87.6850	1/11/91	BB	41.9142	-87.6208	3/10/91		North Ave Beach, Chicago
21927	42.0800	-87.6850	1/20/91	BB	41.7583	-87.5467	5/1/91		72nd St. Beach, Chicago
21928	42.0800	-87.6850	1/20/91	BB	41.9650	-87.6333	5/7/91		Montrose Beach, Chicago
21934	42.0800	-87.6850	1/20/91	BB	41.7583	-87.5467	5/10/91		Rainbow Beach, Chicago
21946	42.0800	-87.6850	1/20/91	BB	41.8000	-86.7500	7/28/91		New Buffalo, MI
21949	42.0800	-87.6850	1/11/91	BB	42.2542	-86.3567	5/6/91		Rodgers Beach, MI
21950	42.0800	-87.6850	1/20/91	BB	41.7183	-86.9167	1/28/92		Michigan City, IN
21953	42.0800	-87.6850	1/20/91	BB	41.6667	-87.0533	3/10/91		Indiana Dunes, IN
21962	42.0800	-87.6850	1/11/91	BB	43.0000	-86.2300	4/5/91		4 mi. S of Grand Haven, MI
21963	42.0800	-87.6850	1/20/91	BB	42.0750	-87.6567	3/10/91	S, W	Loyola Ave Beach, Chicago

¹Type of drifter

BB: Bottom drifter buried in nearshore ice complex

²Recovery status

S: Stem was attached when recovered

W: Weight was attached when recovered

Blank Field: Neither weight or stem attached

No Info: No information returned about drifter condition

Table 4.6. 1992 drifter recoveries in southern Lake Michigan.

Drifter Number	Release Latitude (°)	Release Longitude (°)	Release Date	Type ¹	Recovery Latitude (°)	Recovery Longitude (°)	Recovery Date	Recovery Status ²	Recovery Location
21741	42.0800	-87.6850	2/12/92	B	42.0800	-87.6850	3/1/92	W	Wilmette, IL
21771	42.0800	-87.6850	2/12/92	BB	42.0800	-87.6850	3/1/92	W	Wilmette, Chicago
21987	42.4833	-87.8013	2/13/92	BB	42.3625	-87.8292	3/17/92	NO INFO	South Waukegan, IL
22004	42.4833	-87.8013	2/13/92	BB	42.4650	-87.7975	3/1/92	S, W	Logan Camp, IBSP
22111	42.0800	-87.6850	2/12/92	S	41.6217	-87.2500	3/14/92	NO INFO	Miller Beach, Gary, IN
22122	42.0800	-87.6850	2/12/92	S	41.8933	-87.6133	3/1/92		Grand Ave Beach, Chicago
22125	42.0800	-87.6850	2/12/92	S	41.6217	-87.2500	3/12/92		Miller Beach, Gary, IN
22126	42.2800	-87.8292	2/13/92	S	41.9142	-87.6225	2/24/92	S	North Ave Beach, Chicago
22127	42.2800	-87.8292	2/13/92	S	41.6217	-87.2500	3/14/92	NO INFO	Miller Beach, Gary, IN
22131	42.2800	-87.8292	2/13/92	S	41.7900	-87.5783	3/1/92	S	Rainbow Beach, S. Chicago
22178	42.4833	-87.8013	2/13/92	S	41.6225	-87.2392	3/11/92	S	Miller Beach, Gary, IN
22160	42.0800	-87.6850	2/13/92	S	41.6208	-87.2667	3/24/92		Marquette Park, Gary, IN
22171	42.0800	-87.6850	2/13/92	S	42.0000	-87.6550	4/17/92		North Side Chicago
22172	42.0800	-87.6850	2/13/92	S	41.6217	-87.2500	3/14/92	NO INFO	Miller Beach, Gary, IN
22174	42.4833	-87.8013	2/13/92	S	41.6217	-87.2500	3/17/92		Miller Beach, Gary, IN
22182	42.4833	-87.8013	2/13/92	S	41.6217	-87.2500	3/14/92	NO INFO	Miller Beach, Gary, IN
22197	42.4833	-87.8013	2/13/92	S	41.6215	-87.2553	3/11/92	S	Miller Beach, Gary, IN
22102	42.0800	-87.6850	2/12/92	S	41.6456	-87.6426	5/19/92		E of Burns Harbor, IN
21820	42.0900	-87.7025	2/13/92	S	41.9142	-87.6225	Late Jan 93	NO INFO	PA - Found 'in Chicago'
22184	42.4833	-87.8013	2/13/92	S					Lake Bluff Beach
22159	42.0800	-87.6850	2/13/92	S			10/29/93	NO INFO	Muskegon, MI

¹Type of drifter

BB: Bottom drifter buried in nearshore ice complex

²Recovery status

S: Stem was attached when recovered

W: Weight was attached when recovered

Blank Field: Neither weight or stem attached

No Info: No information returned about drifter condition

"Miller Beach, Gary, Indiana", so the location is not known any better than it was found somewhere on Miller Beach.

The drifter recoveries show that the predominate surface drift direction is to the south during the winter months. The video records from Gillson Beach also record a net southerly and offshore drift during January 1991. This southerly drift direction is the same as the net longshore sediment transport direction along the southwestern shore of Lake Michigan (Chrzastowski and Trask 1995) so the net movement of ice to the south enhances the net southerly sediment transport in this area.

4.6 DISCUSSION

The direction and magnitude of slush ice movement are of geologic importance for determining the net amount of sediment transported by ice. Miner and Powell (1991) noted that random ice drift results in no net sediment transport. A major goal of recent winter coastal studies in southern Lake Michigan has been to determine the magnitude of this ice-induced sediment transport (Barnes *et al.* 1992 and 1994; Reimnitz *et al.* 1991; Miner and Powell 1991). For the six days when ice rafting could be estimated in 1991, the mean longshore ice drift was to the southeast and the mean cross-shore ice drift was offshore. The longshore component of ice drift is the same direction as ice-free, wave-induced longshore transport on the western shore of the lake (Chrzastowski 1990; Chrzastowski and Trask 1995) and the direction of ice rafting observed by Miner and Powell (1991) during winter storms.

Using the video estimates of ice-drift rate and width along with sediment concentrations and ice thickness it was possible to estimate longshore sediment transport rates for 31 daylight hours during parts of six days (Table 4.3). These 31 hours account for 41 percent of the time when slush ice was present in the video record. During this time, calculated longshore sediment transport fluxes varied from 0.004 to 1.06 m³ m⁻¹ hour⁻¹ and calculated longshore sediment transport rates varied from 0.8 to 120 m³ hour⁻¹. Based on dredge records from Wilmette Harbor (Figure 4.1), Chrzastowski and Trask (1995) estimate that the littoral transport rate past the study site is 9000 m³ year⁻¹. Based on the 1989 estimates of 110 m³ day⁻¹ of southward longshore sediment transport and the high hourly rates estimated with the video system (Table 4.3), it is clear that ice moves a significant portion of the sand through this littoral system. This sand is not included in

Chrzastowski and Trask's (1995) estimates of littoral drift because most of the sediment laden ice that is advected to the south during the winter bypasses the Wilmette Harbor jetty and harbor channel. This is because the channel surface is solidly frozen throughout the winter. Ice supplies the buoyancy to keep sand 'suspended' so normal barriers to longshore transport are easily bypassed by ice rafting.

An advantage of the video system is that it allowed the first estimates of cross-shore ice-rafted sand flux. Calculated cross-shore fluxes varied from 0.001 to 0.14 m³ m⁻¹ of beach hour⁻¹ (Table 4.3). The cross shore fluxes ranged from 3% to 27% of the longshore fluxes. The cross-shore component of ice rafting was consistently offshore and accounts for a significant loss of sand from the nearshore zone. These cross-shore fluxes give a conservative picture of offshore ice rafting for the entire seventeen day video record because days when offshore ice-drift components were strong were characterized by dispersed anchor ice so the sediment flux could not be determined. This offshore transport is not associated with streamers from headlands, as Reimnitz *et al.* (1991) noted; instead, it represents a continual loss of sediment from a straight section of beach. The sand fillet at Gillson Beach is one of the larger sand accumulations along the Illinois Coast, containing about 900 m³ of sand per m of beach (Shabica *et al.* 1991). Offshore ice rafting is removing significant amounts of sand from this stretch of sand-starved coast. At present, there is no source of new sand to replace the sand removed from the nearshore zone by ice rafting (Chrzastowski and Trask, 1995).

For a typical (ice-free) nearshore setting, the concept of offshore transport means moving sand from the foreshore of a swell profile to offshore bars in a storm profile (Komar 1976). This cross-shore transport results in little or no long-term loss of littoral sand. In the slush ice zone, ice buoyantly supports sand near the top of the water column, and offshore ice rafting results in a net loss of beach sand from the littoral cell. Ice rafting can occur at very low drift velocities because bed shear stress is not necessary to keep sediment in suspension. Sediment-laden ice may have long drift trajectories over deep water as suggested by the drifter recoveries. The fate of sediment that is ice rafted offshore has been shown by Reimnitz *et al.* (1991). They found that streamers of sediment-laden nearshore ice deflected offshore at promontories dissipate in warmer offshore waters (Figure 1.1). This dissipation releases entrained sand to the muddy lake floor.

On the basis of the amount of sand found in offshore cores, Barnes *et al.* (1994) have determined that each meter of coastline in southern Lake Michigan supplies, on average, $0.5 \text{ m}^3 \text{ year}^{-1}$ of sand to the central Lake Michigan basin. This sand is transported to the deep basin by ice rafting. This offshore sand flux requires only 5 to 250 hours of cross shore ice rafting at the magnitude measured in this study, if it is assumed that all ice transported offshore melts and drops its entrained sand in deep water.

The pattern of drifter returns for 1991 and 1992 show that currents flow to the south along the southwestern shore of Lake Michigan. This supports the observations of Barnes *et al.* (1992, 1994) and Reimnitz *et al.* (1991). It also supports Chrzastowski's (1990a) observation of the net longshore drift rate along the southwestern shore of Lake Michigan. The most interesting returns are the 1991 returns from the eastern shore of Lake Michigan (Figure 4.5). The drifters that were found farthest north along the east coast of Lake Michigan (#21895 and #21876, Table 4.5) were recovered by 10 April 1991. This is just past the end of the normal ice season in the lake, and suggests that ice could have crossed the lake along with the drifters. Observations by Harrington (1894) and modeling by Allender (1977) indicate a counterclockwise gyre in the southern portion of Lake Michigan. With this in mind, I have drawn possible drift trajectories for the 1991 drifters found along the eastern Lake Michigan shore. The recoveries from the eastern shore of Lake Michigan (Figure 4.5) suggest that ice advected offshore may transit the lake, and any entrained sand may end up on the eastern shore of the lake. However, the long drift trajectories suggested by the work of Harrington (1894) and Allender (1977), combined with presence of a core of warm water in the center of the lake during the winter months (Figure 1.1) suggests that most of the ice probably melts before it makes the trip across the lake. Any sediment entrained in this ice would be deposited in the deep lake.

The drifter returns from both years suggest that impediments to longshore sediment transport do not inhibit the movement of surface drifters to reach the southern or eastern shores of the lake. The same should apply to ice during the winter months, and any entrained sediment may end up in the sediment sink at the southern end of the lake. The four recovered weighted drifters that were buried in the NIC in 1992 were recovered very close to their release points (Figure 4.6). This suggests that little or no long-distance transport of NIC ice occurs or that the NIC ice breaks up rapidly after it is released into

the slush ice zone. Breakup of NIC is into small pieces in the slush ice zone may release any entrained sediment in addition to entrained bottom drifters, resulting in relatively short-distance rafting.

4.7 CONCLUSIONS

Kraus (1987) points out that measurement of sand transport in the nearshore zone is a great challenge for coastal engineers. In order to understand sand movement in the nearshore zone it is necessary to make simultaneous measurements of sediment concentrations at several points (horizontally and vertically) across the surf zone and to collect data on waves and currents that are moving the sediment. These same principles apply to evaluating sand transport in the slush ice zone. The problems of sampling in the nearshore zone are exacerbated by cold air temperatures and the presence of ice.

The observations and measurements made in this study show that relatively high concentrations of sand are ubiquitous in the slush ice zone. The presence of slush ice can lead to a sediment concentration inversion in the nearshore zone as the buoyancy of the ice holds sediment near the top of the water column. Sediment that is held in the water column by ice buoyancy is not restricted to transport in the nearshore zone. Drifter returns and video analysis show that sediment is ice rafted to the south and offshore, and possibly to the east shore of the lake. Based on the measurements made in this study, drifting slush ice is responsible for moving a significant portion of sand along and off the sand-starved shoreline of southwestern Lake Michigan.

As Kraus (1987) noted, it is necessary to gather information on nearshore waves and currents in order to understand sediment transport in the (ice-free) nearshore zone. Understanding nearshore waves and currents is also necessary for understanding ice rafting. This study shows that ice rafting is an important process for dispersal of nearshore sand in southwestern Lake Michigan, but does not address the question of what hydrodynamic conditions are necessary for incorporating sand into floating slush ice. Future work should focus on the relationship between nearshore waves and currents, the thickness and width of the slush ice layer, and sediment concentrations in the slush ice layer.

CHAPTER 5: AN INTEGRATED VIEW OF NEARSHORE ICE AND ITS AFFECT ON SEDIMENT TRANSPORT IN SOUTHERN LAKE MICHIGAN

5.1 INTRODUCTION

This thesis divides the nearshore ice in southern Lake Michigan into three separate components (NIC, anchor ice and slush ice) and describes how each of these components interacts with nearshore sediment. These three ice types are so distinct that it is convenient to divide them into these categories. However, these ice types interact simultaneously with each other and with nearshore sediment; to understand the effects of ice on the nearshore zone the ice system must be considered as a gestalt. In this chapter, I compare the different types of ice and discuss the interdependent nature of the NIC, anchor ice and slush ice. This chapter also contains the concluding remarks.

5.2 COMPARISON OF SEDIMENT FOUND IN GILLSON BEACH ICE SAMPLES

Figure 5.1 shows the sediment concentrations of ice samples collected at Gillson Beach in 1989 and 1991. Floating anchor ice concentrations are used to represent the anchor ice component in this figure. For all the samples types, the sediment concentration is given in terms of grams of sediment per liter of drained ice sample. This value was calculated for the NIC samples by dividing the bulk sediment concentration by the ice volume in a core (Table 2.5). Anchor ice samples have the largest range of sediment concentrations and the highest mean sediment concentration (25 g l^{-1} , Figure 5.1). The NIC has a similar concentration range, with a mean sediment concentration of 23 g l^{-1} . Slush ice samples have the lowest range of sediment concentrations and the lowest mean concentration of 8 g l^{-1} . The larger sediment concentrations seen in the anchor ice and NIC ice samples compared to slush ice samples suggests that sediment is preferentially concentrated in anchor ice and NIC ice. When anchor ice is released from the bed, these large sediment concentrations are entrained into the top of the water column. In this study, I observed that anchor ice entrains sediment directly from the bed in relatively quiet conditions. Anchor ice provides a mechanism for entraining sand-sized sediment into the water column during periods when the sand cannot be suspended by bed shear stress. Sand is concentrated in NIC ice ridges by wave overwash. The sand incorporated at this

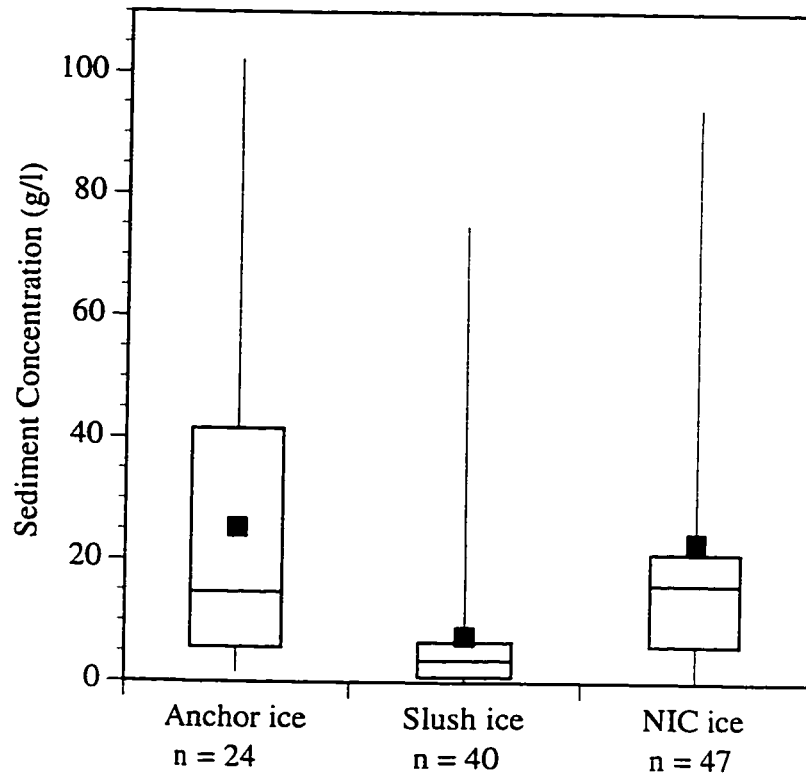


Figure 5.1. Range of sediment concentrations found in Gillson Beach ice samples in 1989 and 1991. Whiskers: range of samples; rectangle: top and bottom quartiles; middle bar: median concentration; black square: mean concentration, n = number of samples.

time is a combination of sand suspended by wave action and sand entrained in the slush ice that is incorporated into the NIC.

Figure 5.2 shows the mean sediment size distributions for the different ice types and lake bottom samples collected at Gillson Beach. The bottom samples have the greatest range of mean grain sizes and the coarsest material found in any type of Gillson Beach sample. The coarsest bed samples are from the plunge point and the longshore trough (Figure 1.4). Based on mean grain sizes, all of the sediment in Gillson Beach ice samples may have been locally derived. Anchor ice has the largest range of mean grain sizes of any ice type. Figure 5.2 shows that anchor ice samples entrained the largest material into the water column. NIC and slush ice samples are very tightly grouped around mean grain size of 2.1ϕ (Figure 5.2). This suggests that NIC and slush ice preferentially entrain the finer sediment at Gillson Beach. This medium sand is the easiest nearshore material to suspend, suggesting that the sediment incorporated into slush ice and NIC ice is entrained from the water column rather than at the bed. The mechanisms of sediment entrainment into ice need more study.

Figures 5.1 and 5.2 summarize what was learned in this study about sediment in southern Lake Michigan ice. The sediment incorporated into southern Lake Michigan ice is predominately sand. Measured sediment concentrations in floating ice ranged from ~ 0 to $\sim 100 \text{ g l}^{-1}$; when concentrations are above 127 g l^{-1} , the ice sinks to the bed and becomes anchor ice. Sediment concentrations in anchor ice samples ranged to $>1000 \text{ g l}^{-1}$. Once sand is incorporated into any type of nearshore ice (NIC, anchor ice, or slush ice), it will probably be ice rafted.

5.3 AN INTEGRATED VIEW OF SEDIMENT/ICE INTERACTIONS IN SOUTHERN LAKE MICHIGAN.

It is clear from this study that the different ice types (NIC, anchor ice and slush ice) found in the Lake Michigan nearshore zone cannot be considered individually in the context of nearshore sediment dynamics. To understand the effects of ice formation on sediment transport, these three ice types must be considered as an integrated whole. Figure 5.3 summarizes the relationships between the different ice types and sediment/ice interactions in the nearshore zone. The open arrows represent pathways for entraining sediment into the ice. These pathways can be divided into two categories:

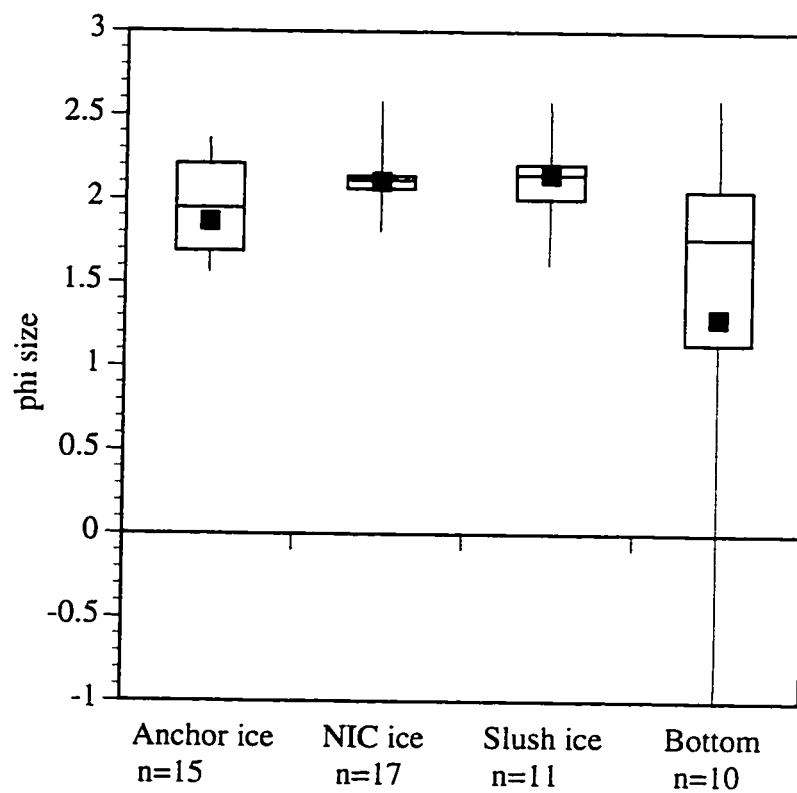


Figure 5.2. Grain size ranges of ice and bed sediment samples from Gillson Beach in 1989 and 1991. See Figure 5.1 for explanation.

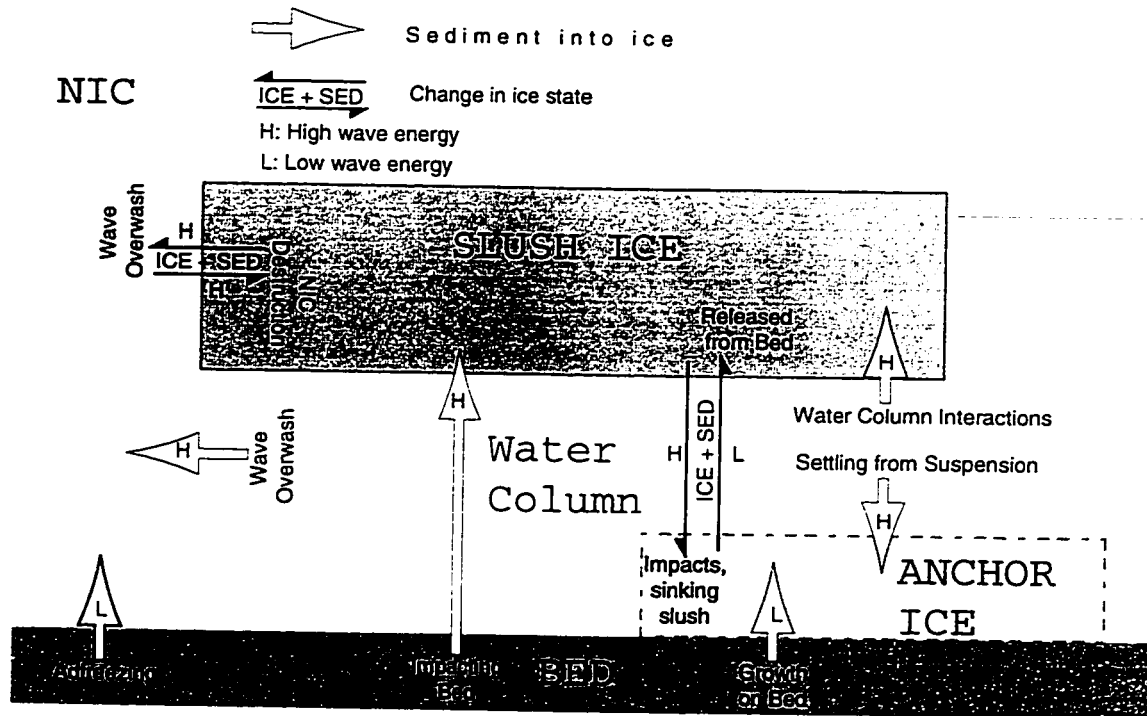


Figure 5.3. A conceptual model of sediment entrainment into Great Lakes ice (open arrows) and transfer of ice from one type to another (closed arrows). The high and low energies (H and L) associated with each path are relative. High wave energy will suspend bed sediment, low wave energy will not.

(1) sediment/ice interactions that occur in the water column and (2) sediment/ice interactions that occur at the bed.

A necessary criteria for sediment/ice interactions in the water column is that the sediment is suspended. This requires relatively energetic conditions that generate bed shear stresses large enough to suspend the nearshore sand. The wave tank studies show that suspended sediment is entrained into frazil ice flocs in the water column. Depending on the amount of sediment entrained into a floc, the floc will either rise to the water surface as slush ice or sink to the bed as anchor ice. As already noted, suspended sediment is incorporated into the NIC by wave overwash.

The other major pathway for entraining sediment into slush ice is via ice impacting the lake bed (Figure 5.3). The wave tank observations show that frazil flocs roll along the bed and entrain sediment. Again, these flocs are either incorporated into the floating slush ice layer or become anchor ice. Another ice/bed sediment interaction occurs when the NIC is grounded. In this case, sediment may be entrained into the NIC by basal freezing, but this process incorporates only small amounts of sediment into nearshore ice (Miner and Powell 1991). The most important sediment/ice interaction at the bed seen in this study is the regular nightly growth of anchor ice on the nearshore lakebed. Anchor ice forms in relatively calm conditions when sediment is not suspended in the water column. Released anchor ice entrains sand and coarser material into the floating slush ice layer where longshore and cross shore ice rafting occurs. This study has shown that regular nightly formation of anchor ice on the sand bed of the nearshore zone in calm conditions incorporates sand into the water column at times when bed shear stress is too small to hydraulically suspend sediment. This regular formation and release of anchor ice is slowly depleting the sand in the southwestern Lake Michigan nearshore zone.

The importance of considering the integrated nature of nearshore ice is indicated by the closed arrows in Figure 5.3. Individual ice parcels readily pass from one ice form to another, taking along entrained sediment. One way to envision the NIC is as a reservoir of ice and sediment that is temporarily stored in the nearshore zone. When there are large waves and thick accumulations of slush ice in the nearshore zone, the NIC is built upward and outward. Waves alone destroy the NIC and release ice and sediment back into the slush ice layer for ice rafting. From this perspective, the NIC is an important component or source of ice and sediment for the slush ice zone. There is a similar exchange of material between anchor ice and slush ice. The most visible exchange is the release of

sediment-laden anchor ice from the bed and its incorporation into the slush ice zone. However, there is also a pathway from slush ice to anchor ice (Figure 5.3). When the sediment concentration in slush ice is above 127 g l^{-1} the slush ice will sink to the bed to become an anchor ice mass.

Until 1991, research on ice in the Great Lakes has focused on the Nearshore Ice Complex. This focus is understandable, because the NIC is the most visible ice morphology in the nearshore zone. The NIC acts as a reservoir of sediment laden ice that remains in place until it is eroded into the slush ice zone. A broad NIC does change littoral cell boundaries by neutralizing barriers to longshore transport by simply engulfing them. Once the NIC ice grows out past a groin, for example, the groin is no longer a barrier to longshore sediment transport or ice rafting. Thus, the presence of a broad NIC enhances sediment transport past normal longshore barriers.

The slush ice zone is the key to understanding sediment dynamics when ice is present in the Great Lakes. The mobile slush ice layer is the only place where ice rafting occurs. In order to move sediment entrained in the NIC or anchor ice, the ice must be transferred into the slush ice layer (Figure 5.3). Unfortunately, the slush ice zone is extremely difficult to work in, and estimates of the slush ice volumes, sediment concentrations, ice concentrations and ice drift rates and directions are extremely difficult to get. This study documents ice rafting by slush ice as an important sediment transport process in southwestern Lake Michigan, resulting in estimated longshore ice-rafting rates of up to $100 \text{ m}^3 \text{ hour}^{-1}$ and in significant offshore ice rafting of sand. However, these are first estimates and will probably be revised as measurements of all the parameters needed to estimate ice rafting are improved. The most important next step in understanding the effects of ice on sediment dynamics in southern Lake Michigan is to get detailed wave data when ice is present to make direct comparisons between hydraulic sediment transport and ice rafting.

5.4 CONCLUSIONS

This study has focused on the effects that ice has on nearshore sediment dynamics in southern Lake Michigan. Nearshore ice in the Great Lakes can be divided into three categories: the Nearshore Ice Complex, anchor ice, and slush ice. Each of these ice types has different effects on nearshore sediment; together they act to enhance normal littoral transport processes.

The NIC is the largest ice feature that forms in the southern Lake Michigan nearshore zone. This ice forms a massive structure that can be 100 m wide, rise to 4 m above lake level, and extends for 10's of kilometers along the coast. The large size of the NIC engulfs many littoral cell boundaries, so nearshore sediment may readily bypass normal littoral cells during the winter months. The total volume of NIC ice that formed at Gillson Beach in January 1991 was 420 m³ of ice per meter of beach. This ice had an entrained sand volume of 2.2 m³ per meter of beach. Wave erosion of the NIC releases sediment laden NIC ice into the slush ice zone. Repeated surveys of nearshore bathymetry lakeward of the NIC at Gillson Beach during the winter of 1991 showed that the bottom profile flattened during the winter and that small scour depressions formed lakeward of the NIC. All evidence of this flattening and the scour depressions was gone by March 1991; the presence of the NIC has little long-term effect on the nearshore bathymetric profile.

Anchor ice forms regularly in the nearshore zone of southern Lake Michigan. Anchor ice forms on cold, clear nights with offshore winds. It forms on sand, pebble, and cobble substrates; the release of anchor ice from the lake bed carries these materials to the top of the water column. Sediment concentrations in floating anchor ice samples range from 1 to 102 g l⁻¹. Anchor ice formed during periods with offshore winds; the release of anchor ice led to offshore ice rafting and removal of sediment from the nearshore zone. Anchor ice formation entrains sand into the water column during relatively calm periods when sand is not suspended by hydraulic forces, so anchor ice formation and release is an important mechanism for moving sand during low-energy periods. A number of different anchor ice morphologies were observed in southern Lake Michigan. I develop a model that relates these morphologies to the nearshore wave energy levels when the anchor ice formed. Four different anchor-ice morphologies that make up a continuum are described. On one end of the continuum is anchor ice that forms in quiet conditions and has large ice crystals and low sediment concentrations. At the other end is anchor ice formed in high energy conditions; this anchor ice has small ice crystals and high sediment concentrations. There is an inverse relationship between the ice crystal size and both the wave energy at the time of formation and the amount of sand incorporated into the anchor ice mass.

Slush ice is the mobile ice type found in the southern Lake Michigan nearshore zone. As such, slush ice is responsible for all ice rafting that occurs. However, both the

NIC and anchor ice contribute material (ice and sediment) to the slush ice layer. Sediment entrained into slush ice is carried to the top of the water column, resulting in sediment concentration inversions in the water column. The buoyancy of ice keeps entrained sediment in the water column, so sediment is easily ice rafted both offshore and along shore past normal littoral cell boundaries. Calculated longshore ice rafting rates at Gillson Beach during 1991 ranged from 0.8 to 120 m³ of sand per hour. Longshore ice rafting is predominately to the south. Cross shore sediment fluxes range from 0.001 to 0.14 m³ of sand per meter of beach per hour. This stretch of shoreline is sediment starved, so these sand volumes represent a significant loss of nearshore sand from this region. Results of a drifter study suggest that slush ice may transport sediment completely across the lake basin

Ice does have a significant effect on nearshore sand in southern Lake Michigan. This study has shown that the old view that formation of a nearshore ice complex locks the beach into place is too simplistic. The formation and movement of ice in the nearshore zone is a dynamic process that redistributes nearshore sand both along shore and offshore throughout the lake basin.

BIBLIOGRAPHY

- Ackerman, N.L., Shen, H.T., and Sanders, B., 1994, Experimental studies of sediment enrichment of arctic ice covers due to wave action and frazil entrainment: *Journal of Geophysical Research*, v. 99, p. 7761-7770.
- Allender, J.H., 1977, Comparison of model and observed currents in Lake Michigan: *Journal of Physical Oceanography*, v. 7, p. 711-718.
- Angel, J.A., 1995, Large-scale storm damage on the U.S. shores of the Great Lakes: *Journal of Great Lakes Research*, v. 21, p. 287-293.
- anon, 1987, Wilmette Park District, Gillson Beach, Wilmette Final Report: W.F. Baird and Associates, p. 22.
- Arden, R.S., 1970, Instrumentation for ice investigations in the Niagara River: *Ice Symposium 1970*, p. 9.
- Arden, R.S., and Wigle, T.S., 1972, Dynamics of ice formation in the upper Niagra River: *International Symposium on the Role of Snow and Ice in Hydrology*, p. 1296-1313.
- Assel, R.A., Quinn, F.H., Leshkevich, G.A., and Bolsenga, S.J., 1983, NOAA Great Lakes Ice Atlas, GLERL Contribution No. 299: Ann Arbor, MI, Great Lakes Environmental Research Laboratory, 116 p.
- Bajorunas, A.J., and Duane, D.B., 1967, Shifting of offshore bars and harbor shoaling: *Journal of Geophysical Research*, v. 72, p. 6195-6205.
- Barnes, P.W., Kempema, E.W., Reimnitz, E., and McCormick, M., 1994, The influence of ice on southern Lake Michigan coastal erosion: *Journal of Great Lakes Research*, v. 20, p. 179-195.
- Barnes, P.W., Kempema, E.W., Reimnitz, E., McCormick, M., Weber, W.S., and Hayden, E.C., 1992, Beach profile modification and sediment transport by ice: an overlooked process on Lake Michigan: *Journal of Coastal Research*, v. 9, p. 65-86.
- Benedicks, C., and Sederholm, P., 1943, Regarding the formation of anchor (ground) ice: *Arkiv for Matematik, Astronomi, och Fysik*, v. 29, p. 1-7.
- Benson, C.S., and Osterkamp, T.E., 1974, Underwater ice formation in rivers as a vehicle for sediment transport, *Oceanography of the Bering Sea*: Fairbanks, Institute of Marine Science, University of Alaska, p. 401-402.
- Booth, J.S., 1994, Wave climate and nearshore lakebed response, Illinois Beach State Park, Lake Michigan: *Journal of Great Lakes Research*, v. 20, p. 163-178.
- Bryan, L.M., and Marcus, M.G., 1972, Physical characteristics of nearshore ice ridges: *Arctic*, v. 25, p. 182-192.
- Carstens, T., 1966, Experiments with supercooling and ice formation in supercooled water: *Geofysiske Publikasjoner*, v. XXVI, p. 1-18.
- Chestnutt, C.B., and Schiller, R.E., 1971, Scour of Simulated Gulf Coast Beaches Due to Wave Action in Front of Seawalls and Dune Barriers: , U.S. Army Corps of Engineers.

- Chrzastowski, M.J., 1990a, Estimate of natural-state littoral transport along the Chicago lakeshore: Coastal Sedimentary Processes in Southern Lake Michigan: Their Influences on Coastal Erosion, p. 19-26.
- Chrzastowski, M.J., 1990b, Late Wisconsinian and Holocene littoral drift patterns in Southern Lake Michigan: Coastal Sedimentary Processes in Southern Lake Michigan: Their Influence on Coastal Erosion, p. 13-18.
- Chrzastowski, m.J., 1991, The building, deterioration, and proposed rebuilding of the Chicago lakefront: Shore and Beach, v. 59, p. 2-10.
- Chrzastowski, M.J., and Thompson, T.A., 1992, Late Wisconsinian and Holocene Coastal Evolution of the Southern Shore of Lake Michigan, Quaternary Coasts of the United States: Marine and Lacustrine Systems: Tulsa, OK, SEPM, p. 397-413.
- Chrzastowski, M.J., Thompson, T.A., and Trask, C.B., 1994, Coastal geomorphology and littoral cell divisions along the Illinois-Indiana coast of Lake Michigan: Journal of Great Lakes Research, v. 20, p. 27-43.
- Chrzastowski, M.J., and Trask, C.B., 1995, Nearshore Geology and Geologic Processes Along the Illinois Shore of Lake Michigan from Waukegan Harbor to Wilmette Harbor: , Illinois State Geologic Survey, p. 93.
- City of Chicago Department of Water, Chicago Water System: City of Chicago Department of Water, p. 24.
- Clifton, H.E., and Dingler, J.R., 1984, Wave-formed structures and paleoenvironmental reconstruction: Marine Geology, v. 60, p. 165-198.
- Colman, S.M., and Foster, D.S., 1994, A sediment budget for southern Lake Michigan: source and sink models for different time intervals: Journal of Great Lakes Research, v. 20, p. 215-228.
- Daly, S.F., 1984, Frazil Ice Dynamics: CRREL Monograph 84-1. Cold Regions Research and Engineering Laboratory, U. S. Army Corps of Engineers, Hanover, NH.
- Daly, S.F., 1991, Frazil ice blockage of intake trash racks: Cold Regions Technical Digest, v. 91-1, p. 12.
- Davis, R.A., 1973, Coastal ice an its effect on beach sedimentation: Shore and Beach, v. 41, p. 3-9.
- Davis, R.A., Goldsmith, V., and Goldsmith, Y.E., 1976, Ice effects on beach sedimentation: examples from Massachusetts and Lake Michigan: La Revue De Geographie De Montreal, v. XXX, p. 201-206.
- Dayton, P.K., 1989, Interdecadal variation in an Antarctic sponge and its predators from oceanographic climate shifts: Science, v. 245, p. 1484-1486.
- Dayton, P.K., Robilliard, G.A., and DeVries, A.L., 1969, Anchor ice formation in McMurdo Sound, Antarctica, and its biological effects: Science, v. 163, p. 273-274.
- Dean, R.G., 1986, Coastal armoring: principles and mitigation: Proceedings of the 20th Coastal Engineering Conference, p. 1843-1857.
- Department of the Army, C.O.E., 1971, Great Lakes Regional Inventory Report National Shoreline Study: U.S. Army, Corps of Engineers, p. 221.

- Dillion, W.P., and Conover, J.T., 1965, Formation of ice-cemented sandstone blocks and lithologic implications: *Journal of Sedimentary Petrology*, p. 964-967.
- Downing, J.P., 1983, Field Studies of Suspended Sand Transport, Twin Harbors Beach, Washington [unpublished Ph.D. thesis]: University of Washington.
- Downing, J.P., Sternberg, R.W., and Lister, C.R.B., 1981, New instrumentation for the investigation of suspended sediment processes in the shallow marine environment: *Marine Geology*, v. 42, p. 19-34.
- Dozier, J., Marsh, B.D., and Marsh, W.M., 1976, Ice cusp formation on Lake Superior icefoots: *La Revue De Geographie De Montreal*, v. XXX, p. 161-179.
- Dyer, K.R., 1986, Coastal and Estuarine Sediment Dynamics: New York, John Wiley and Sons, 342 p.
- Evenson, E.B., and Cohn, B.P., 1979, The ice foot complex: its morphology, formation, and role in sediment transport and shoreline protection: *Zeitschrift fur Geomorphologie*, v. 23, p. 58-75.
- Fahnestock, R.K., Crowley, D.J., Wilson, M., and Schneider, H., 1973, Ice volcanoes of the Lake Erie shore near Dunkirk, New York, U.S.A.: *Journal of Glaciology*, v. 12, p. 93-99.
- Folger, D.W., Colman, S.M., and Barnes, P.W., 1994a, Journal of Great Lakes Research, Special Section on the Southern Lake Michigan Coastal Erosion Study, *Journal of Great Lakes Research: International Association for Great Lakes Research*, p. 326.
- Folger, D.W., Colman, S.M., and Barnes, P.W., 1994b, Overview of Southern Lake Michigan Coastal Erosion Study: *Journal of Great Lakes Research*, v. 20, p. 2-8.
- Folk, R.L., 1974, Petrology of Sedimentary Rocks: Austin, Texas, Hemphill Publishing Company, 182 p.
- Foulds, D.M., and Wigle, T.E., 1977, Frazil - the invisible strangler: *Journal of the American Waterworks Association*, v. April, p. 196-199.
- Fox, W.T., and Davis, R.A., 1976, Weather patterns and coastal processes, in Davis, R.A., and Ethington, R.L., eds., *Beach and Nearshore Sedimentation*: Tulsa, OK, SEPM, p. 1-21.
- Fox, W.T., Ladd, J.W., and Martin, M.K., 1966, A profile of four moment measures perpendicular to a shore line, South Haven, Michigan: *Journal of Sedimentary Petrology*, v. 36, p. 1126-1130.
- Fraser, G.S., Thompson, T.A., Kvale, E.P., Carlson, C.P., Fishbaugh, D.A., Gruver, B.L., Holbrook, J., Kairo, S., Kohler, C.S., Malone, A.E., Moore, C.H., Rachmanto, B., and Rhoades, L., 1991, Sediments and sedimentary structures of a barred, nontidal coastline, southern shore of Lake Michigan: *Journal of Coastal Research*, v. 7, p. 1113-1124.
- Ferguson, H.L., and Cork, H.F., 1972, Regression equations relating ice conditions in the Upper Niagara River to meteorological conditions: The Role of Ice and Snow in Hydrology, Proceedings of the Banff Symposia, September 1972, p. 1314-1327.

- Gilfilian, R.E., Kline, W.L., Osterkamp, T.E., and Benson, C.S., 1972, Ice formation in a small Alaskan stream: The Roll of Snow and Ice in Hydrology, Proceedings of the Banff Symposia, Sept. 1972, p. 505-513.
- Guza, R.T., and Thornton, E.B., 1980, Local and shoaled comparisons of sea surface elevations, pressures, and velocities: *Journal of Geophysical Research*, v. 85, p. 1524-1530.
- Hansel, A.K., Mickelson, D.M., Schneider, A.F., and Larsen, C.E., 1985, Late Wisconsin and early Holocene history of the Lake Michigan Basin, *in* Karrow, P.F., and Calkin, P.E., eds., Geological Survey of Canada Special Publication No. 30: , p. 39-53.
- Harrington, M.W., 1894, Currents of the Great Lakes as Deduced from the Movement of Bottle Papers During the Seasons of 1892 and 1893: , U.S. Department of Agriculture, Weather Service.
- Hough, J.L., 1958, *Geology of the Great Lakes*: Urbana, IL, University of Illinois Press, 313 p.
- Hubertz, J.M., Driver, D.B., and Reinhard, R.D., 1991, Hindcast Wave Information for the Great Lakes: Lake Michigan: , Coastal Engineering Research Center, Department of the Army, Waterways Experimental Station, Corps of Engineers, Vicksburg, MS, p. 36 + Appendices.
- Jonsson, I.G., 1966, Wave boundary layers and friction factors: Proceedings, 10th Conference on Coastal Engineering, p. 127-148.
- Kana, T.W., 1976, A new apparatus for collecting simultaneous water samples in the surf zone: *Journal of Sedimentary Petrology*, v. 46, p. 1031-1034.
- Kempema, E.W., and Holman, R.A., 1994, Video Monitoring of nearshore ice in southern Lake Michigan: *Journal of Great Lakes Research*, v. 20, p. 196-205.
- Kempema, E.W., and Reimnitz, E., 1991, Nearshore sediment transport by slush/brash ice in southern Lake Michigan: Coastal Sediments '91 Proceedings, p. 212-219.
- Kempema, E.W., Reimnitz, E., Clayton, J.R., and Payne, J.R., 1993, Interactions of frazil and anchor ice with sedimentary particles in a flume: *Cold Regions Science and Technology*, v. 21, p. 137-149.
- Kivisild, H.R., 1970, River and lake ice terminology: Proceedings of the IAHR Research Symposium on Ice and Its Action on Hydraulic Structures, p. Paper 1.0.
- Komar, P.D., 1976, *Beach Processes and Sedimentation*: Englewood Cliffs, New Jersey, Prentice-Hall, 429 p.
- Komar, P.D., and Miller, M.C., 1973, The threshold of sediment movement under oscillatory waves: *Journal of Sedimentary Petrology*, v. 43, p. 1101-1110.
- Komar, P.K., and Miller, M.C., 1975, On the comparison between the threshold of sediment motion under waves and unidirectional currents with a discussion of the paractical evaluation of threshold: *Journal of Sedimentary Petrology*, v. 45, p. 362-367.
- Kraus, N.C., 1988, The effects of seawalls on the beach: an extended literature review: *Journal of Coastal Research*, p. 1-28.
- Kraus, N.C., and McDougal, W.G., 1996, The effects of seawalls on the beach: part I, an updated literature review: *Journal of Coastal Research*, v. 12, p. 691-701.

- Kraus, N.C., and Nakasha, L., 1986, Field method for determining rapidly the dry weight of wet sand samples: *Journal of Sedimentary Petrology*, v. 56, p. 550-551.
- Krumbein, W.C., and Pettijohn, F.J., 1938, *Manual of Sedimentary Petrography*: New York, Appleton-Century-Crofts, Inc., 549 p.
- Lee, A.J., Bumpus, D.F., and Lausier, L.M., 1965, The Seabed Drifter: Northwest Atlantic Fisheries Research Bulletin, v. 2, p. 42-47.
- Lesht, B.M., and Brandner, D.J., 1992, Functional representation of Great Lakes surface temperatures: *Journal of Great Lakes Research*, v. 18, p. 98-107.
- Lineback, J.A., Gross, D.L., and Meyer, L.P., 1972, Geologic Cross Sections Derived From Siesmic Cross Profiles and Sediment Cores From Southern Lake Michigan: Illinois State Geologic Survey, p. 43.
- Lippmann, T.C., and Holman, R.A., 1989, Quantification of sand bar morphology: a video technique based on wave dissapation: *Journal of Geophysical Research*, v. 94, p. 995-1011.
- Lippmann, T.C., and Holman, R.H., 1990, The spatial and temporal variability of sand bar morphology: *Journal of Geophysical Research*, v. 95, p. 11575-11590.
- Lyell, C., 1873, *Principles of Geology*.
- Marsh, W.M., Bryan, M.L., and Dozier, J., 1976, Aerial imagery of Lake Superior coastal ice: *La Revue De Geographie De Montreal*, v. XXX, p. 179-186.
- Marsh, W.M., Marsh, B.D., and Dozier, J., 1973, Formation, structure and geomorphic influence of Lake Superior icefoots: *American Journal of Science*, v. 273, p. 38-64.
- Marshall, E.W., 1966, *Air Photo Interpretation of Great Lake Ice Features*: , University of Michigan, p. 92.
- Marshall, E.W., 1967, Lake Superior ice characteristics: Tenth conference on Great Lakes Research, Proceedings, p. 214-220.
- Marshall, E.W., 1977, *The Geology of the Great Lakes Ice Cover* [unpublished Ph.D. thesis]: University of Michigan, Ann Arbor.
- Martin, S., 1981, Frazil ice in rivers and oceans: *Annual Review of Fluid Mechanics*, v. 13, p. 379-397.
- McCormick, M., Hayden, E.C., Weber, W.S., Barnes, P.W., Reimnitz, E., and Kempema, E.W., 1990, Coastal Ice and Sediment Samples; Shoreface and Ice Profiles (Southern Lake Michigan, February, December 1989 and February, April 1990): , U.S. Geological Survey Open File Report 90-537, p. 186.
- McCormick, M., Kempema, E.W., Haines, J., Barnes, P.W., and Reimnitz, E., 1991, Southern Lake Michigan Coastal Ice and Sediment Sample Data: Shoreface and Ice Profiles (Winter 1990/1991): , U.S. Geological Survey Open-File Report 91-619 A & B, p. 32.
- McDougal, W.G., Kraus, N.C., and Ajiwibowo, H., 1996, The effects of seawalls on the beach: part II, numerical modeling of SUPERTANK seawall tests: *Journal of Coastal Research*, v. 12, p. 702-213.
- Michel, A.B., 1971, *Winter Regime of Rivers and Lakes*: U.S. Army Cold Regions Research and Engineering Laboratory, p. 131.

- Michel, B., 1972, Properties and processes of river and lake ice: The Role of Snow and Ice in Hydrology, p. 454-481.
- Miner, J.J., 1990, The Lake Michigan Icefoot Complex: conditions of Formation and Destruction, and and evaluation of Winter Erosion at Wilmette, Illinois. [unpublished Master of Science thesis]: Northern Illinois University.
- Miner, J.J., and Powell, R.D., 1991, An evaluation of ice-rafted erosion caused by an icefoot complex, southwestern Lake Michigan, USA: Journal of Arctic and Alpine Research, v. 23, p. 320-327.
- Navy, U.S., 1952, A Functional Glossary of Ice Terminology.
- Neilsen, P., 1984, Field measurements of time-averaged suspended sediment concentrations under waves: Coastal Engineering, v. 8, p. 51-72.
- Nielsen, N., 1988, Observations of sea ice influence on the littoral sediment exchange, North Zealand, Denmark: Geografisk Tidsskrift, v. 88, p. 61-67.
- O'Hara, N.W., and Ayers, J.C., 1972, Stages of shore ice development: Proceedings, 15th Conference on Great Lakes Research, p. 521-535.
- Osterkamp, T.E., Gilfilian, R.E., Gosink, J.P., and Benson, C.S., 1983, Water temperature measurements in turbulent streams during periods of frazil-ice formation: Annals of Glaciology, v. 4.
- Osterkamp, T.E., and Gosink, J.P., 1982, Frazil ice formation and ice cover development in interior Alaskan streams: Cold Regions Science and Technology, v. 8, p. 43-86.
- Pegau, W.S., Paulson, C.A., and Zaneveld, J.R.V., 1992, Optical techniques for the measurement of frazil ice: Ocean Optics XI, SPIE Proceedings.
- Piotrovich, V.V., 1956, Formation of depth ice, Translated by E.R. Hope, Directorate of Scientific Information Service, DRB Canada, Nov. 1956: Priroda, v. 9.
- Reimnitz, E., Hayden, E., McCormick, M., and Barnes, P.W., 1991, Preliminary observations on coastal sediment loss through ice rafting in Lake Michigan: Journal of Coastal Research, v. 7, p. 653-664.
- Reimnitz, E., Kempema, E.W., and Barnes, P.W., 1987, Anchor ice, seabed freezing, and sediment dynamics of shallow Arctic seas: Journal of Geophysical Research, v. 92, p. 14,671-14,678.
- Sadler, H.E., and Serson, H.V., 1981, Fresh water anchor ice along an arctic beach: Arctic, v. 34, p. 62-63.
- Saulesleja, A., 1986, Great Lakes Climatological Atlas: Ottawa, Atmospheric Environment Service, Environment Canada, p. 145.
- Schaefer, V.J., 1950, The formation of anchor ice in cold water: Transactions, American Geophysical Union, v. 31, p. 885-893.
- Seibel, E., 1986, Lake and shore ice conditions on Southeastern Lake Michigan, in Rossman, R., ed., Impact of the Donald C Cook Nuclear Plant: Ann Arbor, MI, University of Michigan, p. 401-432.
- Seibel, E., Carson, C.T., and Maresca, J.W., 1976, Ice ridge formation: probable control by nearshore bars: Journal of Great Lakes Research, v. 2, p. 384-392.

- Shabica, C., and Pranschke, F., 1994, Survey of littoral sand deposits along the Illinois and Indiana shorelines of Lake Michigan: *Journal of Great Lakes Research*, v. 20, p. 61-72.
- Shabica, C., Pranschke, F., and Chrzastowski, M.J., 1991, Survey of Littoral Drift Sand Deposits Along the Illinois Shore of Lake Michigan from Fort Sheridan to Evanston: Illinois-Indiana Sea Grant Program, p. 15.
- Svensson, U. and Omstedt, A. Simulation of supercooling and size distribution in frazil ice dynamics: *Cold Regions Science and Technology*, v.22, p. 221-233.
- Taylor, J.R., 1982, *An Introduction to Error Analysis: the Study of Uncertainties in Physical Measurements.*: Mill Valley, CA, University Science Books, 270 p.
- Tsang, G., 1982, *Frazil and Anchor Ice: a Mongraph*: Ottawa, Ontario, Canada, Natural Resources Council Subcommittee on Hydraulics of Ice Covered Rivers, 90 p.
- Tsang, G., 1985, An instrument for measuring frazil concentration: *Cold Regions Science and Technology*, v. 10, p. 235-249.
- Weggel, R., 1988, Seawalls: the need for research, dimensional considerations and a suggested classification: *Journal of Coastal Research*, p. 29-40.
- Wickham, J.T., Gross, D.L., Lineback, J.A., and Thomas, R.L., 1978, *Late Quaternary Sediments of Lake Michigan*: , Illinois State Geologic Survey, p. 26.
- Wigle, T.E., 1970, Investigations into frazil, bottom ice and surface ice formation in the Niagara River: *Proceedings of the Symposium on Ice and Its Action on Hydraulic Structures*, p. 16.
- Zampol, J.A., and Inman, D.L., 1989, Suspended sediment measurements: B. discrete measurements of suspended sediment, *in* Seymour, R.J., ed., *Nearshore Sediment Transport*: New York, Plenum Press, p. 259-272.
- Zumberge, J.H., and Wilson, J.T., 1953, Effect of ice on shore development (Michigan): *Proceedings, 4th Coastal Engineering Conference*, Oct, 1953, p. 201-205.

Edward W. Kempema
1657 N 15th
Laramie, WY 82070
(307) 742-8637
kempema@ocean.washington.edu

EDUCATION

Ph.D., Oceanography, 1998, University of Washington, Seattle, WA
M.S., Geology, 1986, San Jose State University, San Jose, CA
B.A., Geology, 1979, Humboldt State University, Arcata, CA

PROFESSIONAL EXPERIENCE

1988 -present	Graduate Student, Research/Teaching Assistant, School of Oceanography, University of Washington, Seattle, WA
1996-1997	Curriculum development/site management, Earth System Science Internet Project (ESSIP), University of Wyoming, Laramie, WY
1981-1988	Geologist, U.S.G.S., Office of Energy and Marine Geology, Branch of Pacific Marine Geology, Menlo Park, CA
1978-1981	Physical Science Technician, U.S.G.S., Office of Energy and Marine Geology, Branch of Pacific Marine Geology, Menlo Park, CA

RESEARCH INTERESTS

Marine sedimentation and sedimentary processes, dynamic ice formation, ice/sediment interactions and ice rafting

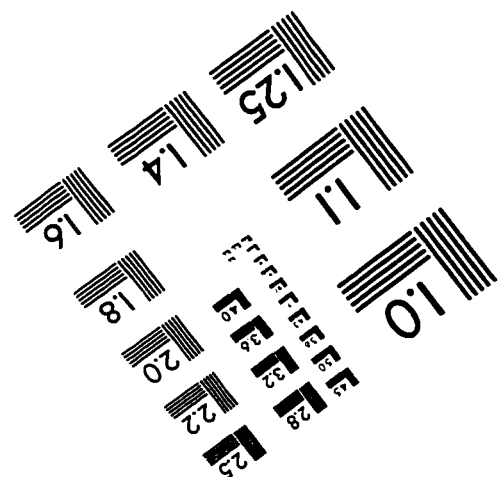
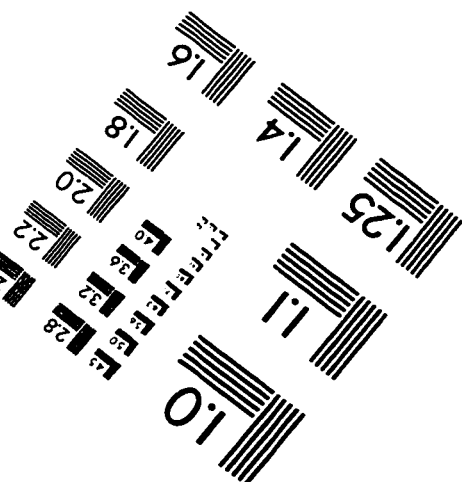
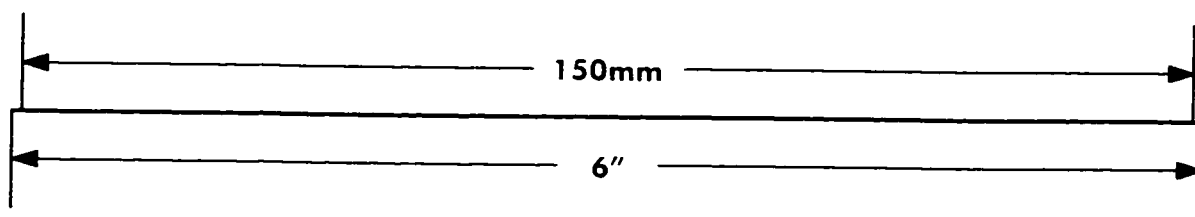
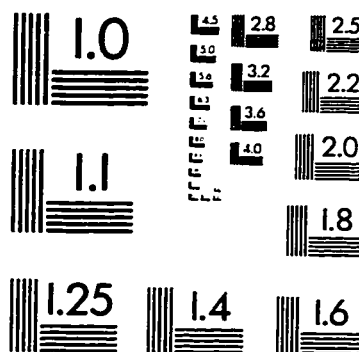
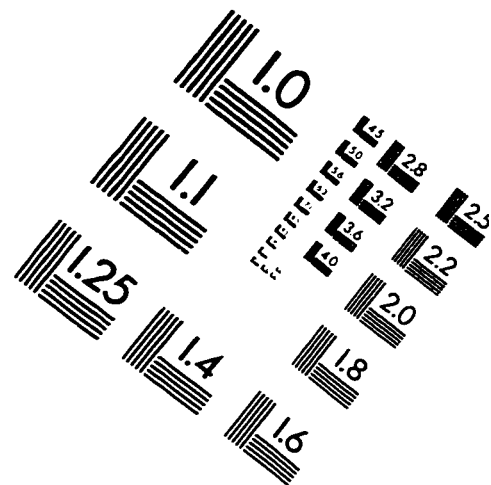
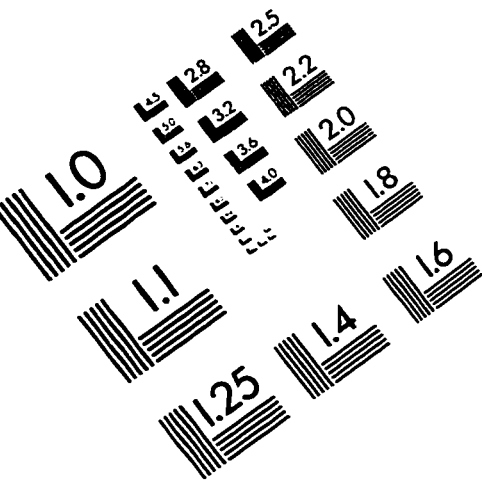
PROFESSIONAL AFFILIATIONS

Society of Economic Paleontologists and Mineralogists
American Geophysical Union

PUBLICATIONS

- Kempema, E.W., 1998, Nearshore Ice and Sediment Transport in Southern Lake Michigan. Ph.D. Dissertaion, University of Washington, Seattle, WA.
- Barnes, P.W., Kempema, E.W., Reimnitz, E., and McCormick, M., 1994, The influence of ice on southern Lake Michigan coastal erosion: *Journal of Great Lakes Research*, v. 20, p. 179-195.
- Kempema, E.W., and Holman, R.A., 1994, Video Monitoring of nearshore ice in southern Lake Michigan: *Journal of Greatr Lakes Research*, v. 20, p. 196-205.
- Barnes, P.W., Kempema, E.W., Reimnitz, E., McCormick, M., Weber, W.S., and Hayden, E.C., 1993, Beach profile modification and sediment transport by ice: an overlooked process on Lake Michigan: *Journal of Coastal Research*, v. 9, p. 65-86.
- Kempema, E.W., Reimnitz, E., Clayton, J.R., and Payne, J.R., 1993, Interactions of frazil and anchor ice with sedimentary particles in a flume: *Cold Regions Science and Technology*, v. 21, p. 137-149.
- Reimnitz, E., Clayton, J.R., Kempema, E.W., Payne, J.R., and Weber, W.S., 1993, Interaction of rising frazil with suspended particles: tank experiments with applications to nature: *Cold Regions Science and Technology*, v. 21, p. 117-135.
- Kempema, E.W., and Reimnitz, E., 1991, Nearshore sediment transport by slush/brash ice in southern Lake Michigan: *Coastal Sediments '91 Proceedings*, p. 212-219.
- Kempema, E.W., Reimnitz, E., and Barnes, P.W., 1989, Sea ice sediment entrainment and rafting in the Arctic: *Journal of Sedimentary Petrology*, v. 59, p. 308-317.
- Reimnitz, E., and Kempema, E.W., 1988, Ice rafting: an indication of glaciation?: *Journal of Glaciology*, v. 34.
- Reimnitz, Erk and Kempema, E.W., 1987, Field observations on slush ice generated during freezeup in Arctic coastal waters, *Marine Geology*, v. 77, p. 219-231.
- Reimnitz, Erk and Kempema, E.W., 1987, Thirty-four-year shoreface evolution at a rapidly retreating. arctic coastal site, in: Hamilton, J.D., and Galloway, J.P., (eds.), *Geological Studies in Alaska by the U.S. Geological Survey During 1986: U.S. Geological Survey Circular*, p 161-164.
- Reimnitz, E., Kempema, E.W., and Barnes, P.W., 1987, Anchor ice, seabed freezing, and sediment dynamics of shallow Arctic seas: *Journal of Geophysical Research*, v. 92, p. 14,671-14,678.
- Kempema, E.W., 1986, Flume studies and field observations of the interaction of frazil ice and anchor ice with sediment, Master's Thesis, San Jose State University, San Jose, CA, 86 p.

IMAGE EVALUATION TEST TARGET (QA-3)



APPLIED IMAGE, Inc
1653 East Main Street
Rochester, NY 14609 USA
Phone: 716/482-0300
Fax: 716/288-5989

© 1993, Applied Image, Inc., All Rights Reserved